WROCŁAW UNIVERSITY OF SCIENCE AND TECHNOLOGY

FACULTY OF CHEMISTRY

DOCTORAL DISSERTATION

STRUVITE PRECIPITATION FROM PROCESSED DAIRY WASTES

mgr Claver NUMVIYIMANA

Supervisor:

dr hab. inż. Jolanta WARCHOL, prof. uczelni

www.ETN-REFLOW.eu
Horizon 2020 Marie Skłodowska-Curie Action Nº· 814258

SUPERVISOR

Associate Professor JOLANTA WARCHOL PhD, DSc

Supervisor approval signature:

Date (dd/mm/yyyy):

This doctoral thesis was conducted in the Department of Advanced Materials Technology in the frame of the Maria Skłodowska-Curie Action H2020-ITN, project REFLOW "Phosphorus recovery for Fertilizers from Dairy processing wastes", No 814258, October 2019 - September 2022.

DEDICATION

I dedicate this work

To the Universe Creator

ACKNOWLEDGEMENT

I would like to acknowledge the Wroclaw University of Science and Technology as well as its community for academic and social support that they offered me.

I would like to acknowledge the role of several individuals whose support made this thesis be completed and to whom I am greatly thankful.

I would like to express my gratitude to Professor Jolanta Warchol for being my work supervisor, and more importantly advisor with inspiration, and correction along the research.

Thanks to Professor Katarzyna Chojnacka, the Head of Department of Advanced Material Technology for entrusting me the role of project implementation, guidance, corrections, and scientific advices.

Thanks to Dr Ewa Pankala, the Director of Department of Research and Innovation, Grupa Azoty, Kędzierzyn-Koźle for hosting me in matters of fertilizer production during my PhD secondment.

My deep gratitude goes to European Commission, Maria Skłodowska-Curie Actions, REFLOW project and all professors in REFLOW for providing inspiring lectures, and modules contents that have been major basics for successful research.

I recognize the support of my referees during my application process: Prof. Jacek Namieśnik, Prof. Agata Kot-Wasik, and Dr eng. Tomasz Chmiel from the Gdansk University of Technology, and Honorable Dr. Laetitia Nyinawamwiza, former Rector of the University of Rwanda College of Agriculture.

All praise be to God, in Jesus, for He makes things possible and he is always in control

Table of content

ACRONYMS

a.g	*analytical grade*	*HTC*	*Hydrothermal carbonization*
AE	*Agronomic efficiency*	*IAP*	*Ion Activity product*
AnD	*Anaerobic digestion*	*ICP-OES*	*Inductively coupled plasma optical emission spectroscopy*
ANR	*Apparent nutrient recovery*	*Ksp*	*Solubility product*
ATP	*Adenosine triphosphate*	*NER*	*Nutrient efficiency ratio*
CA	*Annualized investment cost*	*PE*	*Physiologic efficiency*
CEk	*Cost effectiveness of the production configuration k*	*RE*	*Removal Efficiency*
COM	*Operation and maintenance cost*	*RecP*	*Phosphorus recovery efficiency*
Cs	*Saturation concentration*	*SEM*	*Scanning electron microscopy*
D	*Desirability*	*SI*	*Saturation index*
EBPR	*Enhance Biological Phosphorus Removal*	*TAC*	*Total annualized cost*
EC	*European commission*	*XRD*	*X-ray diffraction*
EDS	*Energy dispersive spectroscopy*		
EU	*European Union*		

SYMBOLS

Symbol	***Meaning***	***Symbol***	***Meaning***
ΔG	*Gibbs free energy*	m_z	*Mass of sorbent materials*
Δm	*Variation of mass*	Q_e, q_e	*Equilibrium sorption capacity*
ΔV	*Variation of volume*	V	*volume*
a_i	*Activity*	α_i	*molar fraction*
C_e	*Equilibrium concentration*	σ	*Supersaturation*
C_o	*Initial Concentration*	τ	*time constant parameter*
DEmax	*Maximum dissolution efficiency*		
K_{sp}	*Solubility product*		

INTRODUCTION

Phosphorus (P) ensures soil fertility, maximizes crop yields, supports farmer livelihoods, and ultimately ensures food security for the world's food systems (Cordell and White, 2013). In living organism, phosphorus (P) is the important element in energy production in animal cells through its dynamic reactions involving phosphorylation and de-phosphorylation, the activities that produce adenosine tri-phosphate (ATP) from their diphosphate congeners (ADP), and vice versa, respectively, with energy exchange (Hardman et al., 2019). Naturally, phosphorus (P) remains bound in nature as ores, e.g., phosphate rocks (Nobel and Nobel, 2009; Samreen and Kausar, 2019). Additionally, phosphorus (P) can exist in matrix as particulate and dissolved species both involving organic and inorganic forms (Jarvie et al., 2002). The inorganic P species include mainly orthophosphate which is the main available form for plant nutrition thus important in soil fertility and problematic in water pollution (Gotsis skretas and Friligos, 1990).

The P reservoirs are irregularly distributed on the globe, with more than 70 percent of them located mainly in Morocco, China, South Africa, Jordan and United states (Schröder et al., 2010). They decrease decently due to multiple uses accompanied with its loss in environment. This causes P soil nutrient depletion inducing the decrease in crop production (Amann et al., 2018; Z. X. et al., 2005). About 82% of the mined phosphorus is used in agriculture, while 7% is used for the production of animal feed. The remaining fraction of mined P is used in industry and medicine for the production of pharmaceuticals, oils, detergents, or even textiles (Cieślik and Konieczka, 2017). The continuous P exploitation without renew will cause a P price growth in near future and problem in P mining (Selby-Pham et al., 2017; Van Vuuren et al., 2010). The P is lost through the sewage, industrial effluents and run off from agricultural activities (Cieślik and Konieczka, 2017; Cieślik et al., 2015).

Dairy processing is one of the largest industry in the European agriculture sector and the EU is the lead global producer of milk with nearly 160 million tones per year (EDA, 2020). This largely contributes to wastewater and agro-food waste generation through dairy processing (Ashekuzzaman et al., 2019). Agro-food industry generates approximately five million metric tonnes of wastes per year. Up to 39% of them come from food processing and manufacturing (Ravindran et al., 2018). Food supply chain including animal derived food waste highlights their use in anaerobic digestion to produce heat fuel and bio-fertilizer (Ravindran and Jaiswal, 2016). Milk industry leads the sources of food industrial effluent water, especially in Europe (Kolev, 2017). The effluent P and nitrogen are the root cause of waterbodies eutrophication, leading to ecological problems such as water anoxia, the increased growth of phytoplankton, periphencton, macrophytes, and more harmful macro and microscopic plants (Lewis et al., 2011). Treated water for reuse should contain 2 $mg \cdot kg^{-1}$ P at most, the range recommended by Food and Agriculture Organization (FAO) being 0-2 $mg \cdot kg^{-1}$ (Almuktar et al., 2018).

Along the wastewater treatment process, nutrients such as P are susceptible to recovery through various processes. The P recovery from wastewater involves its accumulation into the sludge, which becomes a nutrient rich material. The P accumulation methods include physicochemical process, biological process, and their combination (EIP-AGRI, 2017; Izadi et al., 2020). The physicochemical processes are widely applied in wastewater treatment by involving, for example, the use of precipitating agents such as lime, alum, and iron salts; the combination of salts dosing with filtration techniques (Nadeem et al., 2021), and electrochemical precipitation (Lei et al., 2021). The chemical precipitation process demonstrates high P removal efficiency with adverse effect of enormous sludge generation (Bunce et al., 2018).

Research highlighted many challenges caused by wastewater treatment sludge, including their excessive production, the needs for disposal, and limitations of their application in agriculture (Smyth et al., 2010; Tarpani et al., 2020). Different strategies of sludge management have been subjects of studies including their incineration (EurEau, 2021), their use in anaerobic co-digestion for energy recovery (Akhiar et al., 2017), and their use as substrate in production of biochar (Tian et al., 2019). The challenging facts of direct agricultural use of sewage sludge include the environmental risk posed by micro-pollutants and pathogens (Egle et al., 2016). In addition to those limitations, the efficiency of sludge as fertilizer is unstable because of low nutrient content, low nutrient release and variable nutrient composition (Shi et al., 2021). Previous works highlighted that the supply of sludge as a fertilizer with high iron content decreased P availability for some crops (Römer and Samie, 2002). The EU fertilizers regulation 2019/1009 does not include the sludge as fertilizing product on EU market. The limitation does not apply to valuable products obtained by sludge processing designated as STRUBIAS (struvite, biochar, ash) (Gianico et al., 2021). Some processes involve incineration and produce a sludge ash with more than 90% of P recovery (Shaikh, 2018). While others involve production of biochar, a product with better chemical, physical, and fuel properties compared with the raw biomass (Ghanim et al., 2017a). Struvite precipitation presents an advantage for its usability as a fertilizer, with the provision of P and nitrogen in an efficiently available form for plant nutrition (Daneshgar et al., 2018b). Previous works emphasized on phosphorus recovery and precipitation from various wastes (Cieślik and Konieczka, 2017; Cieślik et al., 2015; Corre et al., 2009; Doyle and Parsons, 2002; Kabdaşlı and Tünay, 2018; Kataki et al., 2016a; Sena and Hicks, 2018). The P precipitation produces phosphate salts, e.g., calcium phosphate, hydroxyapatite, and struvite (Cieślik and Konieczka, 2017). The works on coupling waste processing and their P purification into struvite are still limited.

The aim of this work is P recovery from dairy wastes, valorization of the dairy wastes with the focus of their possible use in P recycling and P recovery for fertilizers use (Shaddel et al., 2019). This work collects the knowledge of existing technologies for organic biowastes treatment, their P pathway, dissolution and struvite precipitation. The experimental work focus on study of process conditions for phosphorus recovery as struvite from dairy wastes through their thermochemical treatment and precipitation.

The faster and economic model of coupling thermochemical treatment of sludge and struvite precipitation was studied. In one scenario, the sludge was treated under hydrothermal carbonization process and generate a hydrochar, which is applied as biochar in agriculture. The P in derived HTC process water was then recovered as struvite by precipitation process. The particular attention was given to chemically produced sludge with iron salts, the wastes which studies were previously limited. They were hereby used and resulted into a sterile biosolid (hydrochar), a P inorganic fertilizer (struvite) and iron recycled. A business case was developed for a full scale production implementation.

In second scenario, the sludge was incineration process to generate a P rich ash from the Fe-chemical sludge. The wet chemical extraction followed by struvite precipitation was studied for the obtained ash. For better productivity and cost effectiveness, the combination of dairy sludge ash and magnesite was studied where magnesite served as magnesium source. On the other hand, clinoptilolite natural zeolite was studied for process enhancement and ammonium sorption along with struvite precipitation.

The quality of the obtained products as fertilizers was evaluated by in-vitro assays. For this, nutrients release kinetic models were used. In-vivo assays were used in assessment of nutrient use

efficiencies parameters. Finally, along with the induced chemical reactions and P recovery efficiency, the effects of process conditions on the fertilizer quality were evaluated on plants.

I. THEORITICAL PART

1. Approaches of wastewater phosphorus recovery

1.1. Generalities on P recovery technologies

Phosphorus recovery innovations started within the 1950s with an expanded consideration to eutrophication and the increase of P levels in surface waters (Morse et al., 1998). Phosphorus from wastewater can be accumulated into natural biosolids using biological process or can be removed by physico-chemical treatment or a combination of both strategies (Izadi et al., 2020). The enhanced biological process is done using polyphosphate accumulating microorganisms (PAOs) and removes P more efficiently than activated sludge method. The physicochemical approaches are widely used by e.g, chemical precipitation processes, membrane filtrations, sorption process and ion exchanges. These processes may be combined for better efficiencies where BPR take place in secondary wastewater treatment stages, while the physical chemical process get applied up to tertiary treatment for P removal. The later processes involve mainly the chemical dosing with alumina, iron salts, calcium salts; ion exchanges mechanisms, membrane bioreactor, etc. (Morse et al., 1998). The summary of the processes are presented in the figure 1. For the chemical precipitation applied as the only process of P removal from wastewater, the adverse effect is huge amount of sludge thereby generated due to salts dosing. For process with iron salts, the amount of metal salts added relate with the decrease of P concentration to the needed lower level in treated water. For the chemical precipitation applied as the only process of P removal from wastewater, the adverse effect is huge amount of sludge thereby generated due to salts dosing. For process with iron salts, the amount of metal salts added relate with the decrease of P concentration to the needed lower level in treated water

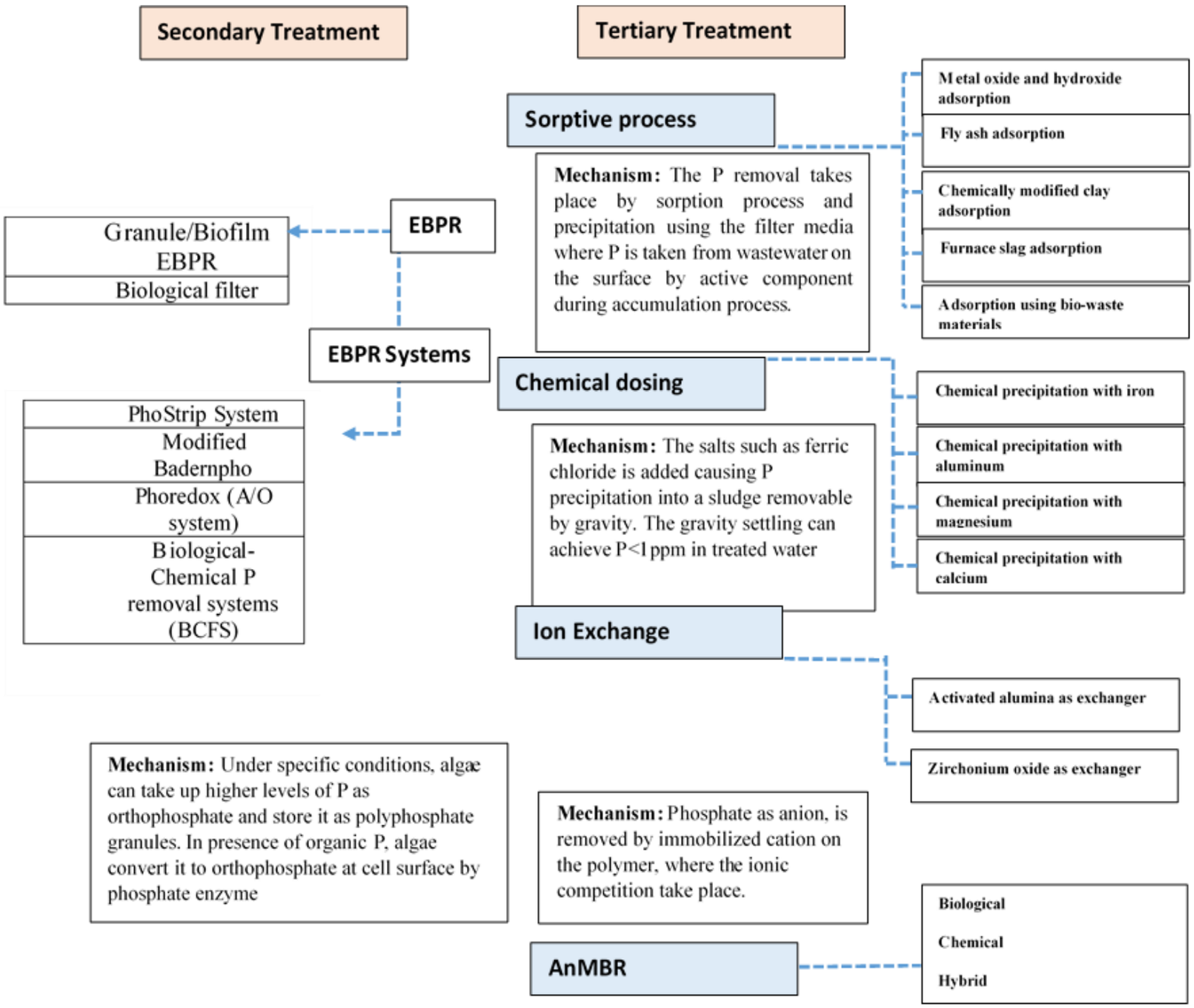

Figure 1. Summary of phosphorus recovery technologies in wastewater treatment (Izadi et al., 2020)

Iron salts dose as coagulants can vary from 1 to 2 mole ratio to P in order to have the P concentration less than 0.2 $mg \cdot L^{-1}$ in treated water (Prot et al., 2020). For the purpose of lowering the P concentration to less than 0.05 $mg \cdot L^{-1}$, the iron dose can be risen to 4 mole ratio to P (Takács et al., 2006).

1.2. Sludge uses limitations in agriculture

The amount of 8.7 million tonnes of sludge were produced in EU-member states in 2020, of which 47.7 % was used in agriculture as fertilizer (EurEau, 2021). Other use of the sludge are summarized on Figure 2a-b. The regulations on fertilizer market in EU member states do not include the sludge as a commercial fertilizing product (Gianico et al., 2021). This follows the suspicion of micro-pollutants and pathogens in the sludge. The reported organic pollutants in sludge with various concentration range include poly-aromatic hydrocarbons (PAHs) which concentration ranged from 0 to 31 $mg \cdot kg^{-1}$, polychlorinated biphenyls (PCBs) with range of 0-3 $mg \cdot kg^{-1}$, and various concentrations of dioxins, and pharmaceuticals (Tavazzi et al., 2012). The micro-organisms are present in sludge with different range of concentration including viruses (87- $417 \cdot 10^7$ $cfu \cdot g^{-1}$), bacteria (2.69-3376 $\cdot 10^5$ $cfu \cdot g^{-1}$), helminths (0.063-453.5 $eggs \cdot g^{-1}$), fungi (114.3-752.3$\cdot 10^6$ $cfu \cdot ml^{-1}$), and protozoa (12-32 $oocyst \cdot g^{-1}$) (Fijalkowski et al., 2017).

On the other hand, the nutrients availability of sludge is limited and unstable. For chemically produced sludge, the P availability to plant for iron based sludge was found to decrease with Fe: P molar ratio, where it was effectively plant-available up to a Fe: P mole ratio of 1.6, and decreased with higher mole ratios (Kahiluoto et al., 2015).

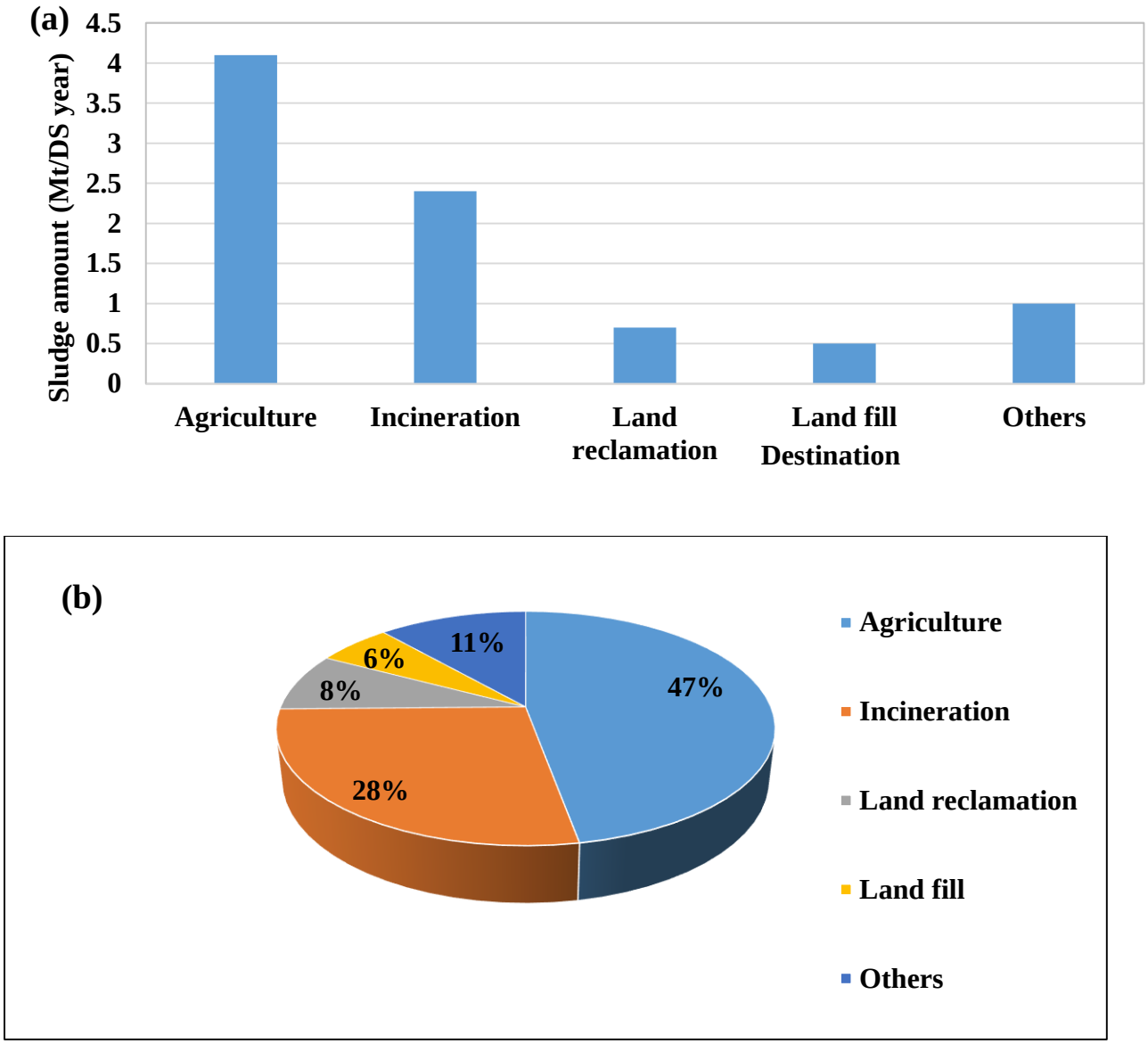

Figure 2. Sludge final destination in EU in Mt/dry sludge (a) and their fraction on total generated sludge (b) (EurEau, 2021)

Such Fe:P mole ratio is easy to exceed in iron based sludge. Ashekuzzaman et al.(2019) has found that iron and P contents in a chemically produced dairy sludge with ferric salts were 162 and 31.6

$g{\cdot}kg^{-1}$, respectively, equivalent to 2.8 of Fe:P mole ratio (Ashekuzzaman et al., 2021). Thus the risk of lower P availability to plant.

2. Phosphorus recovery through struvite precipitation

2.1. Concept of struvite precipitation

The European Innovation Partnership Agricultural Productivity and Sustainability (EIP-AGRI) highlighted the application of precipitation process for P recovery from wastes (EIP-AGRI, 2017). Calcium phosphate was reported to be recovered from manure while struvite is the recommended form for fertilizer use (EIP-AGRI, 2017). The latter is a benefit in agriculture due to its content in nitrogen and phosphorus in the forms efficiently available to plant (Ballirano et al., 2013a; Kataki et al., 2016b). Struvite precipitation reaction is described by reaction$Mg^{2+}{}_{(aq)} + NH_4{}^{+}{}_{(aq)} + H_nPO_4{}^{(3-n)-}{}_{(aq)} + 6H_2O_{(l)} \rightleftharpoons MgNH_4PO_4 \cdot 6H_2O_{(s)} + nH^{+}{}_{(aq)}$:

$$Mg^{2+}{}_{(aq)} + NH_4{}^{+}{}_{(aq)} + H_nPO_4{}^{(3-n)-}{}_{(aq)} + 6H_2O_{(l)} \rightleftharpoons MgNH_4PO_4 \cdot 6H_2O_{(s)} + nH^{+}{}_{(aq)}$$

The product is generally in orthorhombic crystal form (Ulex, 1845). Though the reaction is faster in aqueous solutions by which precipitation term is used, the mechanism of struvite crystallization involves mainly nucleation and crystal growth (Hövelmann et al., 2019). Nucleation is the stage when the first new crystalline nuclei are formed (Le Corre et al., 2009). The crystal growth is subsequent process of incorporating constituent ions into the crystal lattice to form detectable crystals (Abella, 2017). In final stage, the grown crystals aggregate to form a solid-liquid phases equilibrium (Ballirano et al., 2013a). However, different factors influence struvite precipitation including concentration, pH, temperature, and interfering foreign ions. The former two are mainly operational conditions where struvite precipitation is favored in alkaline pH (7.5-11) due to increased molar fraction of reactive phosphate (Daneshgar et al., 2018a; Simoes et al., 2018). The lower temperature (<25°C) is recommended since struvite solubility decreases with temperature

(Capdevielle et al., 2013a; Khater et al., 2015). For struvite precipitation from wastes, the major factors include matrix effects, competitive ions and their concentration.

2.2. Matrix effect and foreign ions

2.2.1. Effect of interfering ions

In solution, besides the contribution to ionic strength, the availability of foreign ions causes co-precipitation with possibility of struvite inhibition. Anions can affect magnesium activity in solution where carbonate salts can potentially co-precipitate in form of huntite ($Mg_3CaCO_3)_2$), hydromagnesite, and magnesite (Ballirano et al., 2013b). On other hand, the precipitation of P is susceptible to happen with a number of cations forming less soluble phosphate salts. The solubility potential of P salts were discussed in several researches (Bell et al., 1978; Bennett et al., 2017; Kazadi Mbamba et al., 2015a; Shih and Yan, 2016), and the summary of typical P precipitation products is described by Figure 3. In multi-component aqueous matrices, phosphate counter-ions can potentially inhibit magnesium and ammonium to pair to phosphate for struvite production (Maneedaeng et al., 2012). More specifically, high level of calcium was pointed out in several researches to inhibit struvite (Ksp = $10^{-13.6}$) formation (Pinatha et al., 2017). In contrast, this favors precipitation of calcium P salts including calcium phosphate ($Ca_3(PO_4)_2$, hydroxyapatite ($Ca_5(PO_4)_3OH$, Ksp = $2.91 \cdot 10^{-58}$), octacalcium phosphate (($Ca_8H_2(PO_4)_6 \cdot 5H_2O$), Ksp = $1.12 \cdot 10^{-48}$), and amorphous calcium phosphate (Bell et al., 1978; Hao et al., 2008; Johansson, 2019). Dairy products make one of groups of calcium source, thus the waste from milk processing plants have high level of calcium and struvite precipitation from DPW needs advanced experimental optimization (Kapsak et al., 2011). In dairy wastewater, other phosphate counterions including silver, aluminum, copper, cadmium, iron and other transition metals, but these are in trace concentrations and their effect in struvite formation is relatively low.

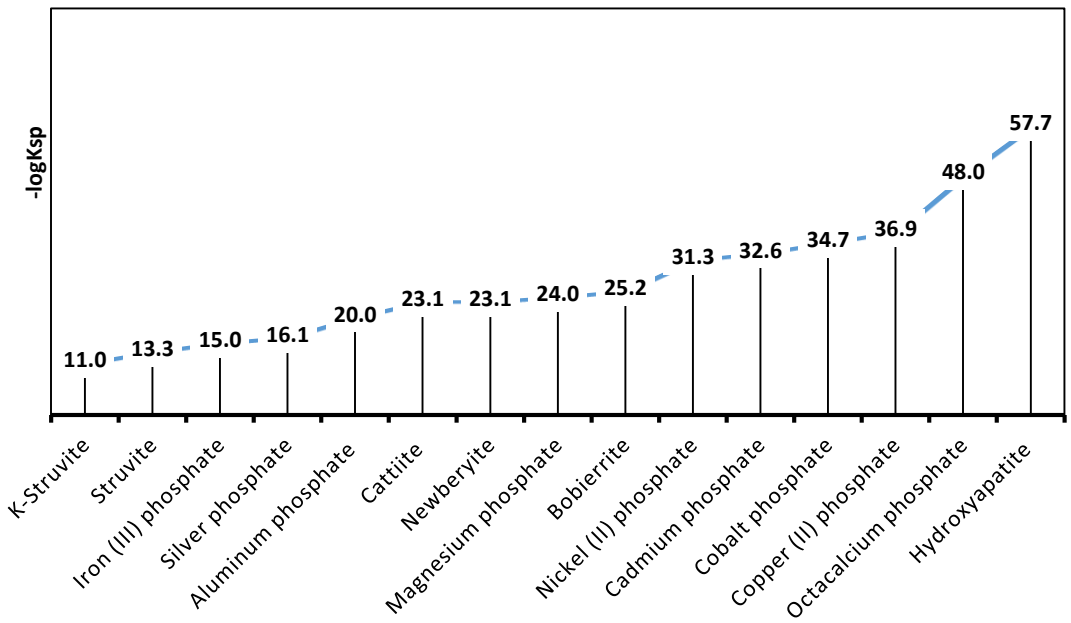

Figure 3. Phosphate counterions and possible phosphate salts precipitation

Thus in light of Ksp (Drahansky et al., 2016), calcium phosphate salts are apt to inhibit struvite. This is underlined by their thermodynamic behaviours where rate expression for precipitation of calcium phosphate salts are higher than magnesium ammonium phosphate (struvite). Such calcium precipitation potential is due to higher saturation index (*SI)* which is inversely proportional to Ksp (up to 10^{-58}) and their SI can reach up to 45 magnitudes higher than struvite.

Table 1. Ion molar ratios in previous works in struvite precipitation

pH	Mg:P	Ca:P	NH_4^+:P	P recovery	References
9.5	4	0.05*	12*	92.60%	(Lavanya and Sri Krishnaperumal Thanga, 2020)
10.89	2.25	-	-	84.70%	(Khater et al., 2015)
8.5, 9.5	5	1.95	5	84%, 94%	(Daneshgar et al., 2018a)
7-10	2.25	1	3.1	>90%	(Capdevielle et al., 2013a)

*Calculated from the composition of used raw material

As a mitigation of struvite inhibition, previous works accounted on optimization of process conditions including pH, and mixing molar ratio of Ca:P, Mg:P, and NH_4:P (Drahansky et al.,

2016; Generalic, 2019; Kataki et al., 2016a; Shalaby et al., 2015; Shih and Yan, 2016; Wang et al., 2005). The data depicted in Table 1 presents some of the mixing molar ratios in recent researches. Prior knowledge of sample characteristics, especially mineral concentration of raw material, is important to have an idea of precipitation pathway. To avoid inhibitory behavior of competitive ions, additional P sources are usually added in the reactor. The previous researches on P recovery as struvite and key process parameters are summarized in Table 2.

a. Additional dose of P and Mg salts

Different techniques have been used to overcome the effect of foreign phosphate counter-ions. One of the ways is to add additional amount of P, magnesium and ammonium salts to increase struvite supersaturation and precipitation potential (Moragaspitiya et al., 2019; Shalaby et al., 2015). Calcium concentration higher than Ca : P > 0.5 molar ratio to P exhibits the progressive inhibition on struvite precipitation due to thermodynamic properties of calcium phosphate salts mainly hydroxyapatite (Khater et al., 2015). Thus mineral adjustment is achieved using additional struvite precursor salts through design of experiments. In this case, the product additionally contains calcium, an important crop secondary macronutrient.

b. Heavy metals and interferences removal

- **Metal removal by precipitation process**

Oxalates precipitates. A number of metals forming phosphate salts in alkaline pH, that can form the oxalate compounds at lower pH thus enabling their removal at lower pH while dissolving the P in supernatant (Verma et al., 2019). The oxalic acid demonstrated settling property of iron thus can be used in its removal (Abis et al., 2018; Elomaa et al., 2019). The additional benefits of oxalic acid are found in significant decrease of calcium concentration thus decreasing the level of struvite inhibitors in the leachate. The need of lower pH of metal oxalate precipitation is due to the ability of the oxalate to undertake both complexation and precipitation reactions. Considering the pKa

values of oxalic acid (pKa_1=1.23, pKa_2=4.19) and the proton transfer speciation model, and the metal complexes eligible of formation with pH dependence, we can draw-out the oxalate behavior in aqueous solution as in Figure 4.

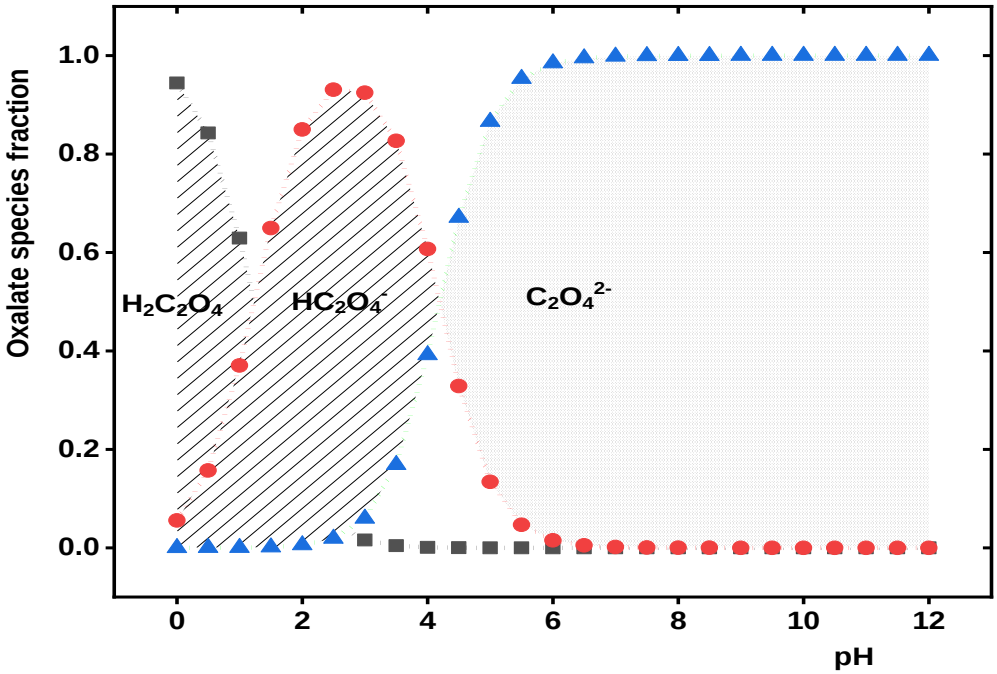

Figure 4. Oxalic acid speciation in function of pH

In this case, the precipitation of metal (M) oxalate is enhanced at lower pH forming precipitates under general form of MC_2O_4 and $M_2(C_2O_4)_3$ for divalent and trivalent metals, respectively. This favors the removal of iron (II), calcium (II) as their oxalates salts. Their removal is decreased by their complexation which start at pH> pKa1 and becomes more predominant at pH>2 as molecular form vanishes from the oxalic acid dynamic equilibria. The divalent metal complexes can thus be formed in pH range of pKa1<pH<pKa2 with $HC_2O_4^-$ ions. At higher pH, the removal becomes quasi impossible due to a full metal complexation by $C_2O_4^{-2}$ ions. This method of oxalic use for previously served in chemical precipitation of calcium by oxalic acid and ammonium oxalate prior to struvite precipitation (Shalaby et al., 2015).

Sulfides precipitates. Most of the heavy metals immediately form low soluble sulfide compounds even in a strong acid solution (Lewis, 2010). These are formed with various metals including iron (II) sulfide which can serve in extraction process for iron recycling from the wastes. Eagle et al., demonstrated that heavy metals can be removed by applying 80g/L Na_2S solution (Egle et al., 2015), and can remove more than 80% of heavy metals. The challenging use of sulfide is the smell released during the process. Once the reaction is done in acidic pH, the hydrolysis of Na_2S releases the H_2S with double negative effects including the decrease in metal settling and the threatening smell for the working environment (Numviyimana et al., 2022).

- **Metal removal by complexation**

The ethylene diamine tetra-acetic acid (EDTA) was used to chelate calcium and release phosphate from calcium phosphate salts (Tianxi Zhang et al., 2010) for enhanced struvite precipitation. The removal using EDTA may also decrease the activity of magnesium in the solution due to complexation. However the $MgEDTA^{2-}$ complex is less stable than $CaEDTA^{2-}$ complex by 2 orders of magnitude ($logK_{25^oC}^{Mg^{2+}} = 8.92\ and\ logK_{25^oC}^{Ca^{2+}} = 10.77$) (Arena et al., 1983). Thus there is negligible effect of EDTA in Mg complexation for struvite enhancement.

c. Adjustment through ion exchange

The selective ion exchange materials were reported as effective in mineral adjustment applicable for either anion and cation removal in prior of precipitation (Liberti, L., Boari, G. and Passino, 1984). Natural zeolite was reported to be a material with appropriate selectivity to remove cations including heavy metals, thus can be applied in mineral adjustment followed by struvite precipitation (Perera et al., 2019). Clinoptilolite, phillipsite and chabazite can be used in ion exchange (Liberti et al., 2001; Xu et al., 2012).

Table 2. Available researches for P recovery as struvite from wastes

Wastes	Reactor	TP/PO_4^{3-}	TN/NH_4^+	Ca	Mg source	Add. Reag.	pH	pH adj	P rec (%)	Reference
Wastewater										
Leather tanning wastewater	Closed stirred batch reactor	NR/12.3	2405	370	$MgCl_2$	Na_2HPO_4	9	NaOH	90	
	Closed stirred batch reactor	NR/2.5-8	NR/119-1076	178–245	$MgCl_2$	Na_2HPO_4	9	NaOH	NR	(Olmez-hanci and Tunay, 2004)
Cochineal insects processing wastewater (Carmine Dye industry)	Agitated batch reactor	NR/3490	NR/2320	42	MgO	Na_2HPO_4	8.5–9	MgO	100	(Chimenos et al., 2003)
Semiconductor wastewater	Jar test with paddle	NR/286	NR/100	5–12	$MgCl_2$	-	9	NaOH	70	(Kim et al., 2009)
Anaerobic effluent from potato processing industries	Continuous aerated stirred reactor	NR/43–127	NR/208–426	36–65	$MgCl_2$	-	8.5–8.7	NaOH	19–89	(Moerman et al., 2009)
Rare-earth wastewater	Stirred jar apparatus	7.8/NR	NR/4535	0.7	Brucite/ H_3PO_4		8.5–9.5	NaOH	97	(Huang et al., 2011)
Fertilizer production waste water	Tube Mixed type continuous crystallizer	NR/4.45 %	NR/0.440 %	-	$MgCl_2$ NH_4Cl		9–11	NaOH	99.5	(Matynia et al., 2013)
Beverages industrial waste water	Agitated glass batch reactor	NR/415	NR/NR	NR	$MgCl_2$ NH_4Cl		9.5	NaOH	97	(Foletto et al., 2013)
Yeast and anaerobic digestion leachates	Stirred batch reactor	22/17.4	354/161	25.6	$MgCl_2$	Na_2HPO_4	9.5	NaOH	83	(Khai, 2012)
	Stirred batch reactor	NR/10.8	595/528	258	$MgSO_4$	H_3PO_4	9	-		(Uysal et al., 2010)
Dairy wastewater (synthetic)	Batch reactors	NR/570	NR/756	200	MgO		9.5	NaOH/ H_2SO_4	93.5	(Lavanya and Sri Krishnaperumal Thanga, 2020)
Ash										
Sewage sludge ash		6.2%	-	6%	$MgCl_2$& NH_4Cl	-	10	NaOH	97%	(Xu et al., 2012)
Biosolids										
Sludge AnD	Batch reactors	37	32.5	101			9.5	NaOH	94	(Daneshgar et al., 2018a)

2.2.2. Matrix effects on struvite precipitation and wastes processing

a. Phosphorus forms in bio-wastes

In organic wastes, the predominant P forms include nucleic acids (ATP), dieters and phytic acid. The latter presents a big fraction of P in agro-food wastes accounting up to 60% of total P in manure (Robinson et al., 2018; Sun et al., 2018). The organic bound P is not reactive in precipitation process. This needs treatment process that break down the organic bond and obtain inorganic P followed by dissolution and precipitation (Ajiboye et al., 2007; Daneshgar et al., 2018a). Different treatment technologies are used to reduce the volume and the mass of wastes including thermochemical treatment, aerobic/anaerobic digestion for material and energy recovery from waste (Kataki et al., 2017). The latter ensures the use of wastes as renewable resources to produce fuel (biogas); fertilizers, and other more added value products (Ravindran and Jaiswal, 2016). The technologies that are coupled with struvite precipitation include anaerobic digestion processes and thermochemical treatment.

b. Anaerobic digestion (AD)

This is a biological process that runs without oxygen supply in built systems referred to as anaerobic digesters. AD systems can minimize odors, reduce pathogens and waste volume, and produces gas, liquid, and solid digestate (Costa et al., 2015; Wahono et al., 2009). It transforms complex organic molecules into small molecules by microbial activity (Moletta et al., 1986). In AD process, fatty acids and carbohydrates are degraded to acetic acid by acetobacteria and form biogas by methanogen activity. Proteins are degraded by proteolytic microorganisms including yeasts (Rodarte et al., 2011) that decompose proteins into small molecules mainly ammonium (Ruiz and Del Carmen Salas, 2019). Inorganic species are dissolved and participate in chemical reactions involving precipitation and volatilization. For AD of sludge, precipitation is enhanced by ferric or ferrous salts of chloride or sulfate, aluminum sulfates and calcium hydroxide added in feedstock of sludge to increase coagulation and chemical precipitation during wastewater treatment (Gutierrez et al., 2010; Möller and Müller, 2012; Ojo and

Ifelebuegu, 2019; USEPA, 1974). Regarding P pathway, Szymańska et al. found that soluble P increased from 41.6 $mg \cdot kg^{-1}$ to 212 $mg \cdot kg^{-1}$ during AD of cattle manure (Szymańska et al., 2019). The ammonium (NH_4^+) and phosphate produced by microbial activity can be trapped in the presence of magnesium to precipitate struvite under optimum conditions. The forward pathway reactions involve precipitation and possible electrochemical reactions (Möller and Müller, 2012).

Nevertheless, other mineral phosphate can precipitate as iron phosphate following their addition as either micronutrient to increase microbial growth or coagulants during wastewater treatment (Möller and Müller, 2012). In addition, struvite, magnesium and calcium phosphate precipitates were found in anaerobic digester liquor (Van Rensburg et al., 2003; Wentzel et al., 2001), revealing therefore, the possibility of struvite production from AD liquor. Furthermore, AD residues dewatering and drying process can produce a biosolid with >90% of dry matter subject to multiple uses or further treatment by thermochemical process (Kijo-Kleczkowska et al., 2015). Technologies of coupling struvite production with anaerobic digestion are installed in different countries in Europe. The summary of the coupled AD and struvite precipitation with example of implemented technologies are presented on Figure 5.

The depicted process has an advantage of production of biogas and struvite for energy and fertilizer applications, respectively. Nevertheless, the application of the technology has many challenges including long hydraulic retention time (HTR) in anaerobic digestion, which can vary from 2 to several days, even a month (Cremonez et al., 2021). Additionally, the performance of sludge dewatering ranges from 40-50°C, and the organic molecules may start to crack at higher temperature (Lv et al., 2019). The obtained sludge is still classified as a waste, limited on fertilizer market due to suspicious presence of harmful microorganisms. The microbial cell walls are destroyed and the proteins are accessible for breakdown after thermal

pre-treatment in the temperature range of 60 to 180°C, a temperature range possible in hydrothermal processes (Neyens and Baeyens, 2003).

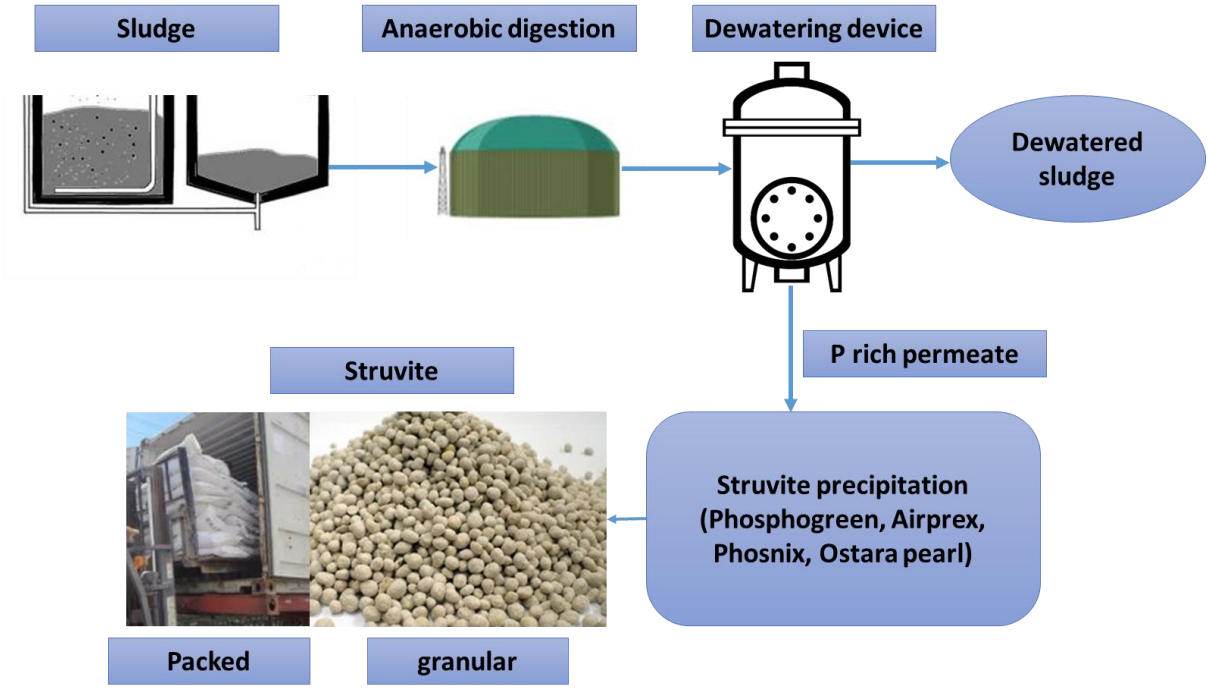

Figure 5. Anaerobic digestion coupled to struvite production

c. Thermochemical treatment

The common sludge disposal include landfill with possibility of agricultural application (Tarpani et al., 2020). The enhanced waste management strategies support the reduction of waste volume where landfill is used as a transit step for further waste treatment process (Smyth et al., 2010). Thermal technologies including incineration, gasification, pyrolysis and hydrothermal carbonization, can be used to convert biological waste into useful products (Ghanim et al., 2017b). The current trademark of fertilizing products from thermochemical treatment of sludge is STRUBIAS (Struvite, Biochar, Ash), products accepted on EU market (Gianico et al., 2021).

Incineration (combustion) reduces the volume of waste and its level of dangerousness. It concentrates minerals and destroys potentially harmful substances. Incineration can also offer the possibility of recovering the heat energy and minerals of waste by accumulation in

ash (Babcock & Willcox Vølund, 2012; Carlos Escobar Palacio et al., 2019). From the mineralization point, incineration is considered as the effective way to reduce mass and volume, disintegrate organic matter, and concentrate phosphorus and microelements in the ash, thus with possibility of further purification in a form of struvite (Egle et al., 2016). Kasina et al (2019) characterized sewage sludge ash generated from wastewater treatment and found an average of 17 wt% of P_2O_5 together with high concentration of microelements and trace metals. Furthermore, the main form was iron (III) phosphate in fly ash and apatite in air pollution residues (Kasina et al., 2019). Nevertheless, European Environmental Agency has reported air pollution associated with incineration of industrial waste and sewage sludge. Greenhouse gases (NOx, and CO_2) are emitted, together with volatile toxic heavy metals including mercury (Hg) and lead (Pb) (Rismiati, 2016). The struvite precipitation from ash is done by P species extraction, heavy metal removal (if needed for product quality) followed by struvite precipitation (Xu et al., 2012). Most of the P in dairy sludge ash is found in the $NaHCO_3$ extract (35%). The rest consists of H_2O (18%), NaOH (10%), and HCl (8%) fractions, with the residual P up to 29% (Ajiboye et al., 2007). The latter value of residual P in sequential extraction is high and can be improved by waste treatment technologies in optimum conditions for further P reclamation and struvite production. According to the used process of sludge generation, the examples of P recovery from ash through precipitation include RecoPhos and SESAL-Phos.

RecoPhos proceeds with P dissolution using phosphoric acid followed by precipitation. It adopts the industrial production of triple superphosphate by use sewage sludge ash as phosphate rock substitute (Weigand et al., 2013a). The addition of phosphoric acid transforms mineral phosphate rock under a generalized formula of $Ca_4Mg_5(PO_4)_6$ to soluble Calcium hydrogen phosphate ($Ca(H_2PO_4)_2$) and Magnesium hydrogen phosphate ($Mg(H_2PO_4)_2$). This process remains unknown in regards of dairy sludge. On the other side of ***SESAL-Phos***, the process is more specific for aluminum based sludge ash. In the first step, the Ca-P and Al-P are

dissolved under hydrochloric acid conditions. The dissolved P is precipitated as Ca-P at pH>13, thus leaving aluminum in supernatant (Petzet et al., 2011). The summary of RecoPhos and SESAL-Phos is presented on Figure 6

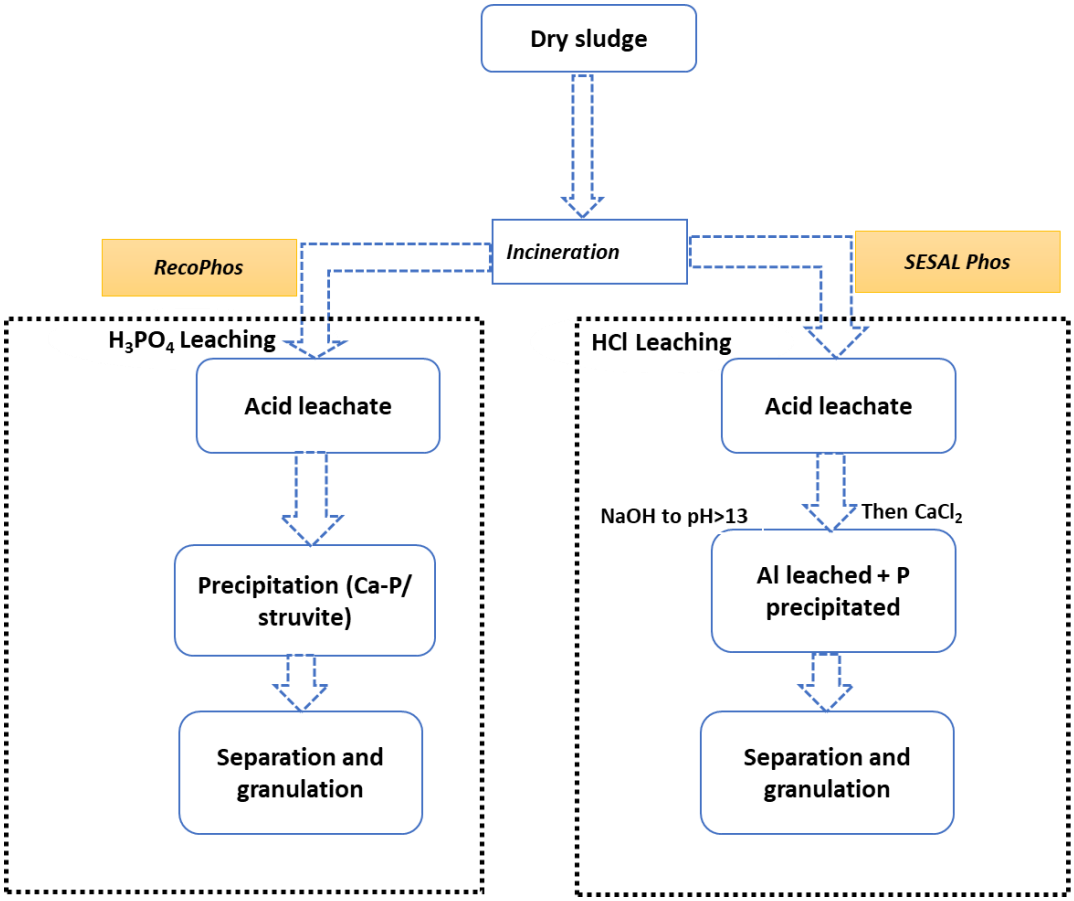

Figure 6. Summary of RecoPhos and SESAL-Phos process of P recovery from ash

Gasification is used to convert solid materials such as coal, coke, biomass and solid waste into a gas, mainly CO, H_2 and CH_4 (Taupe et al., 2016; Xue et al., 2014). It is a thermal process conducted at high temperature (500-1000°C) in presence of limited oxygen for partial oxidation of organic matter (Moharir et al., 2019). In addition to produced synthesis gas mixture (syngas), a liquid fraction of hydrocarbons mixture namely known as tar, and a solid residue known as gasification ash containing minerals were reported as byproducts of organic wastes gasification (Moharir et al., 2019). The derived ash is rich in P and minerals where 20.6% P_2O_5 was reported in previous works (Werle and Sobek, 2019). The species of P in

gasification ash were reported to depend on process conditions where high temperature (>700°C) favors apatite (Müller-Stöver et al., 2018). Furthermore, the feedstock mineral composition determines the P species in solid fraction of gasification products. Gorazda et al. found that phosphate salts of iron (III), calcium and aluminum were the main P species in sludge gasification ash (Gorazda et al., 2018). These findings follow the chemical precipitation process used in municipal wastewater treatment by addition of their coagulants salts (Ojo and Ifelebuegu, 2019). To recover phosphorus by precipitation coupled to gasification process, Siciliano et al. used supercritical water gasification at lower temperature of 450°C and 250 bar pressure. In their work, phosphorus was recovered by precipitation of K-struvite from liquid phase using $KHCO_3$ at pH 10 (Siciliano et al., 2018). In terms of circular economy, gasification score comes from its ability of biofuel production (CH_4) from bio-wastes and the ash used as efficient phosphorus and microelement source in soil fertilizer (Li et al., 2017; Werle and Sobek, 2019). Further P purification in struvite form can be undertaken from the ash since 60-70 percent and more than 95 percent of P from low temperature (500-700°C) gasification ash can be extracted in alkaline and acidic solutions, respectively (Gorazda et al., 2018). Nevertheless, the use of gasification as a tool of P recycling would be discouraging due to high temperature requirement and heavy aromatic tar produced as undesired by-product (Sikarwar et al., 2016).

Pyrolysis is thermal treatment done in the absence of oxygen in closed system and produces pyrolytic-oil, gas and char/biochar (Czajczyńska et al., 2017). The char was defined as a product of decomposition of organic natural or synthetic material by dry pyrolysis (Libra et al., 2011). Low-temperature pyrolysis (<700°C) and long residence time, converting biomass into biochar, involves three core steps: 1) initial volatiles emission; 2) primary biochar formation; and 3) chemical rearrangement to final solid biochar formation (Demirbas, 2004). By such processes, P undergoes transformation and rearrangement into new forms (Sun et al.,

2018). Robinson et al. conducted pyrolysis of bio-waste with aim of P transformation. In raw wastes, the P forms were organic species such as phytic acids, dieters and ATP and inorganic P such as hydroxyapatite. The pyrolysis conducted at 400-600°C resulted in P rich biochar with high content in hydroxyapatite, iron phosphate, and magnesium pyrophosphate (Robinson et al., 2018). Under a certain conditions during a pyrolysis a biochar can be obtained which has significant potential as a tool for climate change mitigation when applied to soil, and it can increase stable soil carbon stocks and increase soil carbon sequestration, while also decreasing atmospheric CO_2 concentrations (Kwapinski et al., 2010). The produced P forms in biochar can be extracted by acidic solution for further P purification into struvite (Sun et al., 2018). Nevertheless, aside the advantage of biochar, the pyrolytic oil contains high aromatic hydrocarbons making it hazardous to environment (Silva et al., 2012). In addition, pyrolysis process conditions involves high temperature that can be beyond 700 ^{O}C thus high energy requirement (Oladejo et al., 2019).

Hydrothermal carbonization **(HTC)** is a process of heating wet biomass together with water at a temperature between 180°C and 250°C under an autogenic pressure vessel for up to several hours (Atallah et al., 2019). The product is hydrochar (HC) composed by a high fraction of aliphatic organic compounds and makes it different from pyrolysis product (char) due to its high aromaticity (Wiedner et al., 2013). The investigation of HTC process conditions extended to temperature higher than 250°C suggested the decrease of organic carbon in aqueous phase thus can be a tool of mineralization of organic wastes (Becker et al., 2014). In addition, acidic pH demonstrated effect of decreasing the HC yield, thus can be a good condition for P dissolution to aqueous phase for prompt recovery by struvite precipitation (Ghanim et al., 2017b). Furthermore, Zhang et al. studied HTC optimum factors for organic P dissolution using swine manure digestate in order to crystallize it into struvite. In their optimization process, volume of hydrochloric acid, hydrogen peroxide, residence time and temperature played a

major role in P dissolution in liquor followed by struvite precipitation (Zhang et al., 2020). In their findings, 88.2 percent of P was dissolved and purified by struvite precipitation which makes a prospect of HTC process for P dissolution followed by struvite precipitation from organic wastes (Zhang et al., 2020).

Besides of process conditions, the portioning of P in HTC products depend on presence of multivalent metals such as calcium, iron, and aluminum that precipitate mineralized P in hydrochar in alkaline pH conditions, otherwise the high fraction of P can be found in liquor (Ghanim et al., 2018). Moreover, mineral portioning can be assessed as a fraction of feed concentration that is dissolved in water phase to assess the dissolution process during HTC (Azzaz et al., 2020). In contrast, immobilization of minerals in hydrochar is explained by concentration partition in liquid and solid phase (Zheng et al., 2020). Dai et al. found that P concentration in cow manure increased by 20% after HTC (Dai et al., 2015). Heilmann et al. found high portion of P in hydrochar of cattle manure following the high level of multivalent metals (Heilmann et al., 2014). These were precursors of P precipitation at pH 9 and are concentrated in hydrochar. Similar results were found by the work of Atallah et al. which, based on ultimate analysis of HTC products, indicates the concentration of phosphorus and multivalent metals in hydrochar. Whereas, alkali metals had their high concentration in the liquor, thus rather dissolved (Atallah et al., 2019). The P salts that are precipitated are calcium phosphates following the recovery of 99% and 98% for Ca and P, respectively, in acid extract. Other possible forms in lower amount are iron phosphates (Heilmann et al., 2014).

Zhao et al found that 79-81% of HC phosphorus was apatite form (a residual form found by $0.5g \cdot 25mL^{-1}$ of hydrochar/NaOH 1M extraction) and underlined that other metal P salts are formed when calcium is exhausted (Zhao et al., 2018). The apatite P form is less efficiently available to plant in soil with alkaline pH (Yadav et al., 2017). Fortunately, a high fraction of it can be leached in acidic solution for further reclamation and purification into struvite as a

better quality fertilizer. In that case, up to 98% of P can be extracted by 4M HCl in a ratio of $10g \cdot 220mL^{-1}$ w/w of hydrochar to acid. In addition to that, 92.5% of P of hydrochar was reclaimed through H_2SO_4 1.5M leaching of aqueous mixture ($10g \cdot 100mL^{-1}$ w/V of water) by acid titration until the pH 2 is reached (Zhao et al., 2018). Thus struvite can be produced from hydrochar leachate by wet chemical extraction process.

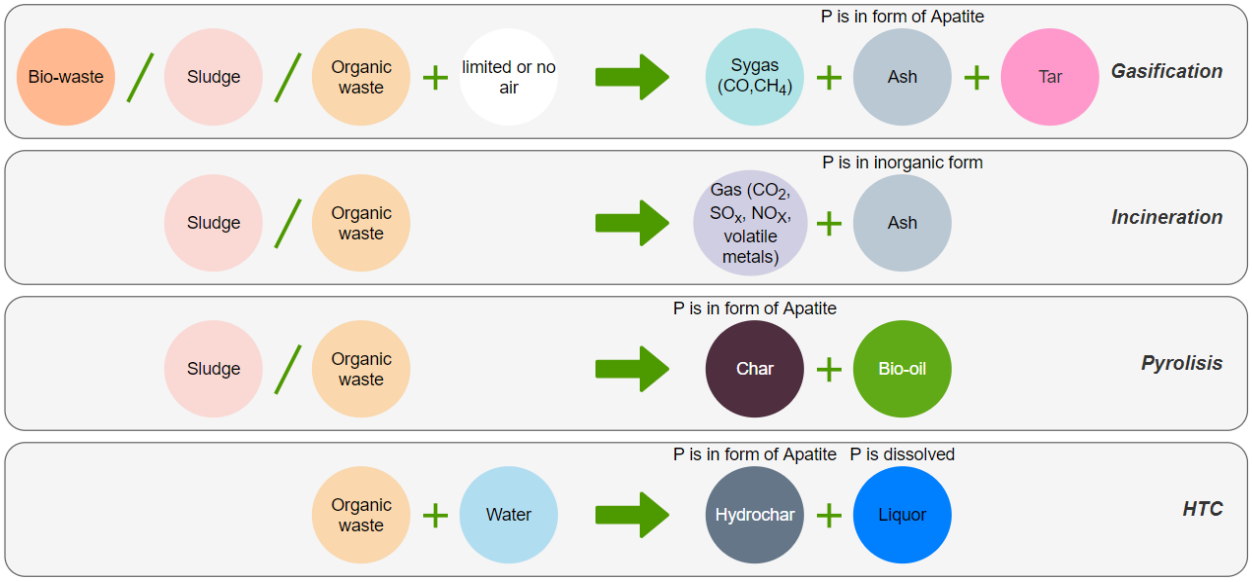

Figure 7: Summary of thermochemical processes: Substrate and main products.

As general view on thermochemical process of wastewater derived organic waste and their products, HTC present an advantage over incineration in terms of greenhouse gases release, volatile micropollutants. The thermochemical process products are summarized on Figure 7. The HTC can be used as a tool of P immobilization in hydrochar, the product that can be applied as biosolid fertilizer (Gianico et al., 2021). The remaining nutrients in HTC liquid phase can be purified by struvite precipitation. Furthermore, in any aspect of the organic and effluent wastes, or their treatment residues, the remaining major challenge for their use as raw material in struvite production is the complexity of matrix mainly underlining interfering elements that becomes a demanding factor in salts dosage for struvite precipitation.

2.3. Full scale struvite production technologies

The existing technologies for struvite precipitation from various wastes base on the reaction of precursors and the nutrients rich-solution.

Table 3. Struvite production technologies and involved processes

Matrix	Technology	Process	Reference
Aqueous phase	AirPrex®	Precipitation	(Hermann, 2009)
	Ostara Pearl	Crystallization	(Ali Adnan, 2002)
	DHV Crystalactor	Crystallization	(Britton et al., 2007)
	P-RoC®	crystallization	(Berg et al., 2007)
Sludge	Gifhorn process	wet-chemical leaching and precipitation	(Muller et al., 2007)
	Stuttgart process	wet-chemical leaching and precipitation	(Ohtake and Tsuneda, 2018)
	PHOXNAN	Wet oxidation	(Blöcher et al., 2012)
Ash	PASCH	acidic wet-chemical leaching and precipitation	(Petzet et al., 2012)
	LEACHPHOS®	acidic wet-chemical, leaching	(Egle et al., 2016)
	RecoPhos®	acidic wet-chemical extraction and precipitation	(Weigand et al., 2013b)
	Fertilizer industry	Acidic wet-chemical, extraction	(Kim ten Wolde, 2013)

They are used to produce struvite at industrial scale using various range of P influent concentrations. Processes of P recovery as struvite from wastewater with lower range of concentration (<500 $mgkg^{-1}$) include PHOSPHAQ, Phosnix, NuReSys, Airprex, and Crystalactor (Desmidt et al., 2015). On the other hand, the higher influent P concentration (> 500 $mg.kg^{-1}$) uses ANPHOS, Scaborne, and Ostara Pearl. The later can recover the P from influent with quite high P concentration (near 1000 $mg.kg^{-1}$). Furthermore, sewage sludge and their ashes involves the combination of chemical extraction/leaching processes followed by precipitation. The examples of some processes are presented in Table 3.

2.4. Review summary

The main preliminary stages of P recovery from wastewater usually consists of its accumulation into a sludge either by activated sludge method, enhanced biological P removal or physicochemical methods. The activated sludge method is mainly a biological process where microorganisms play a major role in all processes. Among those biological processes, the

enhanced biological phosphorus removal (EBPR) is used particularly with aim of phosphorus recovery by using polyphosphate accumulating organisms (PAOs). The P rich biomass thereby obtained can contain nearly 20% of polyphosphates. In terms of physicochemical process, the most famous process of P recovery from wastewater into a sludge is chemical precipitation using iron and alum salts such as ferric chloride and sulfate or aluminum chloride or sulfate, and bases mainly lime.

The widely applied method of coupling sludge treatment and struvite precipitation is anaerobic digestion followed by dewatering where the permeate is flowed to the reactor for struvite crystallization upon proper pH adjustment and magnesium salts dosage. The coupled struvite precipitation is applied by some of the already implemented technologies such as Phosphogreen and Airprex.

In either step of P accumulation to sludge and anaerobic digestions for further struvite precipitation, the challenges are numerous and need to be settled out through the researches. The major challenge in EBPR process is long time required for efficient P removal. The chemical precipitation with coagulants is faster with adverse effect of enormous sludge generation. However, at least one of them has to be applied as preliminary stage of P recovery from wastewater and further improvement is needed for sludge treatment and permeate P purification to struvite.

The anaerobic digestion with microbial activities takes long time which can vary from 2 to several days. Considering the amount of sludge generated (8.7 million in EU in 2020), such retention time is too long and require complex installations for effective sludge treatment for further steps of P recovery by struvite precipitation from P permeate. Additionally, despite of their worldwide production, the involvement of chemically produced sludge has limited valorization study. This makes a gap in nutrient recycling. Compared to amount of iron and

alum salts loaded in sludge production, there are almost no information of their recycling along with phosphorus recovery.

The Ostara Pearl® fluidized bed reactors with proper magnesium and sodium hydroxide satisfy most of the struvite production model for the EBPR sludge liquor. In contrast, the HTC liquor produced from chemically accumulated sludge needs a new model considering prior treatment to remove iron or minimize its levels. The chemical extraction using proper solvents is to be assessed. The sulfides and oxalates are potential precipitating agents able to remove maximum of Fe. Then the supernatant can be used for further steps in the similar process to EBPR-HTC liquor. For the ash from EBPR sludge, wet-chemical extraction and leaching can be applied followed by struvite precipitation using fertilizer industry process (Kim ten Wolde, 2013). In contrast, for chemically produced sludge, the ash contains high level of iron and heavy metals. Thus the PASCH approach uses solvent extraction for leaching and heavy metal removal followed by precipitation of supernatant P to struvite. Considering all involved processes to be applied on the dairy effluent up to struvite precipitation, the summary of scenarios is presented on Figure 8.

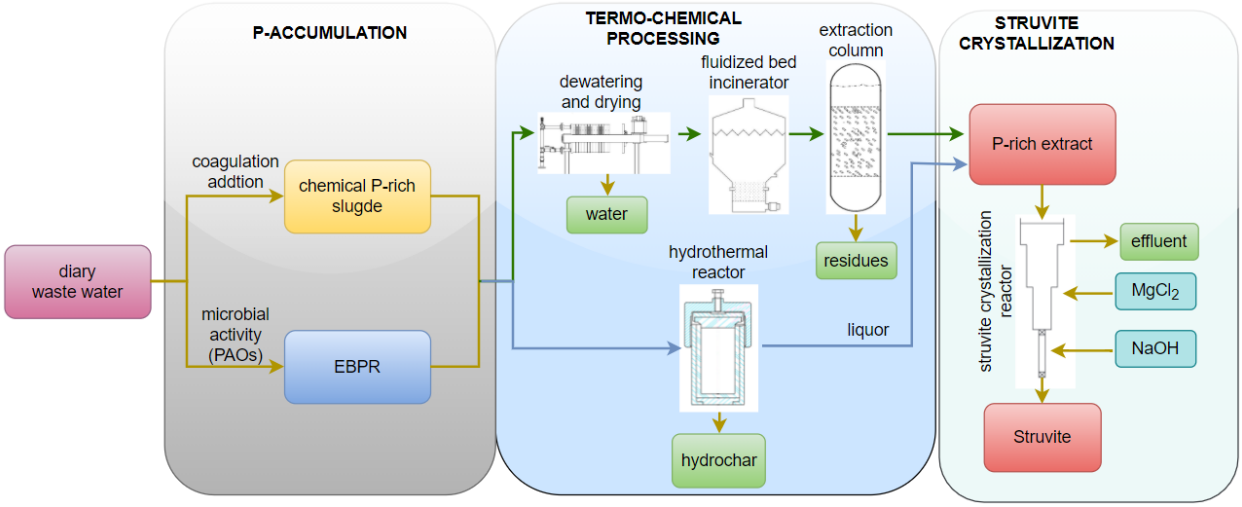

Figure 8. Dairy waste P accumulation and mineralization followed by struvite precipitation

Phosphorus recovery from dairy organic and effluent wastes by struvite precipitation can be achieved after adequate mineralization, and concentration in aqueous solution. Since further objective is to recover phosphorus in struvite form from organic wastes as well as their treatment residues, thermochemical treatment and dissolution are involved as critical stages in organic P mineralization and rendering it reactive for precipitation process. In consideration of aforementioned thermochemical process, three scenarios are proposed for struvite precipitation from dairy organic wastes:

(i) Hydrothermal treatment where moist P rich sludge is treated under acidic conditions (pH < 2) during several hours. In this process, a fraction of P is accumulated in hydrochar applicable in agriculture and the other P is dissolved to liquor as phosphate under acidic aqueous phase followed by precipitation.

(ii) The hydrothermal P immobilization in hydrochar under alkaline (pH nearly 9) followed by either its reclamation into an acidic solution or hydrochar combustion to ash followed by P extraction and precipitation. Nevertheless, this can have no significant economic importance since hydrochar can be applied as a sterile biosolid fertilizer.

(iii) Application of more steps including dairy sludge dewatering, drying, combustion to ash, P leaching, and struvite precipitation.

In case the dissolution is favored, HTC can suffice where P is immobilized in hydrochar (a biosolid fertilizer accepted on EU market under EU regulation 2019/1009 and dissolved P in liquor is purified by struvite precipitation. Thermal technologies of incineration concentrate minerals in ash which is used as raw material in P recovery as struvite. However, ash production is accompanied with emission of micropollutants such as volatile heavy metals as well as organic micropollutants.

II. EXPERIMENTAL PART

1. Aim and scope of the research

The research goal of this work was the determination of optimal process conditions for P recovery from processed dairy wastes through struvite precipitation and evaluation of the product quality as fertilizer.

The utility goal is the mitigation of the environmental impact of P loss through dairy effluents, valorisation of the dairy wastes, especially the sludge derived from wastewater treatment, into commercially acceptable fertilizing products through their thermo-processing, nutrients recovery, nutrients recycling, and fertilizer application.

Hypotheses of the work are pointed out as follow:

- Struvite precipitation from dairy wastes is an effective method for P recovery in a form of high quality fertilizer.
- Dairy wastes resources valorisation need coupling multiple technologies of which thermochemical processing of dairy sludge combined with struvite precipitation represent the best option for P recovery into commercially valuable fertilizing products.

The achievement of research goals was done through the following steps:

- Reviewing literature and documentation on P loss to environment, P reservoirs, P mining and its destination, wastewater P recovery and derived sludge, their treatment and combined techniques of struvite precipitation at experimental and full scale levels.
- Chemical characterization of the cheese production wastewater, and the sludge from dairy wastewater treatment plant.
- Investigation and optimization of effect of potential interfering foreign ions during struvite precipitation.
- Thermochemical treatment of dairy sludge through hydrothermal carbonization and P recovery as struvite from HTC process water.

- Studying the chemically produced sludge with ferric coagulants for iron recycling along with P purification to struvite.
- Identification of the proper initial process conditions of pH and salts dosage in form of mixing molar ratio (Ca:P, Mg:P, NH_4^+:P), for struvite precipitation through experimental design and multiple optimization models.
- Evaluation of natural clinoptilolite zeolitic material as additives to combine struvite precipitation and ammonium sorption.
- Identification of physico-chemical interactions and P speciation through stoichiometry study with accountability of dynamic equilibria in the systems
- Evaluation of the quality of recovered product as fertilizer using kinetic models of nutrients release through the in-vitro assays, and nutrients use efficiencies through in-vivo assays.
- Establishment of economic effective model at full scale for valorisation of chemically produced sludge for both P recovery and iron recycling

2. Methodology

2.1. Chemicals and apparatus

Chemicals	Supplier
Ammonium chloride (NH_4Cl)*	Avantor Performance Materials Poland S.A
Boric Acid	Avantor Performance Materials Poland S.A
Calcium chloride anhydrous ($CaCl_2$)*	Avantor Performance Materials Poland S.A
Deionized water	In-house made
Di-potassium phosphate (K_2HPO_4)*	Avantor Performance Materials Poland S.A
Hydrochloric acid (HCl, 36-38 %)	Avantor Performance Materials Poland S.A
Hydrochloric acid analytical weigh for 0.1N	Avantor Performance Materials Poland S.A
Hydrogen peroxide (H_2O_2, 30%)*	Avantor Performance Materials Poland S.A
Magnesium chloride hexahydrate ($MgCl_2$ $6H_2O$)*	Avantor Performance Materials Poland S.A
Magnesium sulfate heptahydrate a.g ($MgSO_4$ $7H_2O$)	Avantor Performance Materials Poland S.A

Mixed indicator for ammonium titration (green bromocresol and methyl red)	Avantor Performance Materials Poland S.A
Mixed Kjeldhal catalyst (K_2SO4, CuSO4, Se, FeSO4)	Avantor Performance Materials Poland S.A
Multi-elements ICP standard	Avantor Performance Materials Poland S.A
Nitric acid (HNO_3, 65%)*	Avantor Performance Materials Poland S.A
Oxalic acid ($H_2C_2O_4$)	Avantor Performance Materials Poland S.A
Sodium hydroxide (NaOH)*	Avantor Performance Materials Poland S.A
Sodium sufide (Na_2S)	Avantor Performance Materials Poland S.A
Sulphuric acid (H_2SO_4, >95%)*	Avantor Performance Materials Poland S.A
Equipment/Material/Instrument	**Specification**
Batch reactor beaker	Borosilicate glass (0.25,5,1 and 5L)
Batch reactor stirrer	CAT-100, Germany
Batch reactor water bath	PLWC 35 S, Poland
Weighing Balances	Technical (up to 2100g) and Electronic (210g max)
Cellulose syringe filters	MCE (0.22 µm, Whatman),
Hydrogen electrode	LE438 (METTLER TOLEDO)
Holes trial tray plate pot	32 holes, Walmat, USA
ICP- OES	Vista MPX, Varian
Laser diffraction particle size analyser	LS I3 320, BECKMAN COULTER
Microwave digestion system	(Start D, Milestone)
Multifunction meter	CX-705 Elemtron, Poland
pH meter	FiveEasy Plus FEP20
High pressure PARR reactor	7.5 L PARR 4545 reactor
Scanning electron microscopy	SEM/Xe-PFIB Microscope FEI Helios, with EDS detector
Sieve shakers	Gilson 8in Vibratory Sieve Shaker
Stirrer	CAT-100, Germany
Test sieve	Retsch-Allee 1-5, GmbH, Germany
Water bath	PLWC 35S, Poland,
Wattman filter papers	Avantor Performance Materials Poland S.A
Water deionizer	Millipore Simplicity UV,Merck, Germany
X-ray diffraction (XRD) spectrometer	Rigaku MiniFlex diffractometer,Japan
Batch reactor beaker	Borosilicate glass (0.25,0.5, 1,2 and 5L)

2.2. Physico-chemical analysis

2.2.1. Liquid samples analysis

The pH measurements were made in accordance with the standard PN- 90/C- 045400/01, using pH-meter with hydrogen electrode. In summary, the pH meter was calibrated with buffer solutions of pH 4, 7, and 9. The amount of 100 cm^3 of sample was put in 100 cm^3 high density polyethylene bottle and measured directly with hydrogen electrode after proper cleaning with de-ionized water.

Multi-elements analysis was done in accordance with the USEPA method 3051 and by using inductively coupled plasma optical emission spectrometer with vertical plasma ICP-OES (Vista MPX, Varian). The value of the concentration was measured in the range of the calibration curve 0-1000 $mg \cdot dm^{-3}$ for P, alkaline and alkaline earth elements, while the transition metals were calibrated to 0-100 $mg \cdot dm^{-3}$ with a detection limit of 50 $\mu g \cdot dm^{-3}$ for P and up 300 $\mu g \cdot dm^{-3}$ in general for the other elements. Multi-elements Standard for ICP (Fluka) solution with a concentration of 1000 $mg \cdot dm^{-3}$ was used to prepare the standard curve.

Nitrogen and ammonium nitrogen were analyzed in accordance with the standard EPA method 350.1 with modification by Kjeldhal digestion and distillation followed by titration of distilled ammonium nitrogen. In this case for total Kjeldhal nitrogen, the aliquot of liquid (0.2-1g) was measured with electronic balance and mixed with 2g of mixt catalyst, and 10 cm^3 of concentrated surfuric acid, followed by digestion using Kjeldhal digester until the total organic matter is destroyed (digestate usually turned to greenish color). This confirms the conversion of all protein nitrogen, and amines nitrogen to ammonium sulfate. The sodium hydroxide 30% by mass is added in the digestion tube after cooling and distilled with Kjeldhal ammonium distiller. For ammonium analysis only, an aliquot weight of sample was distilled in alkaline conditions, collected in boric acid containing mixed indicator, and titrated with 0.1N HCl.

Total carbon content were analyzed using macro combustion analyzer (Vario Macro Cube elementary analyzer GmbH, made in Germany) for whey samples and HTC liquor.

2.2.2. Solid samples analysis

The solid samples were the dairy sludge, and the hydrochar and ash derived from HTC and incineration process, and the obtained precipitation products. For all solid samples, the analysis parameters were metals and non-metals. The multi-elemental analysis, total carbon, and nitrogen analyses were conducted as described in section 2.2.1. Additional analysis parameters were analyzed on precipitation products. These include microscopic and spectroscopic analysis using nondestructive methods:

Phases analysis was conducted with X-ray diffraction (XRD) spectroscopy that consisted for 2Θ from 10 to 50° with 0.01° steps and 0.50 speeds using the Rigaku MiniFlex diffractometer (Japan, Tokyo) with copper anticathode (λ = 1.54 Å) following standard method EN-13925. The diffraction database was used for pattern phases identification.

Morphology and elemental mapping were analyzed with the scanning electron microscopy SEM/Xe-PFIB (Microscope FEI Helios) following standard method ISO 22309:2011. The microscope was equipped with an Energy-Dispersive X-ray Spectroscopy (EDS) with the Silicon Drift Detector, which enables precise analysis of the elemental composition, with the function of mapping the distribution of elements in the imaged micro-areas.

Particle size analysis was conducted with a laser diffraction particle size analyzer LS I3 320 (BECKMAN COULTER) equipped with a dry powder sample system, sonication control unit, and personal computer.

2.3. Materials and their preparation

2.3.1. Cheese wastewater preparation

Since chemical precipitation involves only dissolved inorganic P, all P forms in sample were transformed into inorganic form where, to dissolve organic fraction of P. The wastewater was electrochemically hydrolyzed under reflux with hydrogen peroxide and hydrochloric acid to have 3% of pure H_2O_2 and 10% of concentrated HCl [44].

2.3.2. Sludge processing and liquor preparation

a. Hydrothermal carbonization of sludge

Dairy sludge was collected from the Arrabawn Company near Limerick (Ireland) and stored in a refrigerator at 4 °C. The hydrothermal carbonization was performed using the 7.5 L PARR 4545 reactor. The sludge water content was 86% and a solution of 1% H_2SO_4 was added to reach a pH of 2.2 as initial conditions. The reaction temperature was controlled and the time needed by the heater to reach the set reaction temperature was 3h. At that point, the stirrer was initiated at 25 rpm, and the temperature and pressure were monitored throughout the residence time. After 2h, the reaction was terminated, and the reactor was left to cool down at ambient temperature, whereas the gases were released into the fume hood. In further steps, after cooling, the products were retrieved and the solid hydrochar was separated from the liquid portion through filtration. The solid fraction was dried in the oven at 105°C for 24h and was subject of study as STRUBIAS material for agricultural application, the work previously co-published by (Shi et al., 2022).

b. Incinerated sludge ash preparation

The sludge incineration was done as per directive 2000/76/EC which aims at mitigating the pollution by reducing emissions into air, soil, surface water and groundwater without endangering human health and environment from incineration or co-incineration of wastes. Under these guidelines, the combustion temperature is in the range of 850-1100 °C (Bontoux, 1999; European commission, 2000).

In summary, the wet sludge was placed in a tray and dried in a fume hood for 7-10 days. After drying was complete, sludge clumps were then ground to fine powder using a Retsch GM 200 mixer grinder for size reduction. Sludge fines hence obtained were then weighed in alumina crucibles and placed in the muffle furnace (30-3000°C) for a specified time and temperature. The parameters for incineration are shown in Table 4.

Table 4. Temperature settings during dairy sludge incineration

Temperature (°C)	Time (hours)	Objectives
0-250	1	Remove volatile matters
250-850	1	Heating up to set temperature
850	1	Maintaining the temperature

c. Magnesite preparation

Magnesite is a mineral of magnesium carbonate with a chemical composition of $MgCO_3$. It is named after the abundance of magnesium in its composition. Magnesite ordinarily shapes amid the change of magnesium-rich rocks or carbonate rocks by geochemical process such as metamorphism or chemical weathering. The magnesite was collected from Kopalnia Wiry Sp. z o. o., based in the village of Wirki, Poland. The rock was ground and sieved with 0.4 mm test sieve and mixed with the dairy sludge ash without further treatment for further acidic leaching and struvite precipitation from the ash.

d. Zeolitic material preparation

These are crystalline materials formed during tectonic movement as basaltic and volcanic rocks. They are characterized with beautiful, very well-formed, and curious crystals with little utility owing to the impossibility of obtaining commercially feasible deposits (Roque-Malherbe, 2001). Nevertheless, these materials were appraised by several researches for sorption capacities of cations. The general chemical formula of zeolites is $M_{x/n}[Al_xSi_yO_{2(x+y)}]\cdot pH_2O$ where M is (Na, K, Li) and/or (Ca, Mg, Ba, Sr), n is cation charge; y/x = 1–6, p/x = 1–4 (Wang and Peng, 2010). One of the reported cation is ammonium, which

clinoptilolite has high sorption capacity (Tang et al., 2020). The natural zeolite was characterized for sorption properties as per referred work (Kotoulas et al., 2019). The zeolitic material was obtained from a mineral deposit located in the Nižný Hrabovec, Slovakia. The material consists of 74% clinoptilolite, 11% cristobalite, 6% plagioclase, 4% illite and smectite, 3% tridymite, 1% kaolinite and 1% quartz. Prior to experiments, the zeolite was sieved to granulometric size of 0.16–0.25 mm and pre-treated to obtain homoionic Mg-form. It was done in three cycles of contact with 3% $MgCl_2$ solution for an overnight, followed by washing with deionized water. Then the material was dried at 105°C referring to existing works of (An et al., 2016).

2.3.3. Phosphorus extraction

(a) P extraction and iron removal from HTC liquor

To decrease the level of iron in the liquor sample, oxalic acid was studied for P extraction and iron removal from HTC liquor using a mimic solution (Elomaa et al., 2019). Different concentrations (0.03, 0.061, 0.125, 0.1875, 0.25, and 0.375 $mol \cdot dm^{-3}$) of oxalic acid were evaluated. For the experiments where the pH failed to reach pH < 2 by the addition of extracting acid, the hydrochloric acid 5M was added drop wise until the pH < 2. In fact, oxalic acid is a diprotic acid with two different acidity constants (pKa_1 = 1.27 and pKa_2 = 4.66) (Gelb, 1971). Below pH 2, this compound is in molecular and mono-protic ionic form, with the ability to form less soluble salts of iron (II) and calcium (II) oxalates. As the pH increases, the ionic form of the acid becomes more predominant and decreases its removal by chelating the metal ions in the supernatant. In addition to iron removal, the use of oxalic acid as an extracting solution removes calcium to a high extent. Despite the enhanced advantage of struvite crystallization, calcium is an important plant macronutrient and is worth keeping in the struvite product. Therefore, sodium sulphide was assessed for selective iron removal using a similar range of concentrations. The artificial solution mimicking HTC liquor was prepared in a 150 cm^3 borosilicate glass beaker together with Na_2S concentration under a fume hood. Four millilitres

of 5M HCl solution were added per 100 cm^3 sample volume to keep the pH less 2.5. The pH adjustment was to favor the dissolution of P and to avoid the precipitation of acidic calcium phosphate probable in the pH range from 4 to 6 (Mekmene et al., 2009). The mixture was capped with parafilm paper and shaken at 20 rpm for 30 min, and settled for 2h for separation. The supernatant was filtered using Wattman filter papers followed by elemental analysis.

(b) Sludge ash wet chemical extraction and precipitation

The ash and magnesite were mixed with the Mg:P molar ratio of 1.73, a ratio that was determined experimentally. The extraction process used the method of RecoPhos technology with some modification. *RecoPhos* proceeds with P dissolution using phosphoric acid followed by precipitation. It adopts the industrial production of triple superphosphate by use sewage sludge ash as phosphate rock substitute (Weigand et al., 2013a). In this work, the addition of phosphoric acid had a double advantage including adjusting mole ratios of struvite inhibitors, i.e (Ca + Fe): P to small value, and transform mineral phosphate rock under a generalized formula of $Ca_4Mg_5(PO_4)_6$ to soluble Calcium hydrogen phosphate ($Ca(H_2PO_4)_2$) and Magnesium hydrogen phosphate ($Mg(H_2PO_4)_2$). The additional acid was needed for efficient dissolution of iron based P rich ash.

To increase the extraction efficiency, hydrochloric acid was added in the mixture as additional extracting reagents. Thus phosphoric acid served as both (Ca+Fe):P mole ratio upgrade and as extracting acid. Since the struvite precipitation from the ash involves wet chemical extraction, this work supplemented the dairy sludge ash with magnesite as a cost free magnesium source. The amount of 0.3g of dairy sludge ash was weighed and placed in test tube. Phosphoric acid was added to different assays with different (Ca:Fe):P mole ratios. These were 1, 0.75, 0.5, 0.25, and 0.15 of (Ca+Fe):P mole ratios. For each test tube, the magnesium source was added to a mole ratio of 1.73. Similarly, to the lower water solubility of the ash, the natural $MgCO_3$

ore is a hardly water soluble salt, but soluble in strong acidic conditions. The magnesite is dissolved by reaction with acid which releases carbon dioxide gas:

$$MgCO_{3\,(s)} + 2H^{+}{}_{(aq)} \rightarrow Mg^{2+}{}_{(aq)} + H_2O_{(l)} + CO_{2(g)}$$

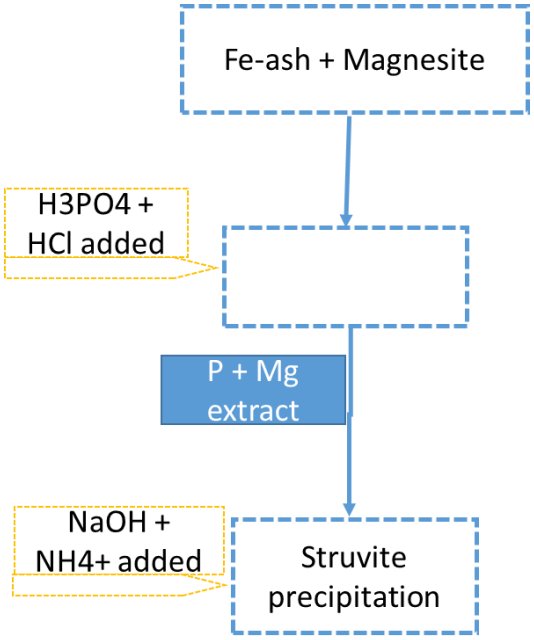

Figure 9. Steps configuration of combined wet chemical extraction and struvite precipitation

The initial volume was made to 5mL in each test tube with deionized water. The assay was repeated with addition of hydrochloric acid to 0M, 2M, and 4M concentrations with final volume of 5, 6, and 8 mL, respectively. The stepwise of wet-chemical extraction and struvite precipitation is described by the Figure 9.

2.4. Struvite precipitation experiments

The precipitation experiments were conducted in stirred batch reactors equipped with a 1L beaker, water bath, and stirrer. The stirring speed was kept at 60 rpm, for 1h, at 22°C (Shaddel et al., 2020b). The pH adjustment was done by the addition of NaOH 6M and monitored using a multifunction meter. The molar ratio of Ca, Mg and NH_4^+ to P were adjusted by adding the pre-calculated quantity of their solution to samples to comply with molar ratio in design of experiments. In this case, ammonium chloride (4 mol·kg^{-1}), dipotassium hydrogen phosphate

(1 mol·kg^{-1}), calcium chloride (1 mol·kg^{-1}) and magnesium sulfate (2 mol·kg^{-1}) were used. For the processed cheese wastewater, the 250 g of sample was brought to 400 g in reactor with deionized water after all doses addition. The calculation procedures for addition of salts doses available in supplementary material *S. 1*. The experimental set up of the used stirred batch reactor system is indicated on the Figure 10.

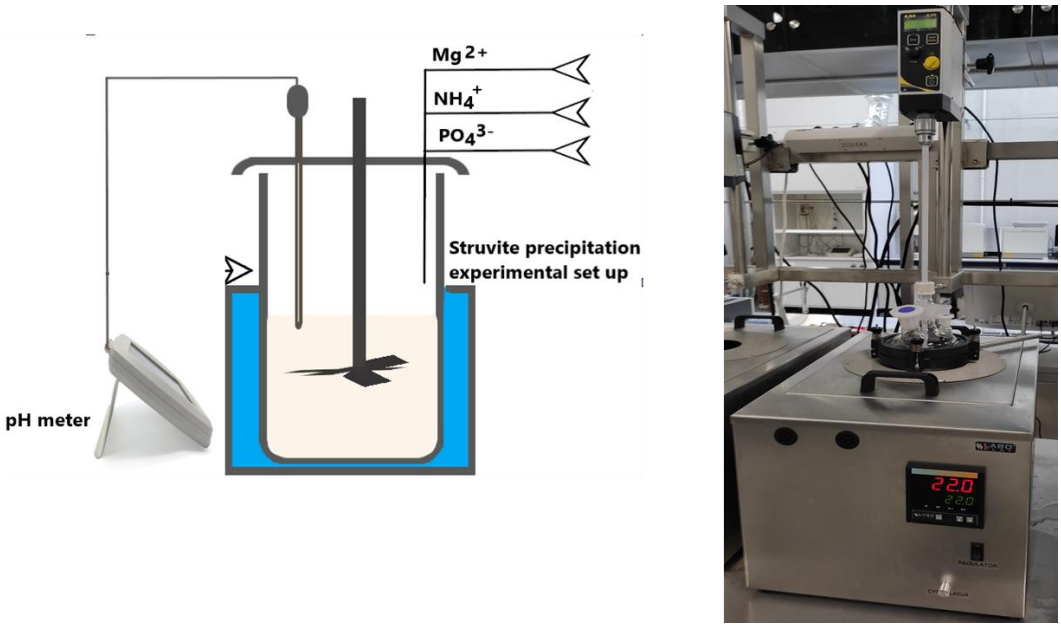

Figure 10. *The batch reactor used in experimental determination of struvite precipitation*

3. DATA ANALYSIS

3.1. Physico-chemical interactions

3.1.1. Proton transfer model

The estimation of the pH levels suitable for experimental investigation was based on sample composition and common proton transfer equilibria of solution components using their acidity constants found in other works (Barnes and Bowers, 2017; Loewenthal, R. E., 1994). The used molar fraction and proton dependent speciation model ($\alpha i = f(H^+)$) for proton acceptor species in acid base equilibria is given by *Eq. 1*

$$\alpha_i = \frac{[H^+]^{n-i} K_0 \ldots K_i}{[H^+]^{n-0} K_0 + [H^+]^{n-1} K_1 + [H^+]^{n-2} K_1 K_2 + \cdots + [H^+]^{n-n} K_1 K_2 \ldots K_n} \quad \textit{Eq. 1}$$

Based on the molar fractions values, the pH suitable for struvite lattice ions saturation was evaluated and used in experimental investigation.

3.1.2. Phosphates saturation and solution speciation

On stoichiometric point, the saturation index (*SI*) of possible P products was estimated from concentration of components in solution based on ion pairing activity products and the solubility products (*Ksp*) described in *Eq.*2

$$SI = logIAP - logKsp \quad \text{Eq. 2}$$

With *IAP*, ion activity product, estimated by $IAP = \prod_i^N a_i^{zi}$ where a_i is activity of iterative ionic species *i* in relation to concentration and activity coefficient ($a_i = C_i \Upsilon_i$). The latter is estimated by extended Debye-Hückel expression which involves ionic strength (*I*), temperature (*T*) and dielectric properties of the system (Baeza Baeza and Ramis-Ramos, 1996). The change of a component activity follows the mass balance equation. In fact, the amount of a component in a system remains constant regardless the undergone transformations (Marinoni et al., 2017). Thus, the component conservation model (*Eq. 3*) is observed for P species in the solution.

$$TOT_j = C_j + \sum_i^N v_{i,j} C_i \quad \text{Eq. 3}$$

Where TOT_j is the total molal concentration of a component *(j)* involved in reactions; C_j, the actual concentration in solution; and the sum of *N* molal concentrations (C_i) of *j* binding species with *v*, the stoichiometric coefficient that equals the number of moles of *j* present in one mole of i^{th} species. For thermodynamic dependence, the concentration was corrected to activity (a_i). The *Eq.3* for a component leads to a stoichiometric matrix of formed species and their components. The speciation takes into account the system's electro-neutrality, acid-base

equilibria, and ionic strength (Nancollas, G.H, Amjad, Z, and Koutsoukos, 1979). For the accountability of all physical chemical interactions, the visual MinteQ v3.1 served in P speciation, ion activity product (IAP) and saturation indices of sparingly soluble compounds (Warmadewanthi et al., 2021). The summary of speciation with MINTEQ V3.1 is given in Figure 11.

3.1.3. Precipitation thermodynamics

Thermodynamic parameters affecting the equilibrium were enclosed in the Gibbs energy of the precipitation spontaneity described by *Eq. 4* (Tao Zhang et al., 2010).

$$\Delta G = -2.303 \frac{RT}{n} \log(\frac{IAP}{Ksp}) \quad \text{Eq. 4}$$

Where ΔG is the the Gibbs free energy in KJ·mol^{-1} for precipitation reaction, *R* is the ideal gas constant ($R = 8.31447 \cdot 10^{-3}$ KJ·mol^{-1}K^{-1}), T is the absolute temperature (295K), *n* is the number of crystal lattice ions, *IAP* is ion activity product which is conditional solubility products ($IAP = \prod_{i=1}^{n} a_i$) and K_{sp}, solubility product; a_i is activity of lattice ion standing for $a_{NH_4^+}$, $a_{Mg^{2+}}$, $a_{PO_4^{3-}}$ for struvite. The activities are obtained from concentration of each component corrected with activity coefficient in dependence of solution ionic strength. The equilibrium is reached when $\Delta G = 0$, spontaneous for precipitation when $\Delta G < 0$, and under-saturation when $\Delta G > 0$. Considering the complexity of the feed sample, the molar balance of each lattice ion component was estimated to find the real activity obtained as dependent to fraction (α_i) of the total activity (a_T) of the component ($a_i = \alpha_i \cdot a_T$). The speciation analysis was done using MINTEQ 3.1 (Figure 11). For the status of equilibrium, the total component influent quantity was preliminary estimated to reach the minimum of P and ammonium.

3.1.4. Ammonium sorption study

Thus the discussion of the effect of zeolite on the process condition was described as extent to which struvite thermodynamic equilibrium is reached. This effect was hypothetically caused by ammonium sorption process. Therefore, the ion exchange of NH_4^+ on Mg-clinoptilolite was examined in batch mode experiments. A measured quantity of mineral (1 g) was added to 50 mL vials containing measured volume of NH_4^+ solution (40 mL), in the range of 10-500 $mg \cdot kg^{-1}$ for a contact time of 24 h to reach the sorption equilibrium. Subsequently, samples were decanted and filtered by using Whatman nylon filters with 0.45 μm of pore size. The amount (q_e) in ($meq.g^{-1}$) adsorbed was calculated in terms of initial (C_o) and equilibrium (C_e) NH_4^+ concentrations in ($mg \cdot dm^{-3}$), mass of mineral (m_z) in (g), and NH_4^+ solution volume (V) in (dm^3) as described by equation (*Eq.*5) (Choi et al., 2016).

$$q_e = \frac{(C_0 - C_e) * V}{m_z} \qquad \text{Eq. 5}$$

For this study, the single ion solution of ammonium was used to find the equilibrium parameters in batch experiments. In order to evaluate the effect of other ions on ammonium sorption, the same equilibrium experiments were conducted on multi-components aqueous solution residue from struvite precipitation with the same range of ammonium concentration. The sorption experiments were additionally done on both raw and Mg-form of zeolitic material to assess their effect on ammonium uptake. The summary of physical chemical parameters and speciation is presented on Figure 11.

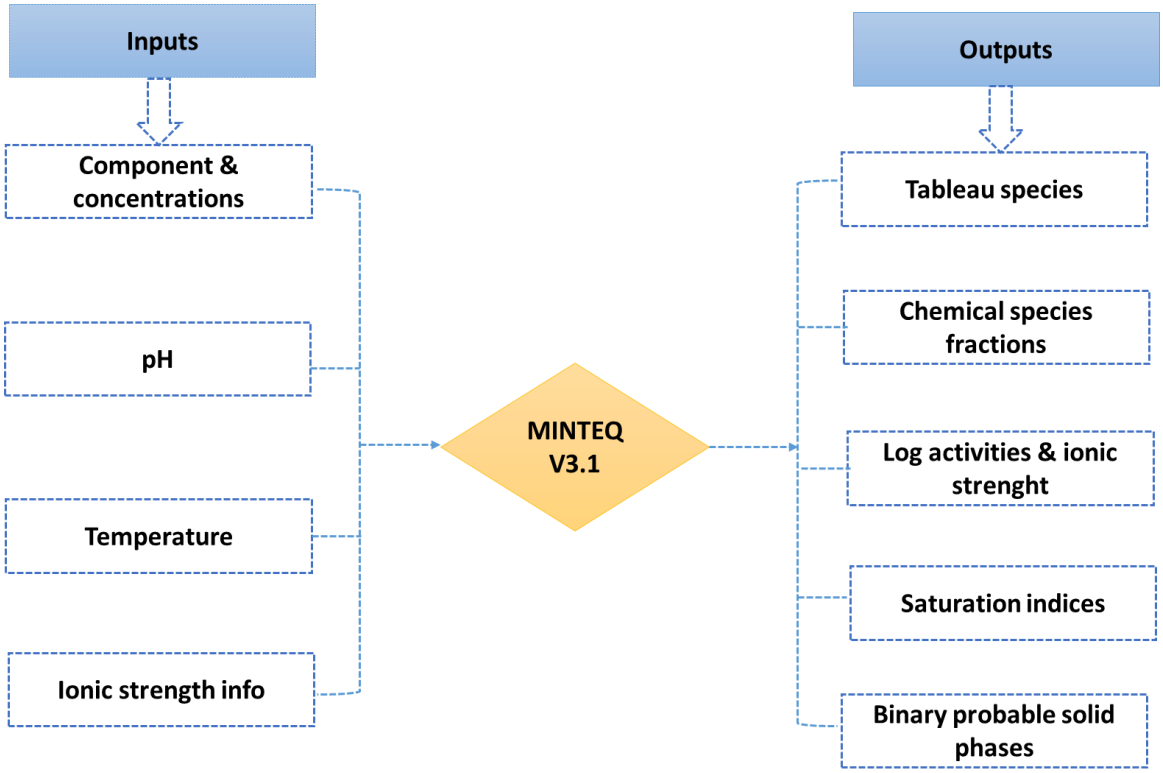

Figure 11. Flow diagram of chemical speciation in MINTEQ software

3.2. Experimental design and optimization

3.2.1. Design of experiments

Experiments were conducted in three level experimental design with four factors. The number N of experiments is generally obtained by $N = n^k$ with *n*, the number of levels (n = 3) corresponding to low, middle and high levels coded by -1; 0; and +1, respectively; *k* stands for the number of factors (*k*) corresponding to pH, Mg:P, Ca:P molar ratios and NH_4^+ doses. In this research, reduced design was adopted to Box-Behnken design to reduce the number of experiments to *Eq.6*

$$N = 2k^2 - 2k + c_p \qquad Eq.\ 6$$

with c_p, center point replications (Polat and Sayan, 2019). For each experiment, the P recovery was calculated from *Eq. 7*

$$RecP = 100 * \left(1 - \frac{C_f}{C_i}\right) \qquad Eq.\ 7$$

With *RecP* as P recovery efficiency estimated as percentage of P removed after precipitation process, C_i and C_f are the P concentration before and after precipitation experiment, respectively.

Struvite production was evaluated as a fraction of ammonium content ($X\text{-}NH_4^+$) in formed solid (Capdevielle et al., 2013b). For struvite precipitation from the liquor, the efficiency of ammonium removal by precipitation (RecN) and the ammonium sorption (q_e) from precipitation effluent were added on the yield parameters.

3.2.2 Experimental modelling

For both percentages of P recovery (X-Rec P) and struvite precipitation estimated experimentally by ammonium content in precipitate (X-NH4+) (Capdevielle et al., 2013b), least square models were studied *Eq.*,8

$$Y - \bar{Y} = \sum SSE \qquad Eq.\ 8$$

The polynomial models (*Eq.9*) with linear (x_i), quadratic (x_i^2) and interaction ($x_i x_j$) terms were chosen (Numviyimana et al., 2019; Polat and Sayan, 2019). The parameters b_0, b_i, b_{ii}, b_{ij}, and *e* are intercept, linear, quadratic, interactions and error coefficients.

$$Y = b_0 + \sum_i^k b_i x_i + \sum_{i=1}^k b_{ii} x_i^2 + \sum_{i<j} \sum_j b_{ij} x_i\, x_j + e \qquad Eq.\ 9$$

Where two results (Y_i) were fractions of P recovery (X-Rec P) and struvite formation ($X\text{-}NH_4^+$), while independent variables are the experimental factors of pH, Mg:P mole ratio, Ca:P mole ratio and NH_4^+ dose.

3.2.3 Models optimization

The optimization of experimental models, *X-Rec P* and $X\text{-}NH_4^+$, was based on maximizing desirability function, d(y_i), described in *Eq. 10* where Y_i is a given specified response, L_i is lower boundary, *T* is the target response. Weight parameters, *s*, are found based on eigen vectors of each response matrix (John, 2013; Varala et al., 2016). With the same response

importance, the overall desirability *D* is obtained as geometric mean of each response desirability d_i in optimization process (*Eq. 11*).

$$d(yi) = \left({Y_i - L_i}/{T - L_i}\right)^s \quad \text{Eq. 10}$$

$$D = (d_1 \cdot d_2 \cdot d_3 \cdot \dots d_n)^{1/n} = (\prod_{i=1}^{n} d_i)^{1/n} \quad \text{Eq. 11}$$

The closer to unit are d_i, the maximum will be *D*; otherwise any null d_i makes null overall desirability (Loewenthal, R. E., 1994).

3.2.4. Precipitation kinetics

The kinetic of struvite crystallization intends to highlights effects of process conditions such as reaction time, and raw materials on crystallization parameters including precipitation rate. Precipitation kinetic was based on monitoring the variation of crystal lattice components concentration in function of time (Musvoto et al., 2000), while crystallization base on variation of crystals parameters in function of time. The struvite precipitation kinetic was studied as variation of concentration of reactant in function of time (*Eq.12*). Various researches use the variation of magnesium concentration (Rahman et al., 2014; Shaddel et al., 2020a), ammonium (Kazadi Mbamba et al., 2015b), or phosphate.

$$r = -dC/dt = k(C - C_e)^x \quad \text{Eq. 12}$$

With r, crystallization rate in mol.kg^{-1}.s^{-1}, C and Ce are concentration at any time and at equilibrium, respectively; k the rate constant in s^{-1} determined experimentally; x the order of reaction. The magnesium was used as struvite lattice ion for kinetic study ($a_i = a_{Mg^{2+}}$). The C_e was estimated as solubility based on struvite solubility product according to reaction:

$$MgNH_4PO_4 \quad \rightleftharpoons \quad Mg^{2+}_{(aq)} + NH^{+}_{4\,(aq)} + PO^{3-}_{4(aq)}$$

At equilibrium, the solubility of struvite involves the equimolar amount of lattice components. Thus the C_e was estimated at equilibrium based on the *Eq.13*.

$$C_e = (Ksp_{struvite})^{1/\sum \nu_i} \quad \textit{Eq. 13}$$

The obtained integrated kinetic model from *Eq.*12 is demonstrated from *Eq. 14* to *Eq. 15*

$$\int_{C_i}^{C} \frac{1}{C-C_e} dc = -\int_0^t k dt \qquad \textit{Eq. 14}$$

$$\frac{C-C_e}{C_i-C_e} = e^{-kt} \qquad \textit{Eq. 15}$$

One can extend the obtained kinetic model with different quantitative parameters where concentration or activity can be expressed in function of time as per *Eq.16*.

$$C_{Mg^{2+}} = \left(C_{i,Mg^{2+}} - C_{e,Mg^{2+}}\right)e^{-kt} + C_{e,Mg^{2+}} \qquad \textit{Eq. 16}$$

with $C_{Mg^{2+}}$, the concentration of magnesium at a given time of precipitation process; $C_{i,Mg^{2+}}$, the initial concentration parameter from the kinetic model; $C_{e,Mg^{2+}}$, the equilibrium concentration of magnesium.

For thermodynamic corrections, the concentration was corrected to activity (a) by multiplication with activity coefficient (γ_i), where activity coefficient is calculated using extended Debye-Huckel relations involving ionic strength (*I*), and parameter *A* that depends on dielectric constant (ε), and the temperature (T). The dielectric constant is matrix dependent, which, in aqueous solutions, is water dependent. The used temperature dependence of dielectric constant was studied by (Malmberg and Maryott, 1956). The concentration correction to activity is summarized in *Eq. 17-22*

$$a_i = C_i\gamma_i \qquad \textit{Eq. 17}$$

$$I = \frac{1}{2}\sum_{i=1}^{n} Z_i^2 C_i \qquad \textit{Eq. 18}$$

$$log\,\gamma_i = -AZ_i^2\left(\frac{\sqrt{I}}{1+\sqrt{I}} + BI\right) \qquad \textit{Eq. 19}$$

(B=0.3 for Davis expression i.e 0<I<0.3)

Or

$$log\,\gamma_i = -AZ_i^2\sqrt{I} \qquad \textit{Eq. 20}$$

(Debye-Huckel expression 0.4 < I <1)

$$\varepsilon = 87.74 - 0.4008t + 9.398(10^{-4})t^2 - 1.41(10^{-6})t^3 \qquad \textit{Eq. 21}$$

Where ***t*** is the temperature in ^oC**,** *an experimental model of Marberg et al.*

$$A = 1.82 * 10^6 * (\varepsilon T)^{-3/2} \qquad Eq.\ 22$$

The validity of ionic strength for model correction is 0<1<1M (Barnes and Bowers, 2017; Solon et al., 2015). The thermodynamic correction of solubility product was done using enthalpy constant van't Hoff relation (*Eq. 23)* and (*Eq. 24*$log\frac{k_2}{k_1} = \frac{\Delta H^\circ}{2.302\ x\ R}\left(\frac{1}{T_1} - \frac{1}{T_2}\right)$

Eq. 24) (Solon et al., 2015)

$$ln\frac{k_2}{k_1} = \frac{\Delta H^\circ}{R}\left(\frac{1}{T_1} - \frac{1}{T_2}\right) \qquad Eq.\ 23$$

$$log\frac{k_2}{k_1} = \frac{\Delta H^\circ}{2.302\ x\ R}\left(\frac{1}{T_1} - \frac{1}{T_2}\right) \qquad Eq.\ 24$$

With k_1 and k_2, the solubility product at absolute temperatures T_1 and T_2, respectively, and R, the ideal gas constant (R = 8.31447 × 10^{-3} KJ·mol^{-1}·K^{-1}). The struvite Ksp values ($Ksp_{struvite}$=$10^{-13.26}$), at standard temperature (T_1 = 298K) and standard enthalpy ΔH° =25.7 kJ mol^{-1} were obtained from MINTEQ database and literature (Zhang et al., 2016), respectively.

3.3. Fertilizer quality

3.3.1. *In-vitro* nutrient release kinetic

The data obtained from experimental essay of product quality as a fertilizer in citric acid were studied as kinetic process. In this case, the release of nutrients in function of time were fitted to dissolution kinetic models (Bruschi, 2015). The latter are diffusion dependent as described in *Eq.25*

$$-dC/_{dt} = (C_s - C)/_{\delta} \qquad Eq.\ 25$$

Where dc/dt is the variation of dissolved concentration over the change of time, Cs is the saturation concentration, C is the concentration at time t, and δ the thickness of solid-liquid interface diffusion layer. The negative sign applied to the normal diffusion law is due to the

change of flux direction where the monitoring of concentration was done from lower to high values, a concept of backward diffusion (Dung and Van Thien, 2014). The *Eq. 25* is changed to rate constant (k) *Eq. 26* which integration from 0 to C in time from the beginning (0 minute) to time t gives an exponential function (*Eq.27*).

$$-{}^{dC}/_{dt} = k(C_s - C) \qquad \textit{Eq. 26}$$

$$C = C_s\,(1 - e^{-kt}) \qquad \textit{Eq. 27}$$

To assess the time required to reach a fraction *X* of saturation C_s, *Eq. 27* is adapted to time constant (τ) expression (*Eq.28*). The latter marks the beginning of first order model in nutrient release.

$$C = C_s\,(1 - e^{-t/\tau}) \qquad \textit{Eq. 28}$$

In fact, *Eq. 28* considers the faster release in first step with limited time to saturation Cs and slow in second step *(-dC/dt = 1/τ * C)* where the first order process starts to be counted (Scholz and Scholz, 2014). The concentration of dissolved nutrients varies with time, where the time (t_x) required to have *C* as fraction *X* of *Cs* can be estimated from *Eq. 28* to *Eq.29*.

$$t_x = -\tau\, ln(1 - X) \qquad \textit{Eq. 29}$$

With t_x in minutes, and *X* as a fraction number ranging from 0 to 1.

Therefore, t_{80} was used to assess the time required for a product to reach 80 % of the maximum nutrient release and played a role in comparative evaluation of struvite production under this study and chemical precipitation used in wastewater treatment plants. The same kinetic models were applied in wet chemical extraction of ash to assess the best time for ash and magnesite mineral dissolution.

The kinetic parameters were estimated by rate constant and time constant exponential growth functions in originPro 2019. The summary of data analysis and softwares for investigation of process conditions, kinetic of nutrient release, and crystallization is presented in Figure 12.

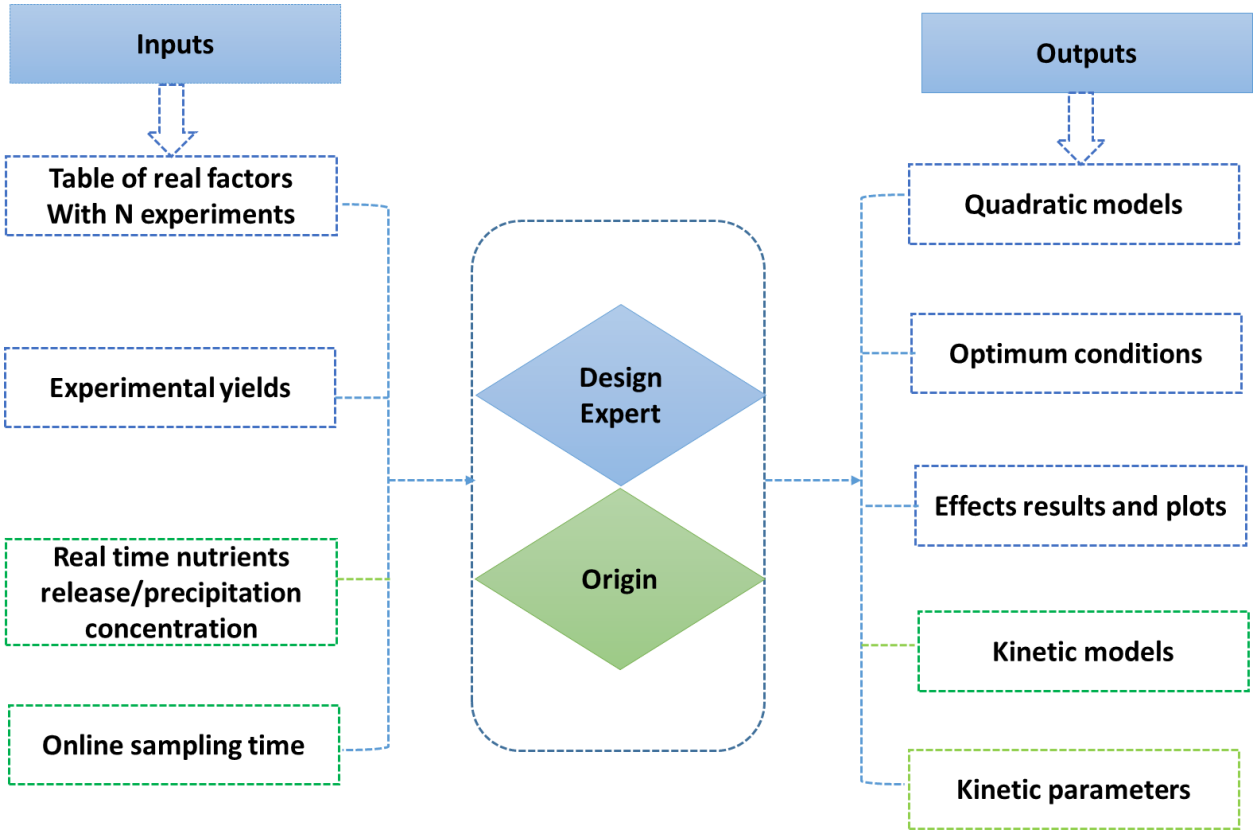

Figure 12. Stepwise flow chat of experimental model parameters

3.3.2. *In-vivo* assay

A germination test was conducted on cucumbers (*Cornichon de Paris*) using a non-fertilized humic soil with a high content of organic matter. The soil and struvite dose was suggested in other work (Ramprasad et al., 2020). In this experiment, 0.2 g of struvite product was used per 35 g of soil in which one seed was placed. The illumination was controlled by an ultraviolet lamp and the plant watering was done daily after 24 h. The germinated seeds were counted after one week and the germination rate was calculated as a percentage of germinated seeds on the placed seeds. The nutrient use efficiency parameters were studied as per Baligar et al. (2001). These include nutrient efficiency ratio (NER) defined as the mass units' ratio of total plant yield to nutrient content; physiological efficiency (PE) defined as the yield mass on nutrient uptake for a fertilized trial after subtraction of control results; agronomic efficiency

(AE) defined as the additional amount of economic yield, i.e., yield minus control per unit nutrient applied (m_f), and apparent nutrient recovery efficiency (ANR) used to reflect plant ability to acquire applied nutrients from soil (Baligar et al., 2001). Those aforementioned nutrient use efficiencies are calculated using *Eq.30-33*

$$NER = \frac{Y}{C_i} \qquad Eq.\ 30$$

$$PE = \frac{Y_F - Y_C}{C_{i,F} - C_{i,C}} \qquad Eq.\ 31$$

$$AE = \frac{Y_F - Y_C}{m_f} \qquad Eq.\ 32$$

$$ANR = \frac{C_F - C_C}{m_f} x100 \qquad Eq.\ 33$$

With *Y*, the yield in kg; C_i, the mass content in kg of nutrient in biomass tissues; Y_F, Y_C, the yield in kg for fertilized and control trials, respectively; $C_{i,F}$, and $C_{i,C}$ are the nutrient uptake in kg for fertilized and control trials, respectively; m_f, amount of nutrient applied.

3.4. Economic model of struvite production

The cost-effectiveness of the P recovery configuration was determined after Bashar et al (2019) using the *Eq. 34* (Bashar et al., 2018):

$$CE_k = \frac{TAC_k}{PE_k} \qquad Eq.\ 34$$

where CE_k is the cost effectiveness in USD or €/kg P removed; TAC_k is the total production cost (USD or €/kg of struvite); PE_k, the total amount of P recovered (Kg). The TAC_k was made by capital annual investment cost (*CA*), and maintenance and operational cost (*COM*) and estimated by *Eq. 35.*

$$TAC_k = CA + COM \qquad Eq.\ 35$$

The estimation of *CA* was done according to Ostara Pearl fluidized bed reactor systems as estimated by (Seymour, 2009). This served in estimation of the cost of alkali, magnesium salt, energy, maintenance, and dumping. The CE_k parameters were calculated by adopting the Pearl® Fluidized Bed Reactors as described in their works (OSTARA, 2018), and the process

conditions and salts dosage obtained at laboratory scale. Further mass, energy and operational costs related formula are given in supplementary *S. 8*

3.5. Infographic of experimental methodology

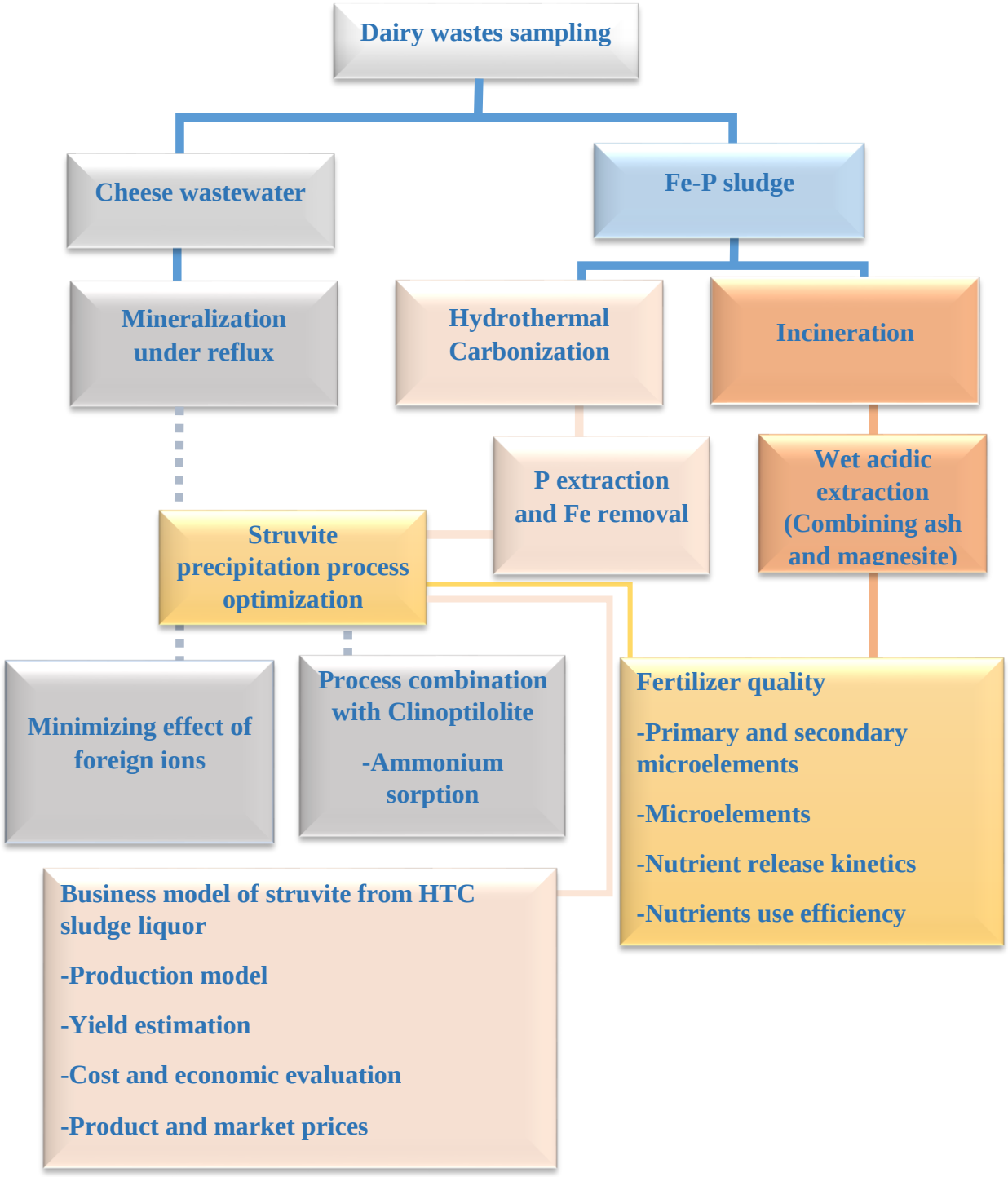

Figure 13. Summary of experimental methodology

4. RESULTS AND DISCUSSION

4.1. Phosphorus recovery from cheese production wastewater

4.1.1. Characterization of cheese production wastewater

The physicochemical analysis of two samples of cheese production wastewater used in in this study is given in Figure 14. The samples are labeled as S1 and S2 representing different sites of samples collection which are the District Dairy Cooperative in Krzepice, Poland and at the Sery Lutomierskie (Poland) cheese producing cooperative, respectively.

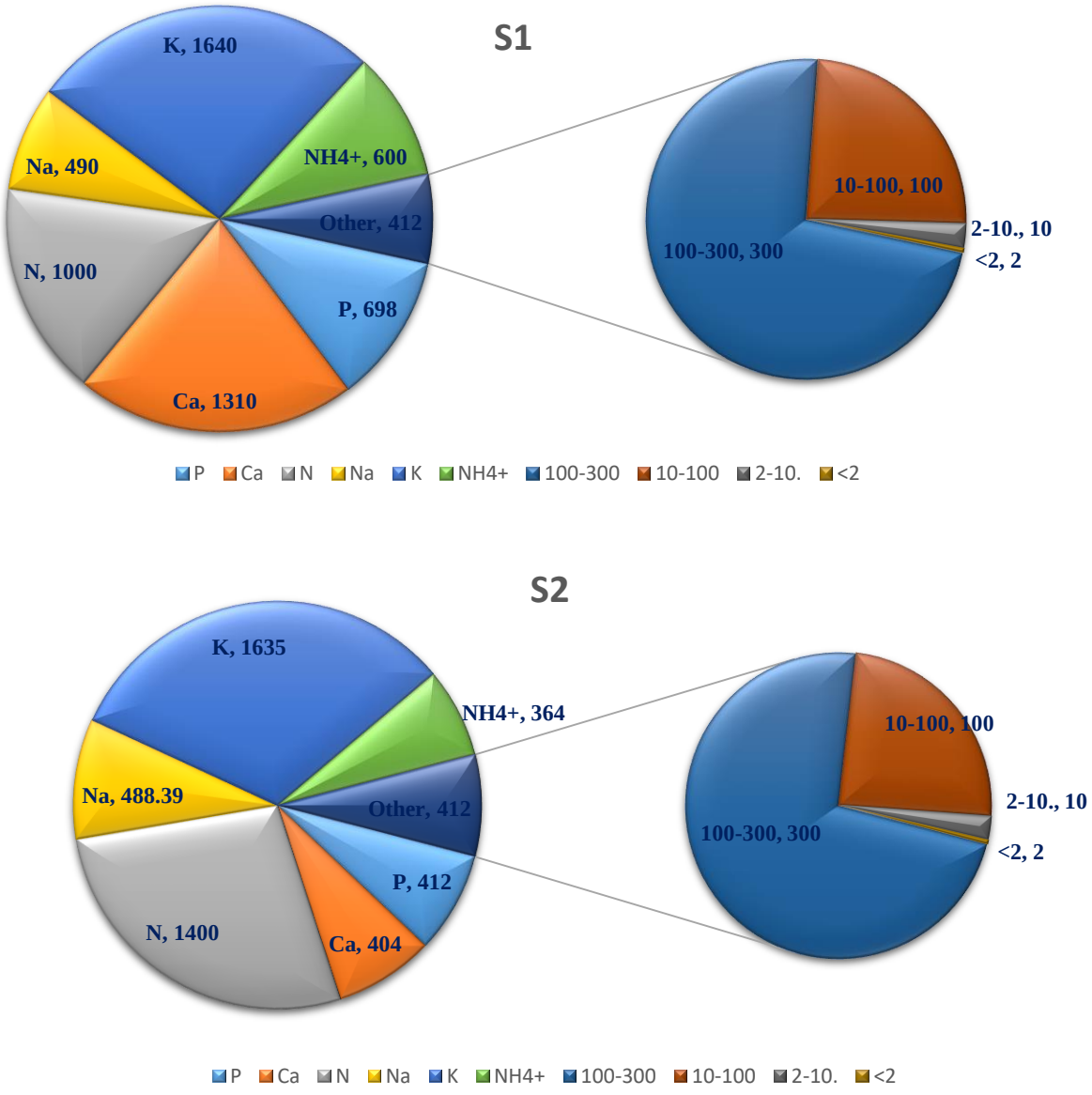

Figure 14: The elemental composition (in mg.kg^{-1}) of wastewater from dairy process: S1and S2

The pH values were 4.35 and 4.34, while the total carbon content were 1.8 % and 3.3% for S1 and S2, respectively. Considering the elemental concentration in different used samples, they show higher concentration of P than accepted limit for wastewater discharge. It should be treated and contain 2 $mg \cdot kg^{-1}$ P at most, the range recommended by Food and Agriculture Organization (FAO) being 0-2 $mg \cdot kg^{-1}$ (Almuktar et al., 2018). Trace elements were considered as Zn, Tl, Si, B, Sb, Mo, Ba, Ti, Ag, Mn, Al. Their concentrations were between 0.01 and 2.6 $mg \cdot kg^{-1}$. Heavy metals were assessed including cadmium (0.002 $mg \cdot kg^{-1}$), lead (1.08 $mg \cdot kg^{-1}$) and chromium (0.204 $mg \cdot kg^{-1}$). Other metals as As, Be, Co, Cu, Fe, Ni, Se, and V were below limit of detection. The levels of heavy metals are low and the wastewater can be used in nutrients recycling (Mansourri and Madani, 2016).

4.1.2. The pH and foreign ions effects on struvite precipitation

a. Effect of pH

The speciation of proton transfer species in function of pH for estimation of best experimental range is depicted on Figure 15. This estimation of the pH range for experiments was based on sample composition and common proton transfer equilibria of solution components using their acidity constants. These include major conjugate acid-base pairs such as (i) phosphate conjugate pairs: $H_3PO_4/H_2PO_4^-$ (pK=2.15); $H_2PO_4^-/HPO_4^{2-}$ (pK=7.20); HPO_4^{2-}/PO_4^{3-} (pK=12.0), (ii) sulfate: H_2SO_4/HSO_4^- (pK = -1.98); HSO_4^-/SO_4^{2-} (pK=1.55), (iii) carbonate: CO_2/H_2CO_3 (pK=1.47); H_2CO_3/HCO_3^- (pK = 6.35); HCO_3^-/CO_3^{2-}(pK=10.3), and (iv) ammonia pair: NH_4^+/NH_3 (pK = 9.25) (Barnes and Bowers, 2017; Loewenthal, R. E., 1994). In that regard, good conditions are alkaline with experimental pH conditions of 8-11. Under these conditions, ammonium and HPO_4^{2-} are predominant with10-90 % of molar fraction in pH range 7.5-10, while PO_4^{3-} is predominant at 7-80% in pH range of 11-13. Thus, alkaline pH enhances supersaturation of phosphate salts.

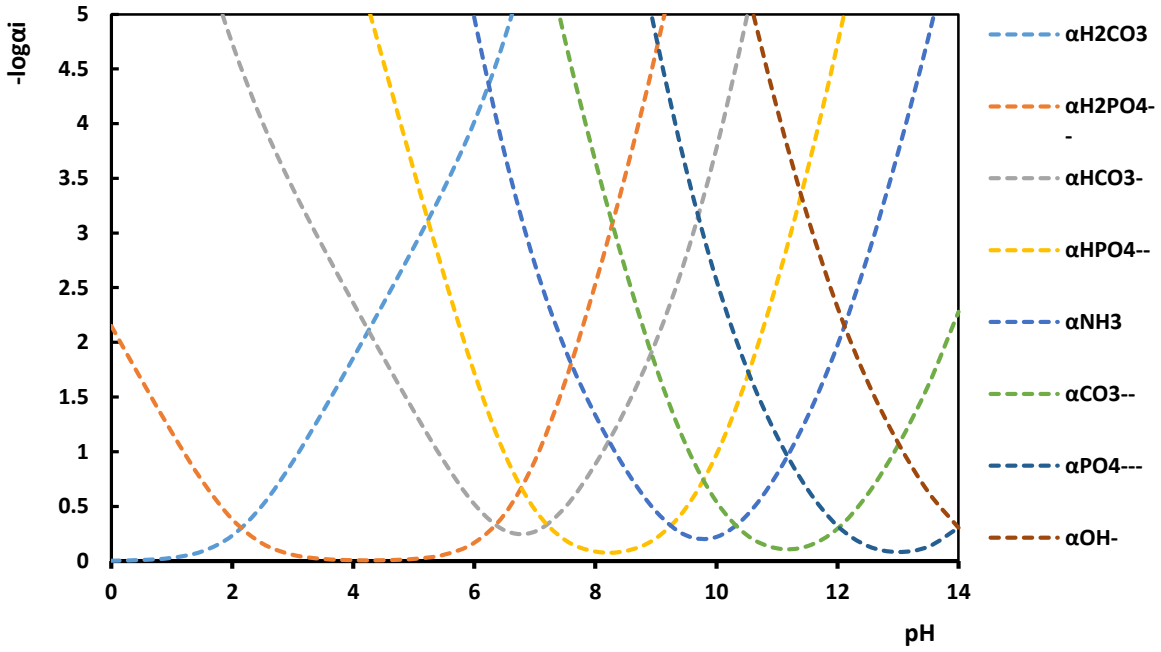

Figure 15. Molar fraction in co-logarithmic scale for potential proton transferring species in function of pH

b. Effects of foreign ions

In light of the elemental composition of sample S1, calcium, potassium, and ammonium have higher molal concentration than P. To find the *SI* for P products to be formed with phosphate, only elements with the concentration higher than 0.1 mmol·kg^{-1} were used, while those equal or below 0.1 mmol·kg^{-1} were considered as traces. The latter have molar ratio on P near to zero thus with negligible contribution in phosphate precipitation. The obtained SI values in relation to phosphate are presented in Table 5.

Table 5. Stoichiometric matrix of phosphate with its possible salts and related saturation indices (SI).

Solid species	**Components**							**log IAP**	**SI**
	K^+	**H^+**	**Ca^{2+}**	**Mg^{2+}**	**NH_4^+**	**PO_4^{3-}**	**H_2O**		
$MgHPO_4 \cdot 3H_2O_{(s)}$		1		1		1	3	-18.75	-0.58
K-struvite	1			1		1	6	-10.78	0.22
$CaHPO_4 \cdot 2H_2O_{(s)}$		1	1			1	2	-18.24	0.76
$Mg_3(PO_4)_{2(s)}$				3		2		-22.37	0.91
$CaHPO_{4(s)}$		1	1			1		-18.22	1.05
Struvite				1	1	1	6	-11.23	2.03
$Ca_3(PO_4)_2$			3			2		-20.85	8.07
$Ca_4H(PO_4)_3 \cdot 3H_2O_{(s)}$		1	4			3	3	-39.10	8.86
Hydroxyapatite		-1	5			3	1	-23.48	20.85

Considering the obtained *SI*, calcium and magnesium are the main phosphate salts with positive *SI* thus possibility of co-precipitation. The calcium phosphate salts have higher *SI* than struvite. This suggests possible inhibition of struvite precipitation. Thus optimizing struvite precursors in reactor is the main way of overcoming more stable calcium phosphate precipitates. Based on acid-base equilibrium model results (Figure 15) and a three level experimental design, *Eq. 6*, the pH range for experimental investigation of effects were chosen and studied using sample S1 (cheese wastewater) after thermochemical treatment.

c. Minimizing effects of foreign ions

The design of experiments on cheese wastewater aimed to find the optimum requirements of overcoming the effect of calcium and enhance struvite precipitation at high concentration. The used factors levels were the lower level (-1) corresponding to 8, 0.5, 0.25 and 1.5; the middle level (0) was 9.5, 1, 0.625 and 2; while the high level (+1) was 11, 1.5, 1, and 3 for pH, M:P, Ca:P, and ammonium excess, respectively. The experimental design matrix and the run yield are presented in supplementary data *S. 2*.

All factors were linearly significant in P recovery and struvite precipitation ($p < 0.05$). By model reduction, the significant interactions ($p < 0.1$) included pH·(Ca:P) for P recovery (Figure 16a) where the increase of both pH and Ca:P enhances P recovery, while the latter factor decreased significantly struvite production (Figure 16b). The additional interaction of pH·(Mg:P) was significant in struvite formation. In fact, the increase of pH with increasing of Mg:P and Ca:P molar ratio enhances P recovery. The detailed analysis of variances of quadratic models is given in supplement *S. 3*.

(a)

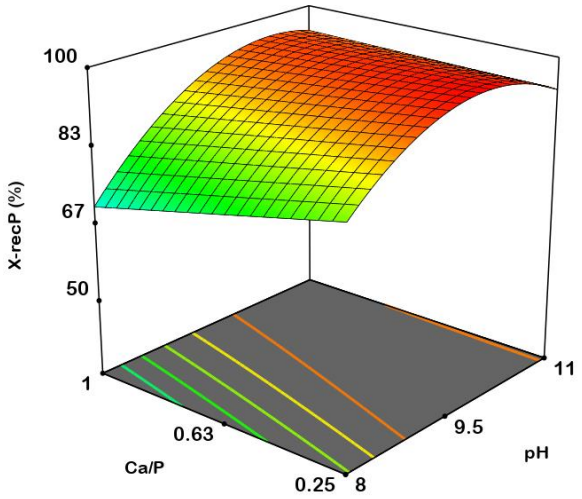

(b)

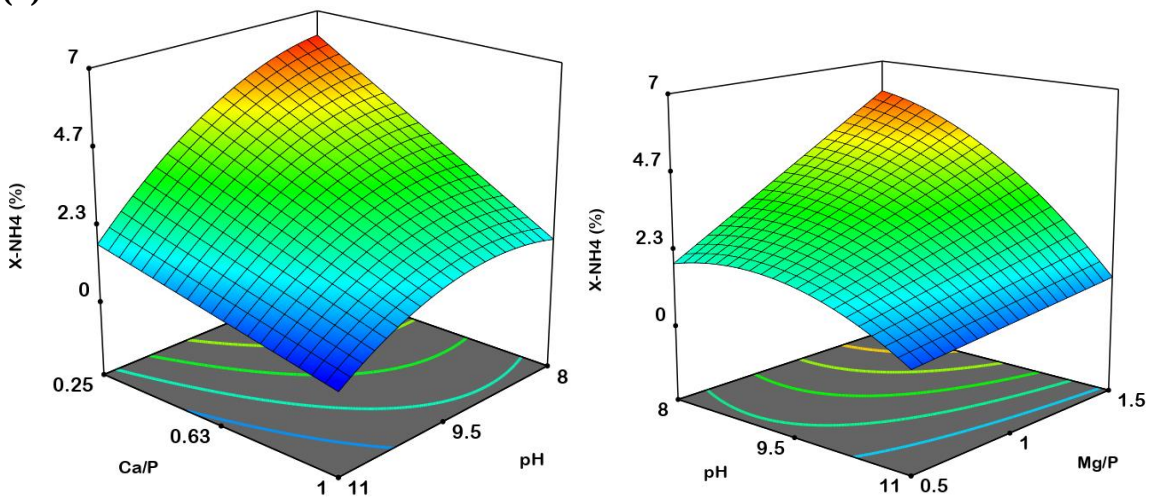

Figure 16. Highlight of factors interactions on P recovery (a) and struvite precipitation (b).

To maximize struvite precipitation, the optimum level of Ca:P mole ratio is needed to be lower than 0.25 while pH keep at 8.3. However, the conditions that maximize both P and struvite precipitation were obtained at pH 8.9. These were achieved with desirability D = 0.995. More factors optimization related to minimizing of effect of foreign ions are given in supplementary *S. 4*. Calcium effect had been pointed out in several researches where its high level favors precipitation of its salts including calcium phosphate ($Ca_3(PO_4)_2$, K_{sp} = 2.07· 0^{-33}), hydroxyapatite ($Ca_5(PO_4)_3OH$, $K_{sp} = 2.1 \cdot 10^{-58}$), octacalcium phosphate ($Ca_8H_2(PO_4)_6 \cdot 5H_2O$, $K_{sp} = 1.12 \cdot 10^{-48}$), and dicalcium phosphate (Bell et al., 1978; Kazadi Mbamba et al., 2015a).

Thus, from cheese wastewater, the calcium at higher molal concentration than magnesium remains the main phosphate counterion with high precipitation potential to inhibit struvite (K_{sp} $=10^{-13.6}$) in non-optimized conditions (Huchzermeier and Tao, 2012). This is in agreement with previous researches where, for example, Wang et al. studied the effect of ion molar ratios in P removal: calcium increased the P recovery with adverse effect on fertilizer quality (Wang et al., 2005). In the published research related to this work, the in-vitro nutrient release was lower for product of precipitation with higher mole ratio Ca:P in feed reactor while it was effective under optimized lower Ca:P mole conditions (Numviyimana et al., 2020).

4.1.3. Struvite precipitation with ammonium sorption onto natural zeolites

a. Ammonium sorption isotherms

Figure 17 represent the equilibrium results obtained for NH_4^+ sorption from synthetic (one-component) solution onto raw and Mg-form of clinoptilolite. The study for multi-ionic solution was conducted by usage of cheese production wastewater (S2). The analysis of the experimental isotherms identifies that the efficiency of NH_4^+ uptake follows the order: homo-ionic form (Mg-Z) > non-modified zeolite (Z-single) > from multi-ionic solution (Z-multi) on raw zeolite. The values of maximum sorption capacity (Q_m) follow the same order $0.48>0.42>0.10$ meq·g^{-1}, respectively.

The elemental analysis of the Mg-form and raw zeolite with XRF are presented in Table 6 and their SEM-EDS results are presented in Figure 18. It is identified that magnesium partially substituted exchangeable ions in the zeolitic stricture. It can result from structural imperfection which probably makes some active (exchangeable) sites unavailable for Mg^{2+} ions. Contact of the homoionic form of zeolite with the NH_4^+ solution resulted in ammonium uptake mainly via ion exchange reaction Mg^{2+}/NH_4^+ as well as adsorption.

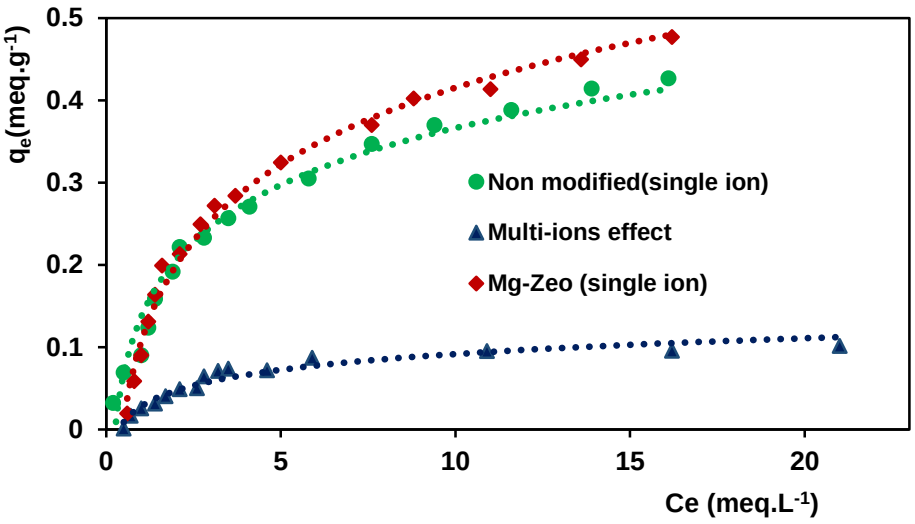

Figure 17. Ammonium sorption isotherms

In raw zeolite case, other ion exchange reactions (Ca^{2+}/NH_4^+, K^+/NH_4^+, Na^+/NH_4^+) occur simultaneously and ions of Ca^{2+}, K^+, and Na^+ are released to the crystallization reactor. Almost five times lower efficiency of NH_4^+ uptake obtained for multi-ionic solution results from competitive sorption of other cations (Na^+, K^+, Ca^{2+}) present in the mixture. They took up some parts of the ion exchange sites available for NH_4^+ on the zeolite surface.

Table 6. XRF characteristic results for row activated (z-Mg) and raw zeolites and after ammonium contact.

Compound	Z-Mg m/m%	raw m/m%	after NH_4^+ contact m/m%
SiO_2	64.22	68.30	59.53
Al_2O3	8.39	14.28	8.01
K_2O	8.33	4.77	11.45
CaO	7.65	6.33	9.94
Fe_2O_3	4.96	2.70	4.90
P_2O_5	4.87	2.74	4.22
BaO	0.55	0.34	0.51
TiO_2	0.29	0.26	0.30
MgO	0.27	-	0.25
SrO	0.11	0.07	0.10
ZrO_2	0.09	0.06	0.08
Co_3O_4	0.04	0.01	-
ZnO	0.01	0.01	0.01
CuO	0.01	-	-
PbO	0.01	-	-
MnO	0.11	0.10	0.06

The obtained XRF results are in agreement with other works (Holub et al., 2013). They highlight the characteristics of Clinoptilolite which alumino-silicates are the major components. Although the main sorption of Mg occurs onto internal porosity of zeolite, the SEM-EDS at randomly chosen surface indicates higher magnesium on the surface of modified zeolite (Figure 1b) than the non-treated zeolite as shown on Figure 18a.

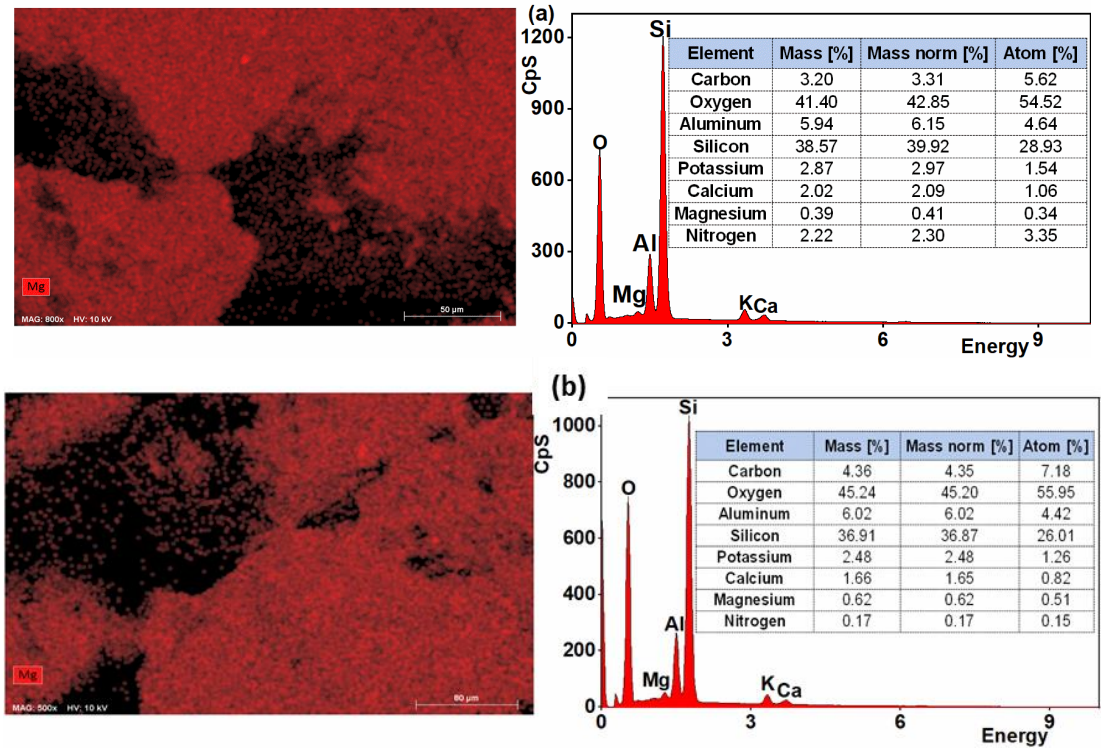

Figure 18. SEM-EDS of zeolite and magnesium mapping (a) Non treated; (b) activated Mg-form.

b. Thermodynamic aspect

The zeolite effect on equilibrium was assessed based on supersaturation ratio with accountability of struvite precursors species at equilibrium. The data presented in Table 7, represent the speciation and indicated different species such as Mg^{2+}, $MgCl^{+}$, and $MgOH^{+}$ which were used to constitute the active molar fraction of magnesium (Stolzenburg et al., 2015); NH_4^{+} and NH_3 to constitute the ammonium molar fraction (Ronteltap et al., 2007); while PO_4^{3-}, HPO_4^{2-} and $H_2PO_4^{-}$ to find the molar fraction of orthophosphate as struvite precursors.

Table 7. Stoichiometric matrix of struvite components and species molar fractions at equilibrium of different experiments.

		Mg^{2+}	NH_4^+	PO_4^{3-}	Na^+	K^+	Ca^{2+}	H^+	CO_3^{2-}	H_2O	Cl^-	GA	GAZ	DA	DAZ
												α_i (%)			
Mg^{+2}	Mg^{+2}	1										46.72	50.43	51.53	51.52
	$Mg_2CO_3^{+2}$	2							1			5.08	5.32	1.39	1.39
	$MgOH^+$									-1		0.05	0.06	0.06	0.06
	$MgCl^+$	1									1	14.74	15.87	16.59	16.60
	$MgHPO_4$ (aq)	1										0.02	0.05	0.20	0.18
	$MgCO_3$ (aq)	1										23.38	19.81	21.23	21.25
	$MgHCO_3^+$	1						1	1			10.01	8.47	8.99	9.00
PO_4^{-3}	PO_4^{-3}			1								0.07	0.06	0.09	0.09
	HPO_4^{-2}			1				1				36.20	31.59	48.06	48.13
	$H_2PO_4^-$			1				2				0.23	0.20	0.30	0.30
	$MgPO_4^-$			1								1.41	1.52	0.57	0.57
	$MgHPO_4$ (aq)	1		1				1				33.56	36.34	13.81	13.84
	$CaHPO_4$ (aq)	1		1				1				0.92	2.26	0.81	0.82
	$CaPO_4^-$			1			1					3.40	8.37	2.98	2.98
	$NaHPO_4^-$			1	1			1				18.09	14.46	25.12	25.02
	$KHPO_4^-$			1		1		1				4.68	4.09	6.18	6.19
	K_2HPO_4 (aq)			1		2						0.26	0.22	0.34	0.34
	KH_2PO_4 (aq)			1		1						0.01	0.01	0.02	0.02
	KPO_4^{-2}			1		1						0.02	0.02	0.02	0.02
	Na_2HPO_4 (aq)			1	2							1.06	0.77	1.54	1.53
	$Na_2PO_4^-$			1	2							0.03	0.02	0.04	0.04
	NaH_2PO_4 (aq)			1	1							0.03	0.03	0.05	0.05
	$NaPO_4^{-2}$			1	1							0.04	0.04	0.06	0.06
NH_4^+	NH_4^+		1									76.31	76.23	76.12	76.12
	NH_3 (aq)		1					1				23.65	23.66	23.85	23.85
	$CaNH_3^{+2}$		1				1					0.04	0.11	0.03	0.03
I (M)												0.36	0.35	0.32	0.32
ΔG (Kj·mol^{-1})												-5.87	-5.42	-9.66	-9.56

The IAP and Δ*G* demonstrated the difference for experiments upon zeolite addition. There is a slight change of Δ*G*, which is due to quantitative expressions involved in estimation of thermodynamic parameters. In fact, the effect of 10 mg kg^{-1} encountered by zeolite addition enhances the change of struvite spontaneity of up to -0.4 and -0.11 KJ mol^{-1} for the molar ratios estimated from GA to GAZ, and DA to DAZ experiments in Table 7, respectively. The Δ*G* in Table 7 highlights the enhanced trend to equilibrium energy (Δ*G* = 0) due to addition of zeolite. The more positive effect is found on final ammonium concentration in the effluent. For P and

ammonium, the effluent concentrations at equilibrium fell from 444.79 to 4.21 mg.dm^{-3} and 1869 to 84.60 7.63 mgkg1, respectively. The ammonium recovery was enhanced to 97.44 percent by adding zeolite up to 1.5 percent of the reaction volume. The applied dose from the gradient descent precipitation supplemented with zeolite enhanced the equilibrium ammonium drop from 84.4 to 48.7 7.63 mg.dm^{-3}, while P remained significantly low at 4.23 mg.dm^{-3}, highlighting natural zeolite's ammonium sorption capacity. This is an advantage in mitigation of the environment pollution caused by excess of ammonium in struvite precipitation effluent. Furthermore, in the related published work, the clinoptilolite formulation with struvite was effective in the increase of crop yield. The in-vivo study indicated that the struvite combined with zeolite is a good formulation which improved the plant harvest dry biomass of cucumber sprout up to the double of the trials without zeolite (Numviyimana et al., 2021).

4.1.4. Summarization of phosphorus recovery from cheese production wastewater

The concentration of P in the used cheese production wastewater is higher than recommended limit of wastewater discharge to environment. The limit of P in wastewater discharge was reported to be in range of 0-2 mg·L^{-1} (Almuktar et al., 2018). Along with P, calcium is a predominant multivalent cation and exhibits high precipitation potential with phosphate. Thus, calcium phosphates can precipitate especially in alkaline conditions (pH > 7). To mitigate it, it would be necessary to minimize the effects of calcium to a mole ratio of Ca^{2+}:PO_4^{3-} below 0.25. These are the conditions that enhanced the struvite product quality as fertilizer (Wang et al., 2005). As was identified in p. 4.1.2, higher mole ratio level decreases the struvite precipitation potential even in the presence of excess of Mg and NH_4^+. An effective tool to optimize the conditions for this process (maximize the P recovery and struvite yield) is desirability function

which allowed for obtaining the optimum molar ratio of Ca:P and the pH conditions for struvite precipitation without inhibition.

Another important approach to favor the struvite production quality is the combination of struvite precipitation and ammonium sorption onto clinoptilolite. This helped to reach the lower levels of P and ammonium in the precipitation effluent. The usage of homoinic form of zeolite not only allow achievement of higher efficiency of NH_4^+ removal but also avoiding Ca^{2+}, Na^+, and K^+, release to reaction solution (Section 4.1.3a). In opposite, the release of Mg^{2+} from homoionic form of zeolite is an additional source of struvite crystal lattice ion. The estimated ΔG values closer to 0 further confirms the process improvement (Table 7). On the other hand, the combination of precipitation process with sorption one allowed obtaining a fertilizer consisting of struvite and zeolite saturated with NH_4^+ ions. This demonstrated a better effect on plant in-vivo assay where the dry mass of sprout was double to the material without zeolite (Numviyimana et al., 2021). On some crops such as straw berry, the effects on the plant, fruit quality, prokaryotic abundances, and relative abundance of bacterial and archaeal functional genes associated to nitrification improved when the ammonium-enriched zeolites were applied as fertilizer to strawberry plants and positively impacted bacterial nitrification. Natural zeolites are proved to have significant sorption characteristics and to be an effective carrier of nitrogen to plants (Costamagna et al., 2020).

4.2. Phosphorus recovery from thermochemically processed sludge

4.2.1. Characterization of sludge and their thermo-chemical processing products

The physicochemical analysis of three samples used in in this study in given in Figure 19 and the related data are presented in supplementary S. 5. These represent the characterization of sludge (S3), the hydrochar (S4) and the liquor (S5) obtaine after HTC process, as well as the incinarated sludge ash (S6).

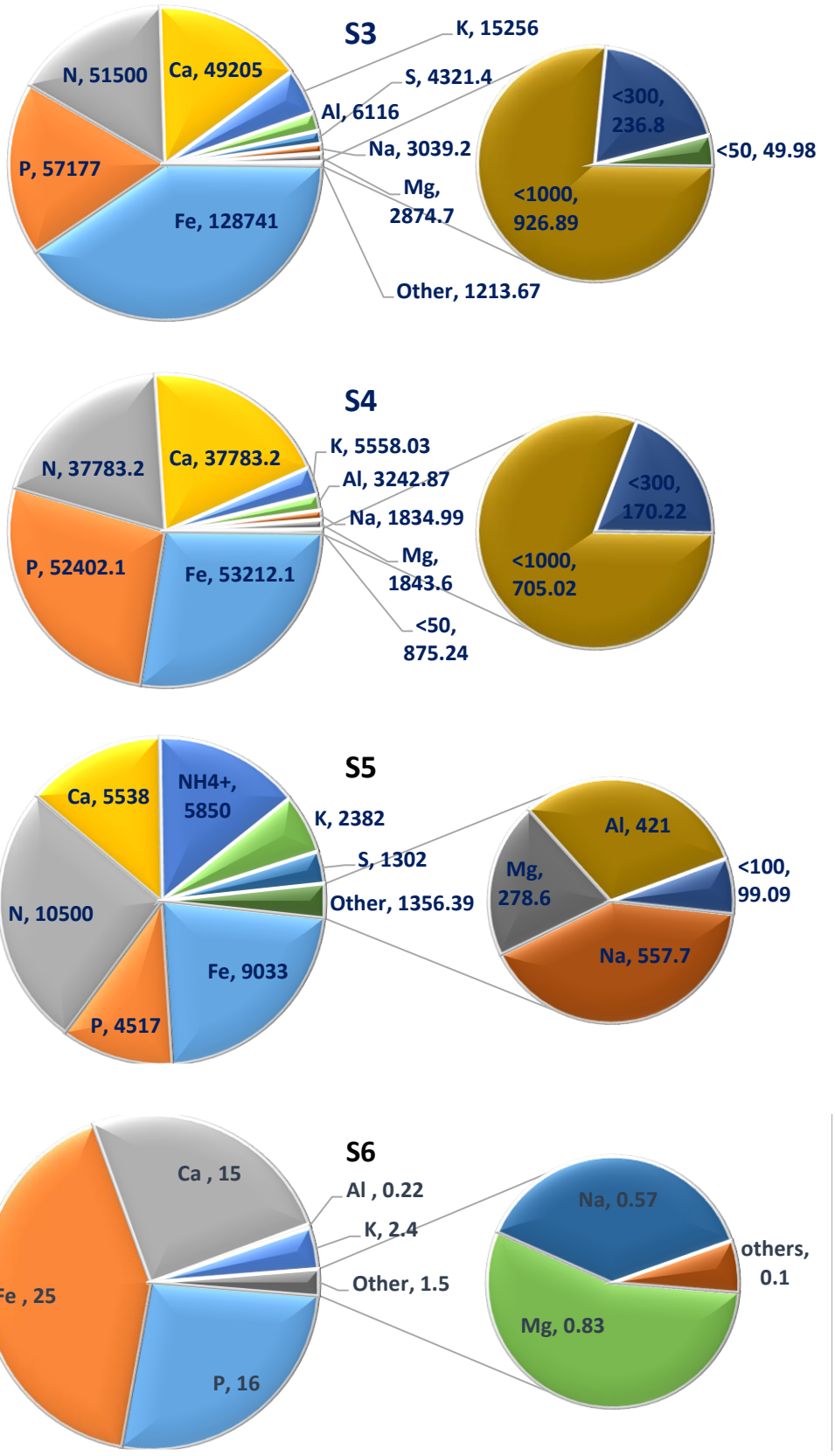

Figure 19. Elemental composition of the sludge (S3) in mg.kg^{-1}, hydrochar (S4) in mg.kg^{-1}, HTC liquor (S5) in mg.Kg^{-1}, and ash (S6) in %.

The comparison of the graphs on Figure 19 indicates significant difference in the quantitative compositions of analysed samples. Firstly, the concentration of P is higher in the sludge than in the wastewater. This highlights the benefits of P accumulation process used in wastewater treatment. Secondly, the use of iron coagulants, makes its concentration becoming very high in the sudge. Upon thermochemical treatment, the concentration varies in each fraction yield compared to feed sludge. The small fraction of metal ions dissolved in the liquid phase (S5) compared to sludge (S3), can results from multivalent metal ions immobilization in hydrochar (S4). Such partition occurs due to the spontaneous binding of these metals with orthophosphate in the solution to form less soluble salts. For calcium, iron, and P, the dissolution rates in the liquor were 11.25%, 7.02%, and 7.9%, respectively. This indicates their accumulation in hydrochar following the supersaturation of their phosphate salts.

The observed elemental partition matches up with the previous research, which found that iron and calcium phosphate were formed in hydrochar following their high content in HTC feedstock (Atallah et al., 2019). Despite the low dissolution rate, the concentration of P in HTC liquor was still high and made it a nutrient rich aqueous mixture for the recovery through precipitation process.

4.2.2. Phosphorus species in the liquor

The phosphorus species in the liquor estimated as per *Eq. 5* are presented in Table 8. The results indicate that $FeHPO_4$ and $FeH_2PO_4^+$ are the predominant phosphate species in the liquor, with 45 and 15% molar fraction of total phosphorus, respectively. Their preeminence is enhanced by high iron concentration and the pH conditions. At pH 6.96 of the liquor, the $H_2PO_4^-$ and HPO_4^{2-} species are the predominant forms of phosphate.

Table 8. Stoichiometric speciation of phosphorus in the liquor

Species	Components								Fraction
	PO_4^{3-}	H^+	Zn^{2+}	Al^{3+}	K^+	Mg^{2+}	Ca^{2+}	Fe^{2+}	%
HPO_4^{2-}	1	1							9.50
$H_2PO_4^-$	1	2							14.31
$FeH_2PO_4^+$	1	2						1	15.46
$FeHPO_4$ (aq)	1	1						1	45.05
$MgHPO_4$ (aq)	1	1				1			1.13
$CaHPO_4$ (aq)	1	1					1		8.44
$CaPO_4^-$	1						1		0.30
$CaH_2PO_4^+$	1	2					1		1.14
$KHPO_4^-$	1	1			1				2.96
$AlHPO_4^+$	1	1		1					0.69
$ZnHPO_4$ (aq)	1	1	1						0.02
K_2HPO_4 (aq)	1	1			2				0.17
KH_2PO_4 (aq)	1	2			1				0.85

Considering the *SI* values of phosphate salts estimated at pH 9, the results show high *SI* for calcium and iron phosphate salts due to their high precipitation potential and the high concentration of P in the sample (Table 9). The salts of prompt recovery at pH 9 are presented in Table 9 with their *SI*. The iron precipitates as vivianite (*SI* = 19.6), while struvite lattice ions are in low concentration in the liquor and their precipitation is at a trace level.

Table 9. Stoichiometric matrix of possible phosphate salts in HTC liquor and their SI

Possible salts	Components									HTC liquor	
	Al^{3+}	PO_4^{3-}	NH_4^+	Mg^{2+}	Ca^{2+}	K^+	Fe^{2+}	H^+	H_2O	log IAP	SI
$Ca_3(PO_4)_2$		2			3					-19.64	9.28
$Ca_4H(PO_4)_3{:}3H_2O$(s)		3			4			1	3	-37.15	10.80
$CaHPO_4$(s)		1			1			1		-17.41	1.87
$CaHPO_4{:}2H_2O$(s)		1			1			1	2	-17.47	1.53
Hydroxyapatite		3			5			-1	1	-21.91	22.42
K-struvite		1		1		1			6	-10.36	0.64
$Mg_3(PO4)_2$(s)		2		3					3	-21.90	1.38
$MgHPO_4{:}3H_2O$(s)		1		1				1	3	-18.25	-0.08
Struvite		1	1	1					6	-9.84	3.42
Variscite	1	1							2	-20.61	1.46
Vivianite		2					3		8	-18.13	19.63

According to Table 9, ammonium precipitates only as struvite and its fraction ($X\text{-}NH_4^+$) in the formed product was used to assess the struvite precipitation efficiency. In this regard, further

steps studied process conditions of iron removal by P extraction and proper dosage of struvite precursor salts.

4.2.3. Phosphorus extraction and iron removal efficiencies

To overcome the complexity of the HTC liquor for struvite precipitation and the product purity, the extraction methods were studied. Oxalic acid was effective to extract P and settle iron and calcium in as their oxalate salts precipitate. The extract underwent the precipitation process after substrate dose optimization. Since the ammonium effluent concentration has a regulated threshold, the natural clinoptilolite was used for ammonium sorption in the struvite precipitation effluent. The extraction using oxalic acid indicated the effect of solvent concentration on removal efficiency (RE). The use of 0.375 mol·L^{-1} solution of oxalic acid decreased iron concentration from 9033 to 1209 mg·L^{-1} (i.e. up to 86.6 % RE); whereas calcium concentration decreased from 5538 to 342 mg·L^{-1} (i.e. up to 93.82% RE). In contrast, the phosphorus level did not change significantly. The latter decreased only by 13.4%. This P decrease in the extract can be due to sorption by calcium and iron oxalates precipitates (Dalahmeh et al., 2020). On the other hand, the use of sodium sulphide was not effective for iron removal. At the same concentration of extracting agent of 0.375 mol·L^{-1}, the iron RE was only 23%. The main reason is the formation and evolution of hydrogen sulphide gas by hydrolysis of sodium sulphide. This phenomenon is caused by pH adjustment to a lower level (< 2.5) to favor P dissolution and to inhibit its precipitation into dicalcium phosphate salts. As pH is lowered by the addition of strong acid, the formed weak and volatile sulphide acid evolves and causes a decrease in iron (II) sulphide precipitation. In addition, the use of sodium sulphide as an extraction solution requires careful handling with sophisticated installation due to the generation of odors by its hydrolysis: $S^{2-} + H_2O \leftrightarrow H_2S + OH^-$. The results for concentrations of extracting solutions in the range of 0.03-0.375 mol·L^{-1} and the variation of

iron and calcium RE are shown in *Figure 20*. Therefore, the struvite inhibition was mitigated through extraction using oxalic acid as the extracting solution. The oxalic acid 0.375 mol·L^{-1} was used in further experiments.

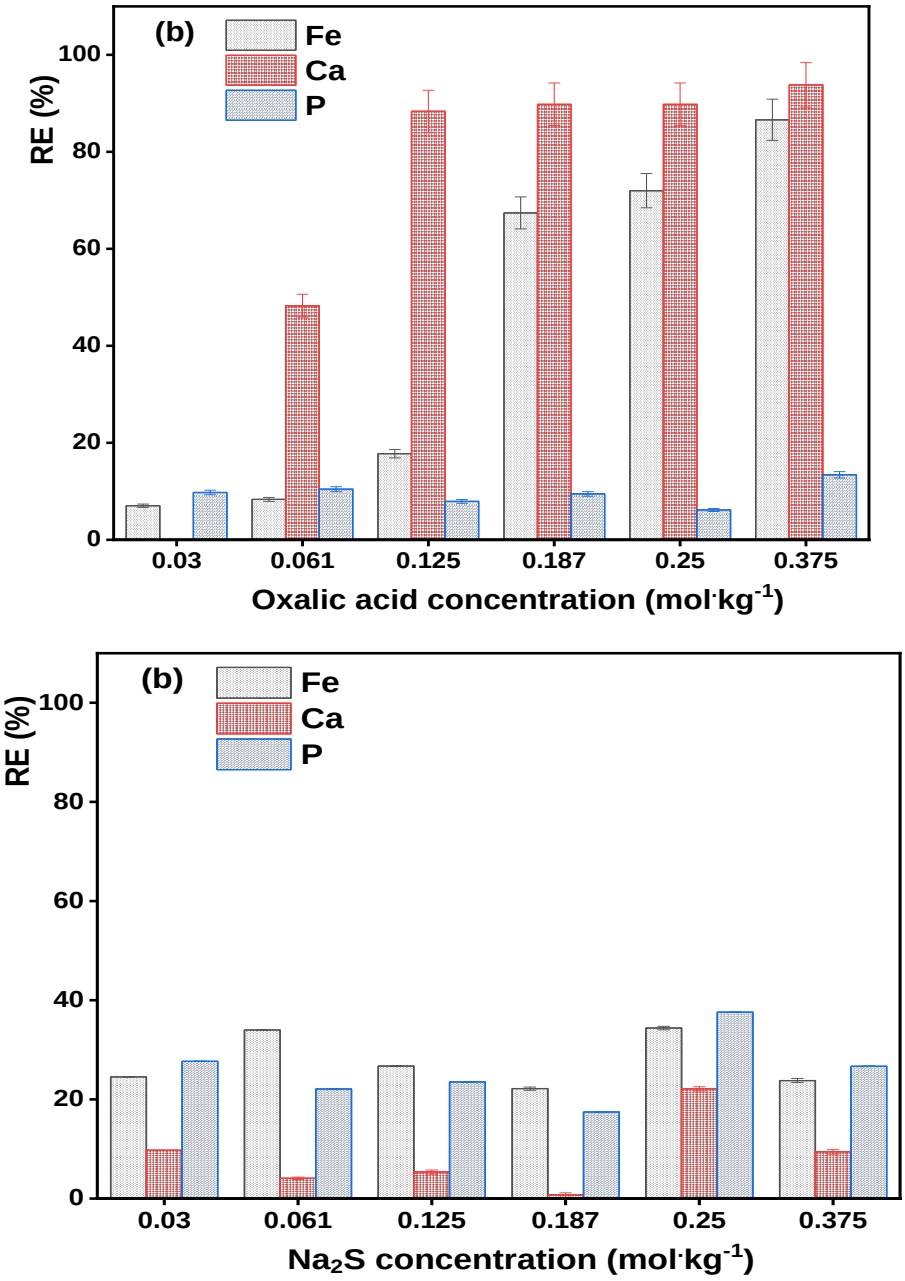

Figure 20. Removal efficiency (RE) of iron and calcium during P extraction with oxalic acid (a) and sodium sulfide (b).

4.2.4. Precipitation and related DOE results

Upon immediate precipitation at pH 9 without additional salt, the obtained product has a high content of calcium, iron, and phosphorus. This is due to the precipitation of amorphous calcium phosphate and vivianite. During this process, the P removal was up to 97.50 and 99.96% by experiments done with real and artificial solutions, respectively. Such removal efficiency highlights the ability of phosphate to form less soluble salts with a number of di- and tri-valent metals (see products *a* and *a'* in Table 9). In fact, the high iron level in the obtained product is restricted to the European market for phosphate fertilizer.

The aim of extraction and DOE application was to extract phosphate, decrease iron and find the proper salt dosage to mitigate the negative effect of liquor composition on product quality. Up to 15 experiments were conducted for each mimic solution of the sample and the extract (Table 10). Nevertheless, due to the quality of final products in regards to fertilizer market (section 4.3), it was mandatory to remove iron in prior of any optimization. Calcium was also decreased along with iron while P passed in supernatant.

Under experimental investigation, the pH, magnesium, and nitrogen feedstock dosage demonstrated their significant effects ($p < 0.05$) on RecP, X-NH_4^+, RecN, and Q_e. The experimental relationships were fitted with a determination coefficient better than 95%, good adequate precision (> 4), and a non-significant lack of fit. All factors were optimized with desirability D = 0.951. The pH was fixed at 9, the obtained optimum salt dosage was 1.73:1.14:1 as initial Mg: NH_4^+: PO_4^{3-} mole ratio. The P recovery from the leachate was RecP = 99.96 ± 0.46 %. The ammonium uptake from the effluent was Q_e = 1.25 mg·g^{-1} of zeolite. The predicted and experimental X-NH_4^+ were 6.76 and 7.28%, respectively.

These conditions were applied to the HTC liquor after P extraction, and the product ammonium content was 6.69 ± 0.01 %. Thus, the struvite in the formed P product is estimated at 91.02%.

The P and Fe concentration in the precipitation effluent was 1.7 and 1.09 $mg \cdot L^{-1}$, respectively. Such concentration levels comply with the threshold limit of a maximum of 2 and 5 $mg \cdot L^{-1}$ of P and iron in industrial effluent, respectively (Almuktar et al., 2018; Tamulonis, 2002). The ammonium in the effluent was 95.82 $mg \cdot L^{-1}$, equivalent to 82.6% of its recovery from the feed sample. The ammonium concentration was decreased to less than 60 $mg \cdot L^{-1}$ by addition of clinoptilolite (Q_e = 1.25 $mg \cdot g^{-1}$) to fall into the accepted range with regard to EU decision 2018/1147 (Sugawara and Nikaido, 2018).

4.2.5. Effect of dilution and residence time.

The growth of phosphate precipitate was time and dilution (DF) dependent. After 1h of precipitation reaction, the evaluated residence time for equilibrium indicated the increase in particle size with the residence time. In the investigated process conditions, Figure 21a shows that the high particle agglomeration is nearly 200 μm of particle diameter. The increase in residence time to 24h indicates the agglomerated particle size up to 600 μm.

Additionally, the high initial concentration enhances the precipitate growth. The high particles' agglomeration was found when the sample was not diluted (DF1). Under these conditions, there is a visible increase in percentage volume with particle size to nearly 1000μm (Figure 21a). Considering the residence time, the particle size increased with equilibrium time. Nonetheless, the effluent P was stabilized to less than 2 $mg \cdot L^{-1}$ in supernatant up to 1h equilibrium time (see Figure 21b). This indicates that the crystal growth is more affected by initial concentration.

Table 10. DOE and optimum results of precipitation.

Factors				Yield without EP*				Yield with PE			
run	**pH**	**Mg:P**	**N:P**	**RecP**	**RecN**	**X-NH_4^+**	**Q_e**	**RecP**	**RecN**	**X-NH_4^+**	**Q_e**
		(mol.mol^{-1})		**(%)**	**(g/100ml)**	**(%)**	**(mg.g^{-1})**	**(%)**	**(g/100ml)**	**(%)**	**(mg.g^{-1})**
1	**7.5**	**1.0**	**0.7**	94.30	0.58	6.33	0.72	82.50	0.30	5.71	0.28
2	**10.5**	**1.5**	**0.2**	99.50	0.11	0.06	1.12	96.90	0.09	0.86	0.00
3	**9.0**	**1.0**	**0.2**	95.50	0.17	1.69	0.46	86.00	0.09	1.13	0.01
4	**9.0**	**1.0**	**1.2**	99.80	0.85	6.60	2.37	94.90	0.48	6.31	0.83
5	**10.5**	**2.0**	**0.7**	99.90	0.52	1.73	1.21	99.40	0.29	4.50	0.47
6	**9.0**	**1.5**	**0.7**	99.80	0.42	6.28	1.94	94.60	0.32	6.21	0.85
7	**7.5**	**1.5**	**1.2**	96.70	0.91	7.34	1.75	90.60	0.51	6.38	0.60
8	**7.5**	**1.5**	**0.2**	90.90	0.15	1.95	1.73	81.20	0.08	1.69	0.25
9	**9.0**	**1.5**	**0.7**	99.70	0.40	6.53	2.08	93.60	0.32	6.11	0.85
10	**9.0**	**2.0**	**0.2**	97.10	0.16	1.94	1.58	93.70	0.10	1.12	0.00
11	**9.0**	**2.0**	**1.2**	99.70	0.89	6.66	2.16	98.40	0.47	6.34	1.64
12	**10.5**	**1.0**	**0.7**	99.20	0.54	3.37	1.84	98.40	0.31	4.62	0.01
13	**7.5**	**2.0**	**0.7**	95.40	0.39	7.05	2.18	86.60	0.29	5.39	1.04
14	**9.0**	**1.5**	**0.7**	99.50	0.42	6.32	1.82	94.00	0.31	6.21	0.85
15	**10.5**	**1.5**	**1.2**	99.90	0.79	3.37	2.52	99.50	0.50	5.91	1.00
Experimental model parameters											
Intercept				-8.330	2.560	-58.300	1.950	-59.00	-0.388	-21.500	-10.60
A-pH				17.900	-0.351	11.700	0.040	21.82	0.050	3.960	2.18
B-Mg:P				10.200	-1.320	11.300	0.217	23.42	0.187	5.700	2.33
C-NH_4^+:P				28.100	0.668	21.200	0.488	34.32	0.563	14.400	-1.62
AB				-0.122	0.058	-0.786	-0.521	-1.07	-0.005	0.069	-0.10
AC				-1.830	-0.029	-0.694	0.346	-2.25	-0.006	0.122	0.22
BC				-1.700	0.042	-0.192	-0.333	-4.17	-0.013	0.041	0.82
A^2				-0.817	0.016	-0.623	-0.161	-0.79	-0.002	-0.246	-0.12
B^2				-2.370	0.242	-1.420	-0.300	-2.25	-0.047	-2.150	-0.49
C^2				-4.190	0.173	-7.190	-0.009	-1.04	-0.064	-7.530	-0.43
p-Value				<0.001	<0.001	<0.001	<0.001	<0.001	<0.001	<0.001	0.035
F				72.3	38.7	45.9	14.7	36	196	255	5.63
R^2				0.992	0.986	0.988	0.963	0.985	0.997	0.998	0.91
P-lack fit				0.058	0.017	0.0501	0.272	0.0825	0.0935	0.0684	-
Precision				27.9	17	21.6	13.3	19.52	37.2	42.2	9.08
Optimum factors level				Ca:P 0.25** pH =9.0, Mg:P=1.4, N:P=1.14				pH =9.0, Mg:P=1.73, N:P=1.14,			
Optimum pred. yields				RecP =100 ± 0.13, RecN = 0.761, X-NH_4^+ = 7.01 ± 0.15, Q_e = 2.37, D = 0.964				RecP = 97 ± 0.41 %, RecN = 0.467, X-NH_4^+ = 6.76 ± 0.06, Q_e =1.35, D = 0.951			
Experimental yields				RecP = 99.96 ± 0.22, RecN = 0.768, X-NH_4^+ = 6.76 ± 0.15				RecP = 99.96 ± 0.46 %, RecN = 0.502, X-NH_4^+ = 7.28 ± 0.05, Q_e = 1.25			

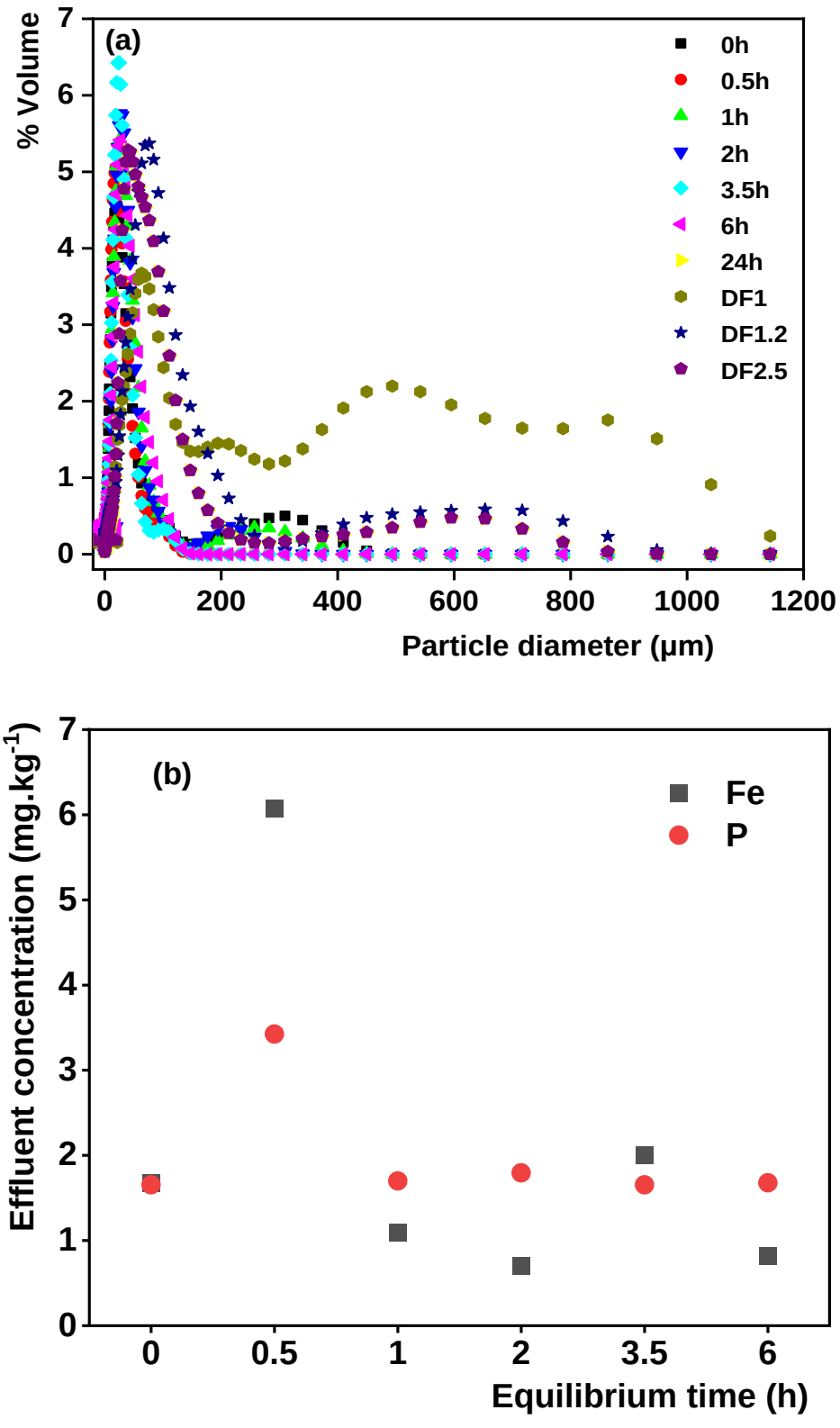

Figure 21. Particle size variation with residence time and dilution factor (a), and effect of equilibrium time on P effluent concentration (b).

4.2.6. Characterization of recovered products from the liquor

a. Physicochemical characterization

The products of direct salt recovery from the HTC liquor are highly iron and calcium-based phosphate products. This was observed for both real (*a*) and mimic (*a'*) samples in *Table 11*. The optimized salt dosages without P extraction by additional ammonium, magnesium, and phosphorus sources to the HTC liquor enhanced struvite content (*b* and *b'* in *Table 11*). The product nitrogen content was improved, and the iron decreased from 17.42 to 6.16 %. Despite the applied additional dose of struvite precursors, the obtained product does not meet the regulations of the phosphate fertilizer market with regard to iron content. This was mitigated by P extraction for iron removal followed by struvite precipitation from the extract (*c* and *c'* in *Table 11*). By applying the optimum dosage on the P extract, the product iron content was less than 2%, the P content was up to 28.18 and 31% obtained experimentally on real (product c) and artificial (product c') samples, respectively. The products comply with the European regulation 2019/1009 regarding the market for phosphorus fertilizers (EU, 2019).

The used combination of extraction with oxalic acid and struvite precipitation is a beneficial process for its ability to recover iron and P into two separate and valuable products. Struvite, thereby recovered, is used as an efficient P fertilizer.

Table 11. Elemental characteristics of products obtained under different conditions

ID	Ca	Fe	K	Mg	P_2O_5	NH_4^+	Na	Tot. C
			(%)					
a	8.04	17.91	0.33	0.74	28.20	0.43	1.23	0.49
a'	9.68	17.42	1.05	0.44	22.57	2.33	5.63	0.61
b	3.43	6.65	1.26	6.23	31.60	6.49	1.06	4.83
b'	5.21	6.16	0.84	8.43	25.05	6.06	1.56	0.17
c	1.99	1.88	0.53	9.93	28.18	6.69	5.64	5.21
c'	1.19	1.11	0.55	11.17	31.44	7.28	0.77	0.18
d	7.33	11.04	0.21	1.53	0.34	1.72	0.61	18.71
d'	11.94	16.02	0.65	0.19	3.68	1.53	0.18	18.17

In contrast, the extraction solid product of iron (II) and calcium oxalates have been reported for further use, either as sorbent material or as carbonate salts after their thermo-treatment

(Dhal et al., 2015). In particular, ferrous oxalate is a useful product member of metal organic framework polymers (Li et al., 2019). The elemental characterization of recovered products is presented in *Table 11*.

b. Spectroscopic and microscopic characterization

The XRD characterization of the precipitates indicates various aspects of the crystallinity of the recovered products. The direct precipitation at pH 9 leads to the production of amorphous salts. The predominant products are iron phosphate and calcium phosphate following their high concentration in the liquor, their decrease in precipitation effluent, and their high concentration in the products. This is highlighted by their SEM-EDS images showing the elemental mapping on the material surface (Figure 22a), and their products' analytical results (*Table 11*, products *a* and *a'*).

In contrast, the struvite rich products were produced at optimum dosage and exhibited closer crystal lattice parameters with a struvite pattern. For those products, the crystal lattice parameters a: 6.955, b:6.142, and c: 11.218 A^{o} for struvite crystals were observed, and the characteristic peaks were at 15.9, 20.8, 21.5, and 31-32 Ɵ. The XRD spectra of all products are presented in Figure 22a-d in which the struvite pattern is marked by the letter *S*. The same struvite crystal properties were identified in specific works by Whitaker et al. (1970), thus highlighting the achieved struvite predominance in the products (Whitaker and Jeffery, 1970).

Furthermore, microscopic images correlate with XRD results. In addition to the lower intensity caused by the formation of amorphous phosphate salts, the SEM-EDS image in Figure 22*a* indicates a non-crystalline structure with calcium phosphate as the major element with high signal on the product surface elemental mapping. The results improve in Figure 22b after addition of magnesium salts.

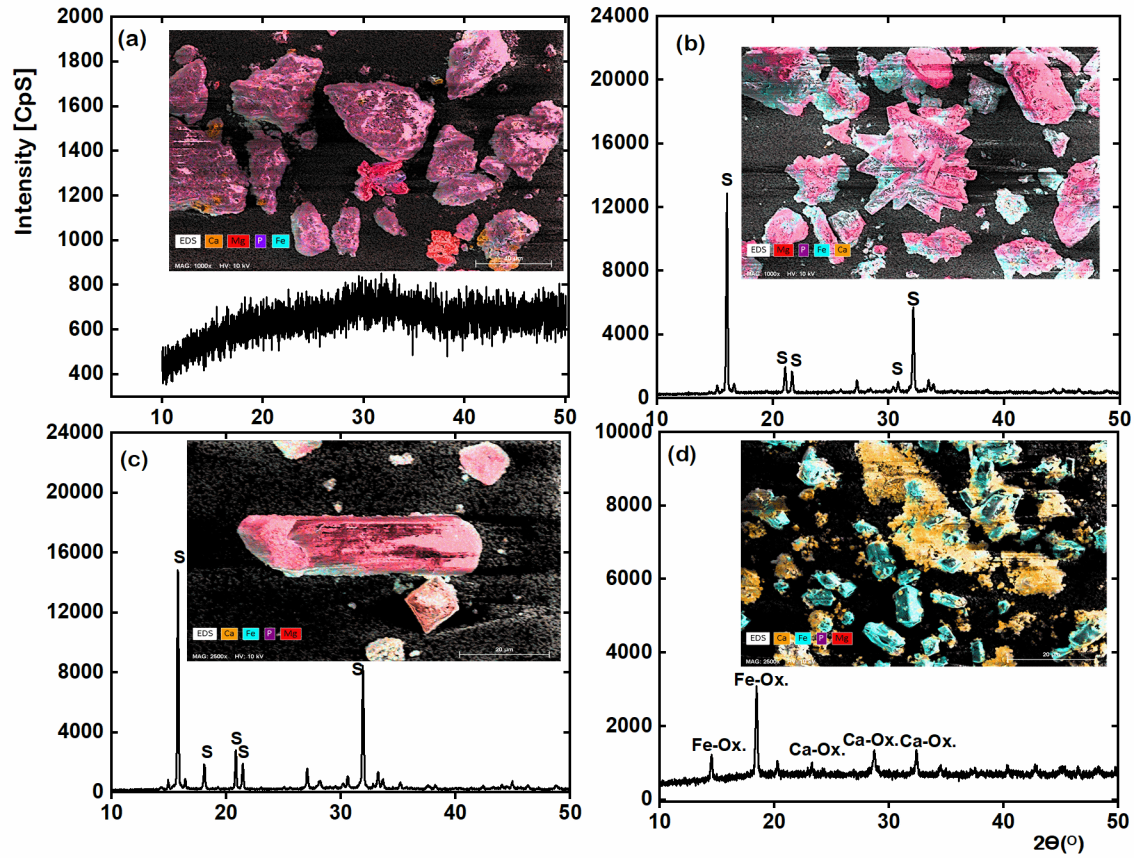

Figure 22. XRD and SEM-EDS graphs of recovered salts from the HTC liquor (a), struvite (s) precipitation without iron removal (b), and after iron removal (c), and the extraction residue with iron oxalate (Fe-ox.) and calcium oxalate (Ca-ox.) (d).

The higher XRD intensity and best crystal structures are obtained after P extraction and iron removal. In this case, the big portion of P is precipitated as struvite (Figure 22c). On the other hand, the solid phase obtained through extraction is an iron and calcium product of the oxalate solid mixture. Its XRD diffraction shows lower peak intensity, while the SEM-EDS indicates high iron and calcium on surface elemental mapping Figure 22b. Furthermore, microscopic images correlate with XRD results. In addition to the lower intensity caused by the formation of amorphous phosphate salts, the SEM-EDS image in Figure 22a indicates a non-crystalline

structure with calcium phosphate as the major element with high signal on the product surface elemental mapping. The results improve in Figure 22b after addition of magnesium salts.
The responsible products are their oxalates salts. They are materials with orthorhombic shapes and their structures were confirmed by XRD analysis.

4.2.7. Struvite precipitation from incinerated sludge ash

a. Wet chemical leaching efficiencies

The solvent composition demonstrated strong effect on magnesite and ash metal dissolution. The magnesite was mixed with ash to have a final ratio of 1.73 of Mg:P mole ratio after addition of phosphoric acid. In contrary of *RecoPhos* process, the use of phosphoric acid was not effective to dissolve both magnesium and ash minerals. The combination of phosphoric acid and hydrochloric acid improved the dissolution efficiencies of magnesium, calcium and iron from their matrices. The increment of hydrochloric acid solvent strength increased the dissolution efficiencies. Compared to the 2M HCl strength, the 4M HCl reached the highest magnesium dissolution of up to 80%. The dissolution efficiencies are depicted on Figure 23 and related efficiencies in percentage are presented in supplementary S. 6. In the same conditions at mixing mole ratio (Ca+Fe):P of 0.25, the calcium and iron dissolution efficiencies were up to 90 and 52% of dissolution efficiencies, respectively. The ash phosphorus dissolution assessed in HCl was 73%.

a. Ash mineral **dissolution** *kinetic*

The dissolution assay is presented on Figure 24 and dissolution model parameters are presented in Table 12. The assay on dissolution time in 4M HCl shows that the upper plateau is reached after 1h. However, the changes become less noticeable in 15 mins. Consideration prediction with dissolution model *Eq. 28,* the maximum dissolution requires 248 min to reach 99.9 % of maximum magnesium dissolution. This can extract up to 88.97 % of magnesite and ash

magnesium, 81.47 and 21.47% of calcium and iron, respectively. The associated kinetic data of measured concentration in function of time are presented in supplementary material S. 7

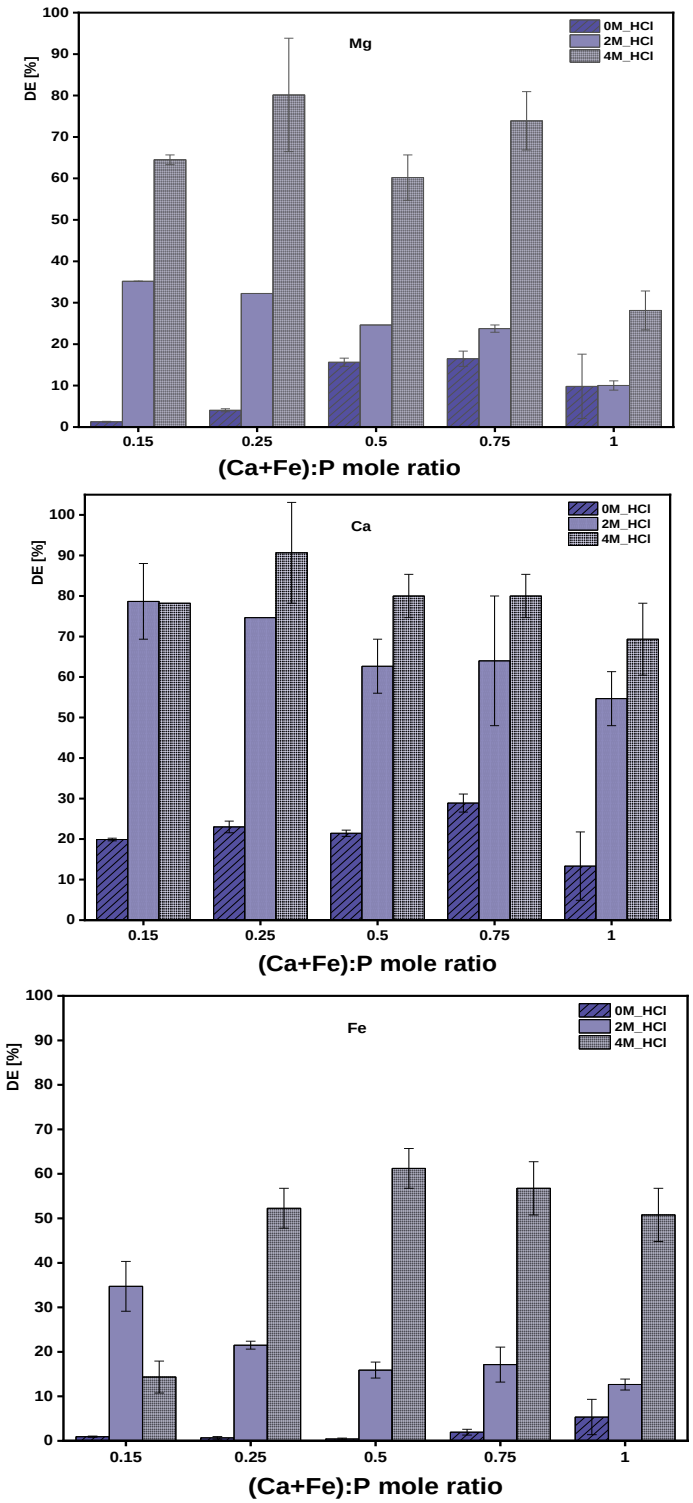

Figure 23. Mineral dissolution efficiencies from ash and magnesite mixture in function of (Ca+Fe): P mole ratios.

Table 12. Kinetic parameters of ash minerals dissolution

Model	C_s(mgkg^{-1})	k (min^{-1})	R^2	τ	T_{80}	$T_{99.9}$	DEmax (%)
P	3335.64 ± 91	0.062	0.978	16.229 ± 1.81	26.12 ± 2.91	112.11 ± 12	54.34 ± 1.5
Ca	4716.96 ± 118	0.069	0.98	14.472 ± 1.54	23.29 ± 2.47	99.97 ± 11	81.97 ± 2.1
Fe	2059.08 ± 41	0.044	0.991	22.863 ± 1.67	36.80 ± 2.69	157.93 ± 12	21.47 ± 0.4
Mg	27577.37 ± 626	0.028	0.992	35.963 ± 2.74	57.88 ± 4.41	248.42 ± 19	88.90 ± 2
K	815.10 ± 34	0.046	0.963	21.809 ± 3.30	35.10 ± 5.30	150.65 ± 22	88.52 ± 3.7

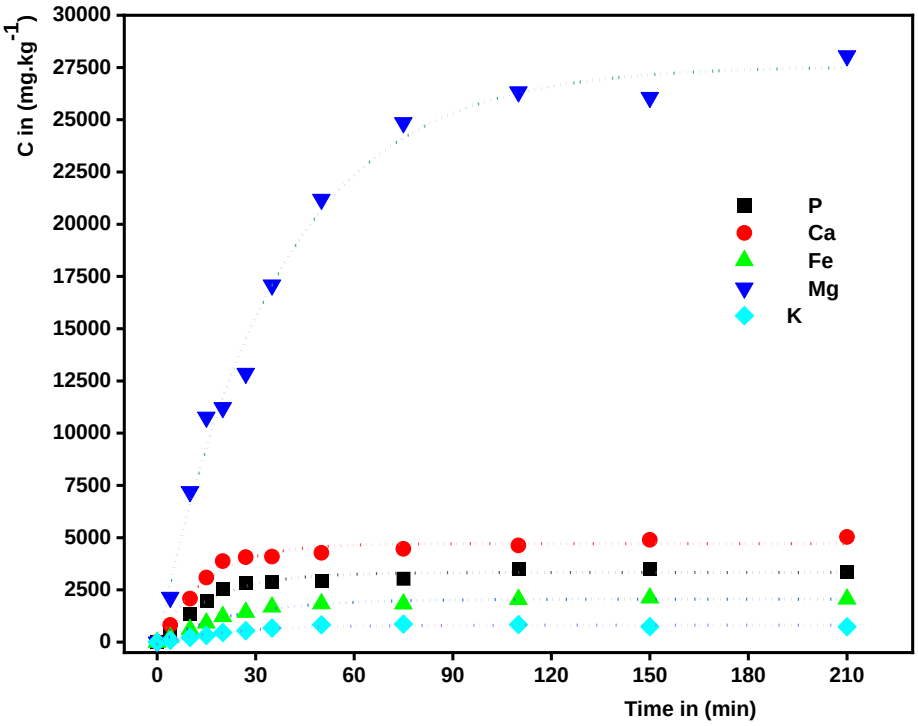

Figure 24. Ash mineral dissolution in function of time.

b. Struvite precipitation from ash leachate

The incinerated dairy sludge ash dissolution in phosphoric acid and hydrochloric acid was followed by struvite precipitation. The best mixing ratios were 0.25 as (Ca+Fe):P mole ratios adjusted by addition of phosphoric acid. The magnesite was then added to a mole ratio of 1.73. The mineral dissolution required the supplementation with hydrochloric acid up 4M HCl in the final mixture until the solid liquid ratio of 1:27 mass/mass of ash and acid extracting solution. It required the time range of 57 to 248 min to reach 80 to 99.9% of mineral dissolution from the ash combined with magnesite, the 1h as time period for struvite precipitation from the

leachate. The ammonium dosage is done on the ash leachate with similar mole ratios of 1.14 NH_4^+:P and the pH 9, as found during the work of struvite precipitation from the HTC liquor.

In this, three products were synthetized where two were synthetized from mimic solution of ash leachate and precipitated at pH 9, with additional 1.14 NH_4+: P and 1.73 Mg:P mole ratio dose using ammonium chloride and magnesium source, respectively. The product (a) was synthetized with magnesium chloride as Mg source, while product (b) was synthetized with magnesite acidic solution as Mg source. The third product (c) was synthetized by addition of ammonium and alkali to the ash and magnesite mixture. Compared to their original ash, the results show that the products were enriched in nitrogen and magnesium. The concentration of nitrogen in the product decreased with matrix effect. This was higher in synthetized struvite from mimic extract with magnesium chloride, and lower by use of magnesite and much lower when magnesite was combined from the ash. Nevertheless, these effects are inversely proportional to the productivity where the mass of product increases with matrix effects. Thus the combination of dairy sludge ash and magnesite for struvite precipitation can yield a better primary macro nutrient profile (N,P,Mg) in the product than the ash and in plenty amount. The comparative table of chemical characteristics of recovered products are highlighted in Table 13.

Table 13. Elemental characteristics of products obtained from ash leachate under different conditions.

ID	Ca	Fe	K	Mg	P_2O_5	NH_4^+	Na	Tot. C
			[%]					
a	0.87	1.87	0.18	12.78	24.20	5.67	2.86	0.15
b	1.39	0.91	0.02	15.50	16.86	3.24	3.29	2.99
c	1.53	2.97	0.22	11.84	19.90	2.48	6.62	0.54

c. Microscopic and spectroscopic characterization of the ash products

The crystalline, orthorhombic structures were observed in all products of struvite precipitation from ash leachate. In mimic solutions and real ash sample, the structures are visible and reflects the struvite products. The SEM images of struvite products are presented in Figure 25.

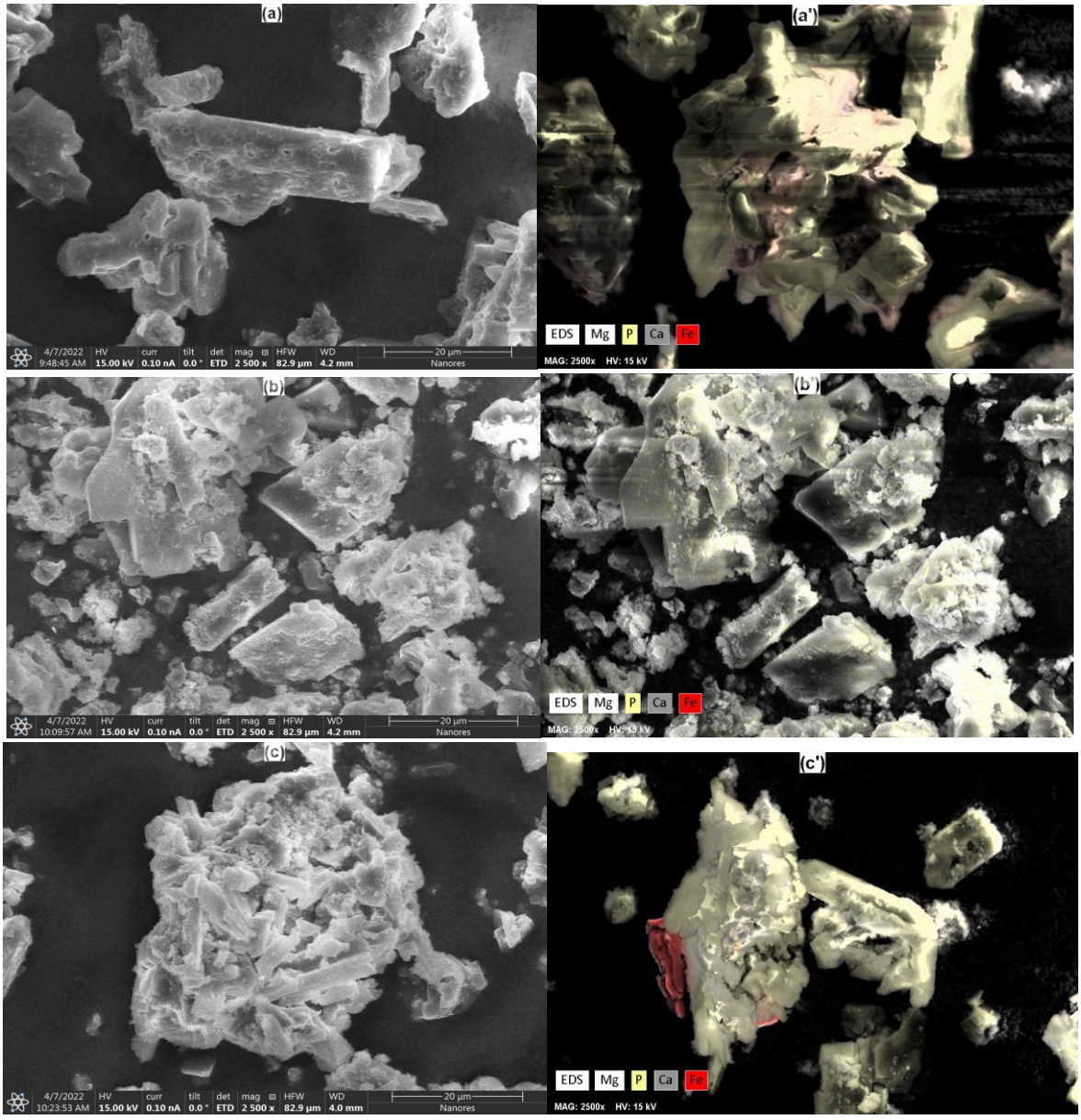

Figure 25. SEM images of synthetic struvite from mimic ash leachate: (a): with magnesium chloride as Mg source, (b): with magnesite as Mg source, (c): struvite from real ash combined with magnesite, and a', b', c', their respective EDS images with elemental mapping

The struvite was confirmed using XRD analysis where it was a predominant phase in the obtained products. As observed in struvite from the liquor, the crystal lattice parameters a: 6.955, b:6.142, and c: 11.218 A^{O} for struvite crystals were observed, as well, in the ash products, and the characteristic peaks were at 15.9, 20.8, 21.5, and 31-32 Θ. The use of magnesite as Mg-source did not affect crystallinity of the products. In Figure 25c, the combination of dairy sludge ash and magnesite highlights big agglomeration of crystals. Thus playing a role of seed materials providing a surface for crystal growth and agglomeration. They show the same crystal properties in products (b) and (c) as in their congeners produced with magnesium chloride (a) (Figure 26a-c). On the other hand, the magnesite used in this work was confirmed by XRD pattern, where it was made by magnesium carbonate (Figure 26d).

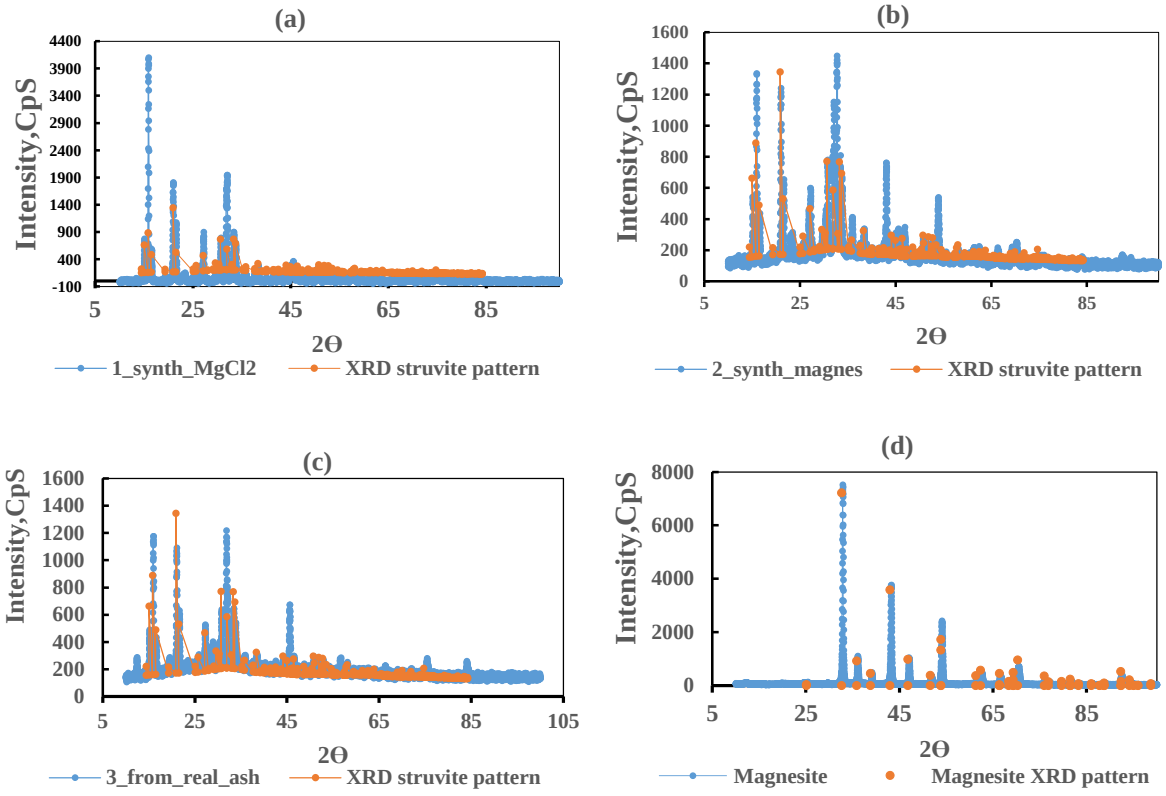

Figure 26. XRD spectra of struvite synthetized from mimic solution of ash extract with different magnesium sources (a): with $MgCl_2$, (b): with magnesite, (c): struvite synthesized from ash combined with magnesite, (d): magnesite.

d. Magnesite and magnesium chloride in struvite precipitation kinetic

Struvite precipitation was effective in the presence of magnesium supplied as magnesium chloride as well as the magnesium supplied as magnesite. In the latter case, the equilibrium is achieved with higher supersaturation due to lower magnesite dissolution requiring the addition of excessive amount with accountability to dissolution rate. In both cases, the P is recovered efficiently > 99% and the final effluent concentration is lower than 2 $mg \cdot kg^{-1}$, a value in the recommended range of P levels in water discharge to environment. Nevertheless, the ionic strenght of initial concentration were higher than validity values, i.e, I>1M.

In fact, the I changed from 1.1 to 0.78 for initial and final values, respectively, during precipitration process with magnesium chloride as Mg source, while the I changed from 1.15 to 0.95M for initial and final I values, respectively, during the struvite precipitation process with magnesite as Mg source. Those *I* values are not reliable and have not a valid correction in thermodynamic correction of precipitation models. It is due to high concentration of minerals that the initial state can not exist in homogeneous equilibrium.

They immediately undergo precipitation process. Therefore, for modelling purposes, the Davis maximal value ($I=0.3M$) was used in thermodynamic correction of the concentration. The comparative aspect of magnesite and magnesium chloride performance in struvite precipitation process is highlighted in Figure 27.

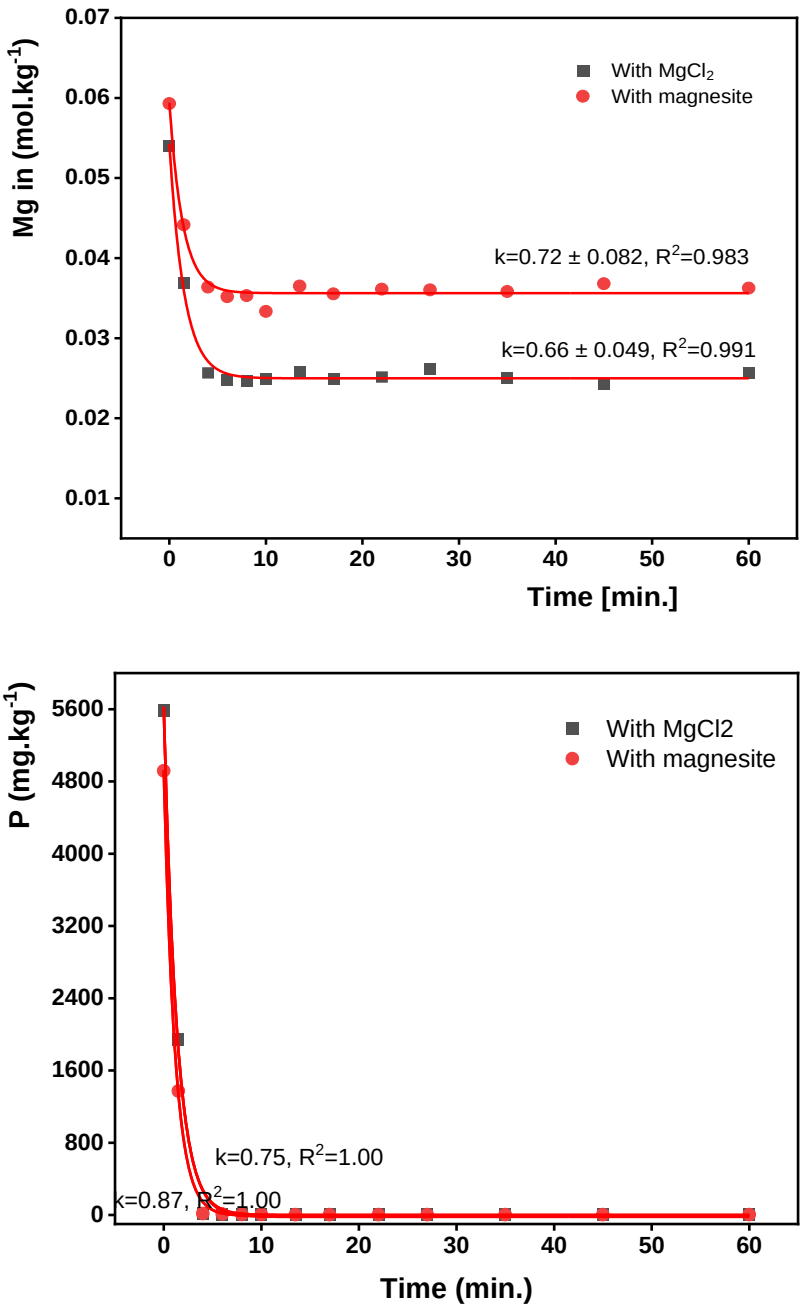

Figure 27. Precipitation kinetic for magnesium and Phosphorus in function with time

4.2.8. Summarisation of phosphorus recovery from thermochemically processed sludge

During hydrothermal processing of dairy sludge, the P and multivalent metals likely partition in the hydrochar than in the liquor. This is due to thermodynamic properties of phosphate salts formed with these metals. They are potentially prompt of precipitation and settle in hydrochar

at equilibrium (Section 4.2.1). This partition induced by the presence of multi-valent metals is in agreement with previous works by (Atallah et al., 2019).

The P species in the liquor are mostly iron phosphate species with more than 60% of molar fraction on total P. The direct precipitation upon pH adjustment to 9, resulted in the vivianite, which is the main iron phosphate salt with high saturation index, and calcium phosphate salts, which present the highest saturation indices. These two metals are the main metal components in recovered salts and have the main effect on the quality of recovered products. In the worst case, the recovered product has high iron concentration, which makes it restricted on EU market as an alternative to conventional phosphate fertilizer.

The mitigation of iron effect on the final product was favored by use of extraction process. Oxalic acid was found to be the best to settle iron and extract P to supernatant. This achieved the settling of 86.6% of iron and 93% of calcium from hydrothermal carbonization liquor of iron based sludge by precipitation using oxalic acid followed by struvite precipitation. The obtained iron removal efficiency confirms the settling property of ferrous ions by oxalic acid thus can be applied in extraction process of iron-P rich liquor for their purification into separate products (Abis et al., 2018; Elomaa et al., 2019). The oxalate product is reportedly useful in sorption materials and nanomaterials synthesis, and other products recycling (Li et al., 2019).

The optimization of process conditions and salts dosage indicated the pH 9 and the optimum dosage in terms of molar ratios is 1.73, and 1.14 for Mg^{2+}:P and NH_4^+:P, respectively. When an excess of ammonium was in the liquor, the ratio of NH_4^+:P is initially adjusted to 1.14 by additional source of P such as K_2HPO_4 or H_3PO_4. The Mg addition must then take into account the update value. As presented in theoretical part (Table 2) of previous researches, the addition of extra P source is the main option to mitigate the effect of competing ions, the amount needed for proper adjustment is obtained under experimental studies of each matrix. These optimum conditions enhance the HTC liquor P recovery of 99.96% and the struvite yield up to 91.02%.

The P, and Fe in effluent are in acceptable limits of environmental safety for production discharges. The ammonium level was a bit higher than the recommended levels, which would require the striping or sorption process to remove it. Clinoptilolite demonstrated the properties to remove ammonium with Q_e of 1.25 $mg \cdot g^{-1}$. This *Qe* value is equivalent to 0.07 meq·g-1, a value lower to 0.1 $meq \cdot g^{-1}$ obtained by zeolite modification to Mg-homoionic form (Numviyimana et al., 2021).

Struvite precipitation from sludge ash needed the wet chemical extraction with acids. Since Mg is needed as struvite precursor, the magnesite was combined with ash. The use of phosphoric acid alone as leaching acid is not effective to dissolve the minerals and P from the iron based ash. The supplementation with hydrochloric acid up to 4 M efficiently dissolved magnesite combined with the ash. The best mixing is (Ca + Fe):P mole ratio of 0.25 adjusted with P acid and 1.73 Mg:P mole ratio in 4 M HCl and solid liquid ratio of 1:21.

The struvite produced with magnesite had similar crystal lattice properties as the one produced with magnesium chloride in ash extract mimic solutions. In both production processes, the final P concentration was lower than 2 $mg.dm^{-3}$. The struvite precipitation product from magnesite-ash leachate was much more agglomerated, which highlight the seeding properties of the undissolved ash matter.

The struvite products from both HTC liquor and sludge ash had high level of phosphorus (24-28 %P_2O_5), Nitrogen (2-6.69 NH_4^+) and magnesium (10-12 %) (see *Table 11* product c and *Table 13*, product c). Except sodium, other metals in struvite from the liquor were less than 2%. This indicates that the products can be used as fertilizer accepted on the market with ability to provide primary plant macronutrients (N and P), secondary plant macronutrient (Mg), and a micronutrient (Fe) with its appropriate content.

Considering the obtained optimum conditions and the yields, the results are in good range of P recovery as struvite. The advantage of using iron based sludge include the production of struvite with proper amount of iron as micronutrient. The comparison with previous work is presented in Table 14. By use of multiple optimization approach, it was possible to reach lower mixing ratios and achieve higher P recovery.

Table 14. Comparative table of mixing ratios and P recovery under this work and in literature

	This work					**Others' works**			
Ref.	(Numviyimana et al., 2020)		(Numviyimana et al., 2021)		(Numviyimana et al., 2022)	(Lavanya and Sri Krishnaperumal Thanga, 2020)	(Khater et al., 2015)	(Daneshgar et al., 2018a)	(Capdevielle et al., 2013a)
Matrix	Cheese wastewater		Cheese wastewater		HTC sludge liquor*	Dairy wastewater	Waste-water	Sludge liquor	Swine wastewater
pH	8.3	8.9	8.9	8.9	9	9.5	10.89	8.5, 9.5	10.7
Mg:P	1.26	1.21	1.51	1.51	1.73	4	2.25	5	2.25
Ca:P	0.25	0.26	0.26	0.05	-	0.05*	-	1.95	1
NH_4^+:P	2.32	2.69	0.8	0.61	1.14	12*	-	5	3.1
P rec.	**92%**	**99**	**99**	**99.05**	**99.96**	**92.60%**	**84.70%**	**84%, 94%**	**>90%**

*Iron and calcium were firstly removed by precipitation as oxalate

4.3. Qualification of phosphorus fertilizers

4.3.1. In-vitro nutrient release assay

The *in vitro* nutrient release assay in 2% citric acid solution demonstrated a significant difference in P release and availability. The P purification from the sludge liquor by extraction followed by precipitation demonstrated the advantage in nutrients availability. The in-vitro nutrient release assay is presented in Figure 28.

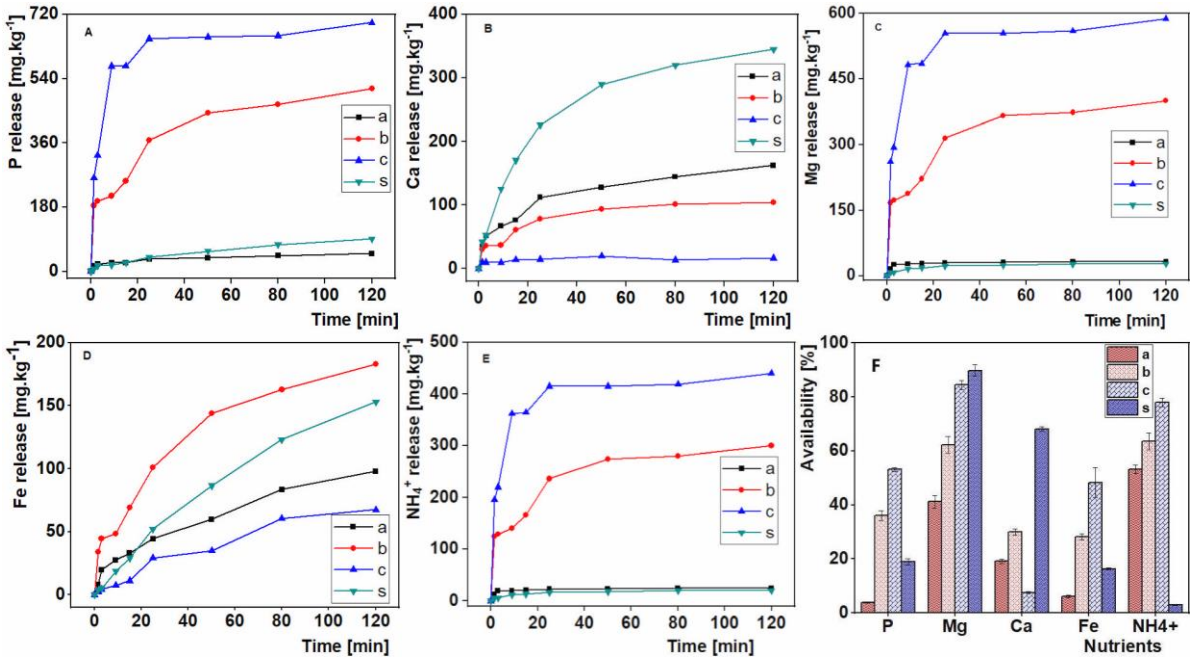

Figure 28. In vitro nutrient release assay in citrate solution for phosphorus (A), calcium (B), magnesium (C), iron (D), ammonium (E), and their availability (F)

The P release in terms of C_{max} for the raw sludge (*s*) was lower than their purified products. The product (c) of P extraction combined with precipitation exhibits better nutrient availability with higher C_s than others. This property is affected by increased iron and calcium content, where C_s was lower in precipitation products obtained without iron removal (a, b). The effect was even stronger in the case of HTC liquor recovered salts, where P release was the lowest of phosphate precipitates (*Figure 28*a). Nutrient availability was more decreased with a lower level of struvite content, and high iron and calcium content. The latter reached a higher concentration of release in citric acid for products *a*, *b*, and *s*. In particular, for P and N availability, the product *c* of P extract reached the highest percentage of solubility in citric acid solution (*Figure 28*F and *Table 15*).

Table 15. Kinetic parameters of the in-vitro nutrient release assay for recovered products (a, b, c) and their raw sludge (s)

Model	Product	C_{max}(mg.kg^{-1})	k [min^{-1}]	R^2	τ	t_{80}	Availability [%]
P release	**a**	46.42	0.04	0.894	22.50	36.22	3.77
	b	497.08	0.04	0.92	23.72	38.18	36.03
	c	653.32	0.23	0.981	4.28	6.88	53.10
	s	108.39	0.01	0.988	69.39	111.67	18.96
Mg Release	a	30.49	0.55	0.965	1.84	2.95	41.20
	b	387.63	0.05	0.899	18.68	30.06	62.22
	c	547.92	0.27	0.968	3.68	5.93	84.42
	s	25.81	0.08	0.975	12.16	19.58	89.78
Ca release	a	153.47	0.04	0.958	23.44	37.73	19.09
	b	102.80	0.05	0.956	20.31	32.69	29.97
	c	14.82	0.41	0.760	2.42	3.90	7.45
	s	335.40	0.04	0.996	22.76	36.63	68.16
Fe release	a	109.87	0.02	0.979	59.67	96.04	6.13
	b	187.91	0.03	0.979	38.12	61.36	28.26
	c	90.83	0.01	0.979	83.93	135	48.31
	s	210.37	0.01	0.999	91.78	147.71	16.34
NH_4^+ release	a	22.86	0.55	0.965	1.84	2.95	53.16
	b	290.72	0.05	0.899	18.68	30.06	63.61
	c	410.94	0.27	0.968	3.68	5.93	77.98
	s	19.36	0.08	0.975	12.16	19.58	2.92

4.3.2. In-vivo nutrients use efficiencies

The *in*-vivo assay on the cucumber demonstrated similar effects. The germination test showed a difference in terms of plant health and nutrient effects. After one week, the seeds were effectively germinated at 80, 32, and 88% for the control, and the soil fertilized with P products *b* and *c*, respectively. The lower germination rate observed for high iron content products (*b*) highlights the risk of phyto-toxicity. On the other hand, removing a large fraction of iron makes the product more valuable for fertilizer application. The Iron content in the product is within the accepted range and becomes a benefit to the plant for the production of a micronutrient bio-fortified diet. After two weeks, the harvested fresh biomass was weighed, dried, and analyzed on a dry matter basis.

With consideration of nutrient efficiency ratio, the NER parameter is lower for fertilized biomass than the control, thus highlighting the higher uptake of nutrients in the fertilized trials. The comparative experiments were aimed at highlighting the effect of iron on fertilizer quality. The high efficiency parameters were found with product *c* (L-HTC), the product after iron removal.

Table 16. In-vivo assay and nutrient use efficiencies for different struvite products

		Control (a)	HTC (b)	L-HTC (c)
	Mass soil (kg)	0.874	0.874	0.874
	Number Seeds	25	25	25
	Fertilizer used	0	5	5
	Germinated	18	8	22
	Germ. Rate (%)	80	32	88
Applied nutrient ($x10^{-5}$ kg)	N	0	17.8	28.5
	Mg	0	31.2	55.9
	P	0	56.4	56.1
	Fe	0	33.3	5.55
	Fresh biomass (g)	26	16	57
	Dry biomass (g)	4.6	2.6	5.9
	%DM	17.40	16.67	10.23
DM conc ($g.kg^{-1}$)	N (%)	2.86	4.22	3.18
	Mg ($g.kg^{-1}$)	8.07	10.41	9.99
	P($g.kg^{-1}$)	1.41	14.93	14.27
	Fe ($g.kg^{-1}$)	0.11	0.19	0.09
NER	N	34.96	23.68	31.45
	Mg	123.97	96.05	100.07
	P	310.35	29.24	30.60
	Fe	9.01	5.35	10.72
PE	N	-	101.41	23.26
	Mg	-	206.79	59.76
	P	-	-25.34	7.37
	Fe	-	378.61	-112.22
AE	N	-	-0.44	0.30
	Mg	-	-6.15	2.33
	P	-	-3.40	2.32
	Fe	-	-5.77	23.48
NAR	N	-	-10.64	19.66
	Mg	-	-2.98	3.9
	P	-	16.01	34.12
	Fe	-	1.49	9.85

On the other hand, the efficiency parameters decreased on trials fertilized with *b* (HTC) due to an excess of iron content. This observation is an emphasis on iron content limitation in phosphate fertilizers. Additionally, this negative effect was studied and confirmed elsewhere (Römer and Samie, 2002). Nevertheless, the iron optimum content in the product demonstrated

the improvement of AE and ANR parameter. The latter became worse for trials fertilized with high iron content where they became negative, thus the applied nutrients remained almost unused compared to the control trial. In contrast, the PE results demonstrate the potential of micro-elements in plant growth, where the PE was improved. Similar effects were previously reported by other research where iron was particularly the major micro-element in the fertilizer formulation (Popko et al., 2018). This plays a major role in the bio-fortification and the production of micronutrients-based functional foods. In addition, previous research found that application of 2.5 g struvite per kg of soil increased the amount of cucumber harvested plant biomass by 64% versus control treatment (Yetilmezsoy et al., 2020). The nutrients use efficiency parameters that include NER, PE, AE, and ANR for *Eq. 30-33* are reported in *Figure 29*a-e.

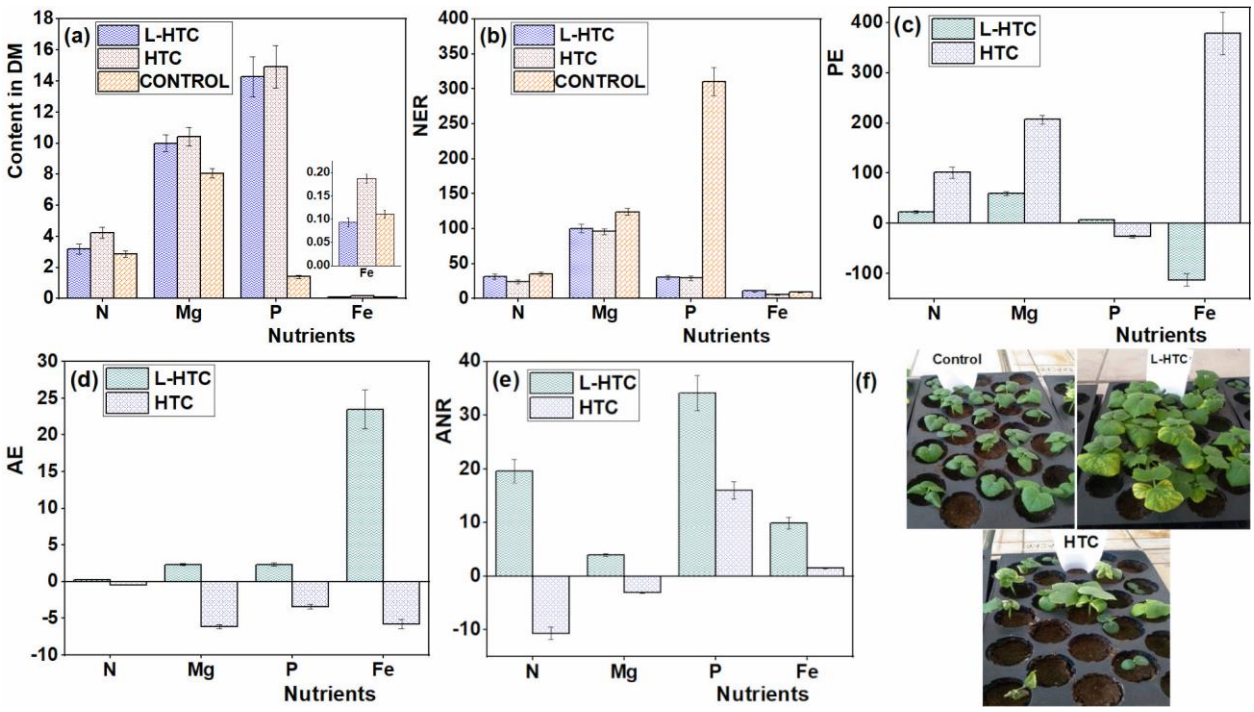

Figure 29. Nutrient content (a) on the basis of dry biomass for N (%), and other elements (g·kg^{-1}); their use efficiency parameters: (b) NER (kg DM·kg^{-1}); (c) PE in kg net DM yield per unit mass of nutrient uptake; (d) AE as kg net DM per unit mass of applied nutrient; (e) ANR as the % of uptake by net DM on the unit mass of applied nutrient, and (f) the plant status for control, fertilized soil by struvite with (L-HTC) and without (HTC) iron removal.

4.3.3. Summarization of phosphorus fertilizers qualification

The dairy sludge has lower nutrients availability than their purified products. The P product obtained by direct precipitation process has also lower P availability due to high iron and calcium concentration forming less soluble P compounds of vivianite and calcium phosphate, respectively. The extraction with oxalic acid removes iron followed by struvite precipitation from the extract mitigated this problem resulting in product with better nutrients availability.

The nutrients use efficiency parameters on plant were worse on high iron content products accompanied with germination inhibition. The germination rate was effective with struvite produced after extraction process. Therefore, it is evident that fertilizer quality of the recovered product is affected by iron content. Removing iron enhances the production of struvite with good level of that micronutrient (Fe), thus making plant healthier. The agronomic efficiency and apparent nutrients recovery parameters are thereby improved.

4.4. Business case and cost effectiveness

The business case is presented for producing the struvite with the use of raw materials of dairy sludge HTC process water.

Potential applications of the obtained preparations are:

1. An alternative conventional P fertilizer for supply of P and nitrogen as plant primary macronutrients, and magnesium as the secondary macronutrient for different crops.
2. Maintain a small content of iron (<2%) in the product for both product purity and optimum micronutrient composition
3. To recover both phosphorus and Iron into two separate products with agricultural and chemical applications, respectively. The production model involving sludge processing and resources recoveries is presented as in
4. Figure 30

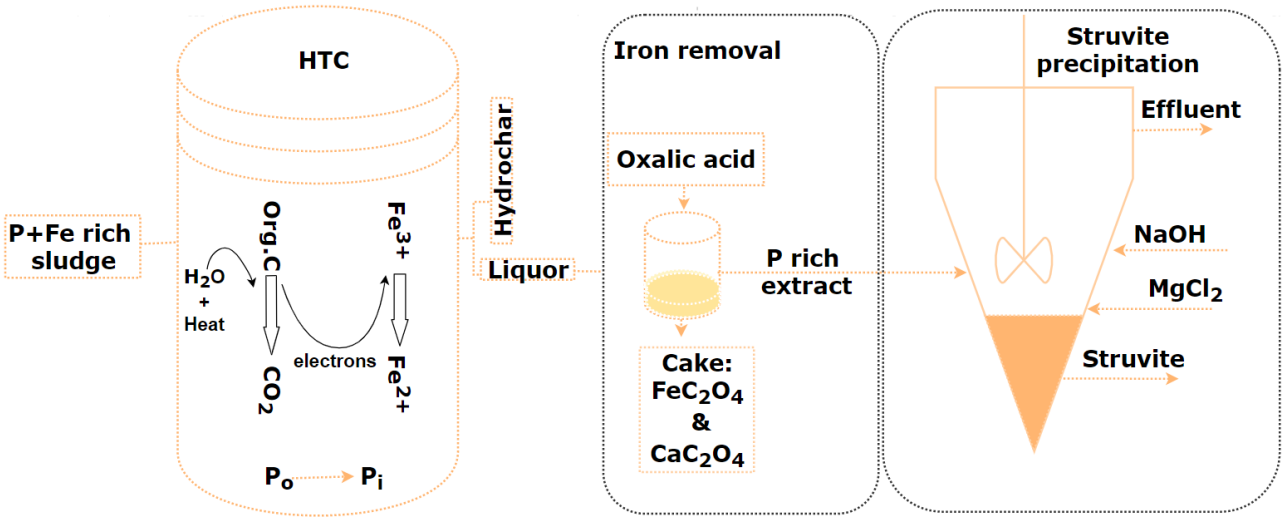

Figure 30. *Model of coupled dairy sludge hydrothermal processing and struvite precipitation*

From the HTC process water (liquor), the implementation of struvite precipitation cannot suit to Ostara system due to involvement of double precipitation process, which one consists of iron and calcium precipitation as oxalate salts (Reactor 1, R1), and extract P precipitation as struvite (Reactor2, R2), both in separate reactors. Thus we design a system of double connected reactors with the similar mechanical properties.

In the first tank, the iron and calcium are precipitated by oxalic acid and the supernatant rich in P is continued to struvite precipitation reactor. The extraction time is 30-60min. In the second tank, the liquor leachate, the magnesium chloride, and sodium hydroxide are added up to pH 9 for struvite crystallization. Adopting the famous reactors of Pearl® Fluidized Bed Reactors as described in their works (OSTARA, 2018), the combination of two sequential reactors both serving in precipitation of oxalates salts and struvite, respectively is described by the drawing in Figure 31

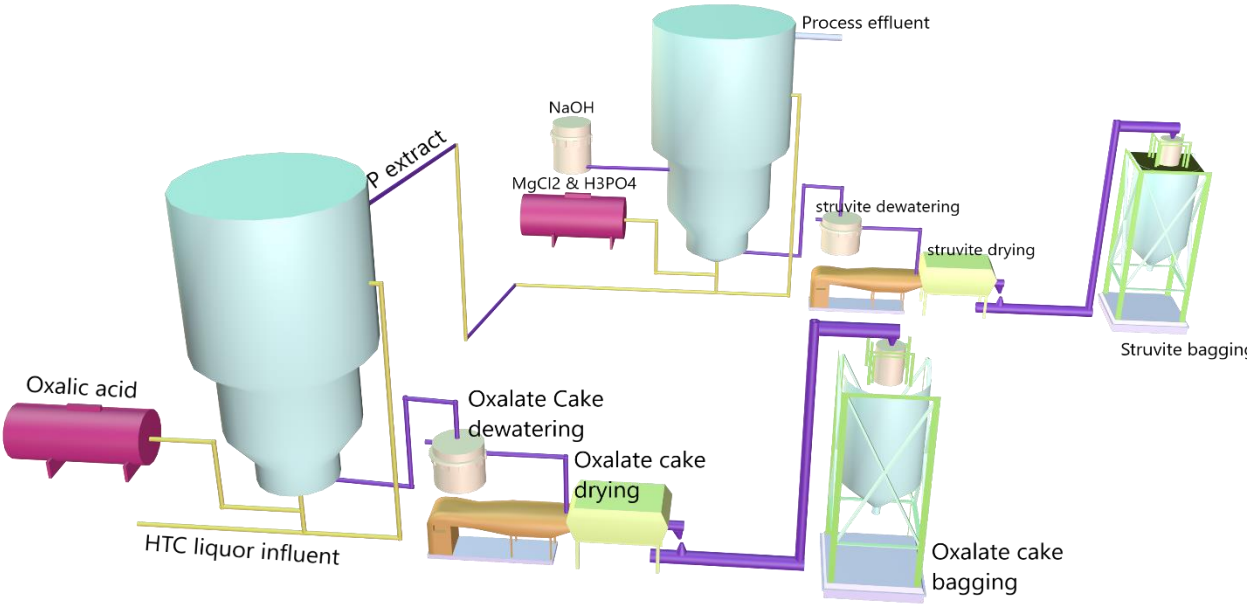

Figure 31. Illustration of industrial plant set-up for iron recovery as oxalates and phosphorus recovery as struvite

Considering previously published work on coupling hydrothermal process with chemical extraction and struvite precipitation (Numviyimana et al., 2022), the respective reactions occurs in consecutive reactors as illustrated in *Figure 31*. The production yield, energy and material balances, operational, maintenance, installation, and chemical costs related to the configuration and the cost effectiveness are presented in supplementary

S. 9.

For the cost effectiveness, the full scale with 10K Ostara fluidized bed reactor system makes 1.11 USD·kg^{-1} and 9.01 USD·kg^{-1} to struvite production and P recovery costs, respectively. The high production cost was previously reported per 1kg P in range from 11USD to 55 USD (i.e. nearly 9.52 to 47.61 €) while their products market prices ranges from 0.95 to 4 USD per 1 kg (i.e. nearly 0.82 to 3.46 €) (Kim et al., 2021). Additionally, the iron and calcium oxalates were recovered. This cost is affordable view the value of produced struvite enriched with proper content of iron, a plant essential micronutrient.

5. CONCLUSIONS

1. The P recovery as struvite encounters interfering ions that, when available at high concentration, they inhibit struvite precipitation. These include mainly calcium and iron. Both metals are the most abundant in chemically accumulated sludge with iron salts as coagulants. Their precipitation potential can reach 45 magnitudes higher than that of struvite. This affects both the process efficiency and the quality of the product as fertilizer.

2. The coupling hydrothermal processing of sludge and struvite precipitation presented a prominent approach in dairy sludge valorisation. The obtained hydrochar can serve as biochar usable as accepted fertilizing biosolid. The obtained nutrients rich liquor is valorised by P and N recovery through struvite precipitation.

3. Stoichiometric analysis indicated that P species are more iron bound which $FeHPO_4$ and $FeH_2PO_4^+$ have 60% of fraction of total P in the HTC liquor of iron based sludge. Similarly, the precipitation directly applied on the liquor by pH adjustment to 9 produces a high iron content product with lower P availability and the risk of phyton-toxicity to plant for uncontrolled fertilizer dose.

4. Chemically produced sludge required the use of extracting agent to remove iron followed by struvite precipitation. The use of oxalic acid up to 0.375M was effective to extract 86.7% of P and remove 86.6% of iron. This enhances both P recovery and iron recycling into two separate products for agricultural and chemical applications, respectively. The fraction of 58% of P in feed stock came from dairy sludge liquor which is a big contribution to waste resources valorisation and non-renewable nutrient recovery.

5. The experimental design and multiple optimization process is accurate for determination of the optimal process conditions of pH and salts dosage in form of mixing molar ratio (Ca:P, Mg:P, NH_4^+:P) for struvite precipitation. The optimum initial conditions were pH

~9, mixing rations of 1.73 and 1.14 as Mg:P and N:P mole ratios of magnesium and ammonium to phosphate, respectively. The P recovery efficiency is up to 99.96% and 82% of nitrogen recovery.

6. The obtained products of struvite precipitation from HTC liquor demonstrated good quality as fertilizer. Struvite showed better nutrient release with higher Cs for P in citric acid. This value was decreased with the increase of Fe level in the initial mixing conditions. The nutrients use efficiency was better on struvite than the phosphate products obtained without iron removal. In contrast, at the same application dose with high iron level caused lower germination rates.
7. The use of zeolitic material either as additive to the reactor or in the effluent enhanced the ammonium removal to lower level as well as process thermodynamics. These combined precipitation and sorption processes beneficiate to obtaining two fertilizing materials: struvite and ammonium saturated natural zeolite.
8. The cost effective way of struvite production is the coupling of hydrothermal processing and precipitation through extraction. The adopted Ostara fluidized bed reactors with 10K reactor system, the struvite production cost is approximately 1.11 USD/Kg. It makes a promising and cheap technology to contribute to dairy wastes management by valorising them into a micronutrient enriched struvite fertilizer.

6. RECOMMENDATIONS FOR FUTHER RESEARCH

The research on dairy wastes processing and struvite precipitation using EBPR sludge is worth being conducted and compared with the chemically produced sludge. The EBPR sludge involves longer production time, however the struvite precipitation from their processing liquor may not need any further metal removal. This can decrease the number of steps such as the skipping of extraction and addition of oxalic acid associated reagents. The alternative P accumulation that is recommended for further researches is lime based sludge. These technologies are left on bench scale. However, once performed they can produce a raw sludge with the liquor of good chemical profile for struvite and calcium phosphate salts. Along with magnesium, calcium is an important plant secondary macronutrient.

The production of struvite from dairy wastes for commercial purposes needs awareness of all stakeholders involved in wastes generation. The financial contribution of all involved parties can mitigate the final product costs thus making the process more sustainable. Thus, there is a need for a business model involving the contribution of wastes generators, wastewater treatment, their sludge thermochemical treatment, and struvite precipitation. Establishing a pilot plant for dairy sludge hydrothermal processing, coupled to HTC liquor nutrients extraction and precipitation as illustrated in the business model presented in this study is recommended for implementation.

This work involved recovery of iron along with P. The iron and calcium were precipitated separately during extraction process and produced solid products of crystalline iron (II) oxalate and calcium oxalate. Further research on their application as sorbents, or in synthesis of metal organic frameworks and nanomaterials, or in coagulants recycling could allow achievement of the circular economy.

III. REFERENCES

Abella, E.T., 2017. Assessment of Struvite and K-Struvite Recovery From Digested Manure.

Abis, M., Calmano, W., Kuchta, K., 2018. Innovative technologies for phosphorus recovery from sewage sludge ash. Detritus 1, 23–29. https://doi.org/10.26403/detritus/2018.23

Ajiboye, B., Akinremi, O.O., Hu, Y., Flaten, D.N., 2007. Phosphorus Speciation of Sequential Extracts of Organic Amendments Using Nuclear Magnetic Resonance and X-ray Absorption Near-Edge Structure Spectroscopies. J. Environ. Qual. 36, 1563–1576. https://doi.org/10.2134/jeq2006.0541

Akhiar, A., Battimelli, A., Torrijos, M., Carrere, H., 2017. Comprehensive characterization of the liquid fraction of digestates from full-scale anaerobic co-digestion. Waste Manag. 59, 118–128. https://doi.org/10.1016/j.wasman.2016.11.005

Ali Adnan, 2002. Pilot-scale study of phosphorus recovery through struvite crystallization. THE UNIVERSITY OF BRITISH COLUMBIA.

Almuktar, S.A.A.A.N., Abed, S.N., Scholz, M., 2018. Wetlands for wastewater treatment and subsequent recycling of treated effluent: a review. Environ. Sci. Pollut. Res. 25, 23595–23623. https://doi.org/10.1007/s11356-018-2629-3

Amann, A., Zoboli, O., Krampe, J., Rechberger, H., Zessner, M., Egle, L., 2018. Environmental impacts of phosphorus recovery from municipal wastewater. Resour. Conserv. Recycl. 130, 127–139. https://doi.org/10.1016/j.resconrec.2017.11.002

An, S.W., Jeong, Y.C., Cho, H.H., Park, J.W., 2016. Adsorption of NH4+-N and E. coli onto Mg2+-modified zeolites. Environ. Earth Sci. 75, 1–11. https://doi.org/10.1007/s12665-016-5476-x

Arena, G., Musumeci, S., Purrello, R., Sammartano, S., 1983. Calcium- and magnesium-EDTA complexes. Stability constants and their dependence on temperature and ionic strength. Thermochim. Acta 61, 129–138. https://doi.org/10.1016/0040-6031(83)80309-8

Ashekuzzaman, S.M., Forrestal, P., Richards, K., Fenton, O., 2019. Dairy industry derived wastewater treatment sludge: Generation, type and characterization of nutrients and metals for agricultural reuse. J. Clean. Prod. 230, 1266–1275. https://doi.org/10.1016/j.jclepro.2019.05.025

Ashekuzzaman, S.M., Forrestal, P., Richards, K.G., Daly, K., Fenton, O., 2021. Grassland Phosphorus and Nitrogen Fertiliser Replacement value of Dairy Processing Dewatered Sludge. Sustain. Prod. Consum. 25, 363–373. https://doi.org/10.1016/j.spc.2020.11.017

Atallah, E., Kwapinski, W., Ahmad, M.N., Leahy, J.J., Zeaiter, J., 2019. Effect of water-sludge ratio and reaction time on the hydrothermal carbonization of olive oil mill wastewater treatment: Hydrochar characterization. J. Water Process Eng. 31, 100813. https://doi.org/10.1016/j.jwpe.2019.100813

Azzaz, A.A., Jeguirim, M., Kinigopoulou, V., Doulgeris, C., Goddard, M.L., Jellali, S., Matei Ghimbeu, C., 2020. Olive mill wastewater: From a pollutant to green fuels, agricultural and water source and bio-fertilizer – Hydrothermal carbonization. Sci. Total Environ. 733, 139314. https://doi.org/10.1016/j.scitotenv.2020.139314

Babcock & Willcox Vølund, 2012. 21’ Century Advanced Concept for Waste-Fired Power Plants.

Baeza Baeza, J.J., Ramis-Ramos, G., 1996. A series expansion of the extended Debye-Huckel equation and application to linear prediction of stability constants. Talanta 43, 1579–1587. https://doi.org/10.1016/0039-9140(96)01942-X

Baligar, V.C., Fageria, N.K., He, Z.L., 2001. Nutrient use efficiency in plants. Commun. Soil Sci. Plant Anal. 32, 921–950. https://doi.org/10.1081/CSS-100104098

Ballirano, P., De Vito, C., Mignardi, S., Ferrini, V., 2013a. Phase transitions in the MgCO2H2O system

and the thermal decomposition of dypingite, Mg5(CO3)4(OH)2·5H2O: Implications for geosequestration of carbon dioxide. Chem. Geol. 340, 59–67. https://doi.org/10.1016/j.chemgeo.2012.12.005

Ballirano, P., De Vito, C., Mignardi, S., Ferrini, V., 2013b. Phase transitions in the MgCO2H2O system and the thermal decomposition of dypingite, Mg5(CO3)4(OH)2 · 5H2O: Implications for geosequestration of carbon dioxide. Chem. Geol. 340, 59–67. https://doi.org/10.1016/J.CHEMGEO.2012.12.005

Barnes, N.J., Bowers, A.R., 2017. A probabilistic approach to modeling struvite precipitation with uncertain equilibrium parameters. Chem. Eng. Sci. 161, 178–186. https://doi.org/10.1016/j.ces.2016.12.026

Bashar, R., Gungor, K., Karthikeyan, K.G., Barak, P., 2018. Cost effectiveness of phosphorus removal processes in municipal wastewater treatment. Chemosphere 197, 280–290. https://doi.org/10.1016/j.chemosphere.2017.12.169

Becker, R., Dorgerloh, U., Paulke, E., Mumme, J., Nehls, I., 2014. Hydrothermal carbonization of biomass: Major organic components of the aqueous phase. Chem. Eng. Technol. 37, 511–518. https://doi.org/10.1002/ceat.201300401

Bell, L.C., Mika, H., Kruger, B.J., 1978. Synthetic hydroxyapatite-solubility product and stoichiometry of dissolution. Arch. Oral Biol. 23, 329–336. https://doi.org/10.1016/0003-9969(78)90089-4

Bennett, A.M., Lobanov, S., Koch, F.A., Mavinic, D.S., 2017. Improving potassium recovery with new solubility product values for K-struvite. J. Environ. Eng. Sci. 12, 93–103. https://doi.org/10.1680/jenes.17.00019

Berg, U., Ehbrecht, A., Röhm, E., Weidler, P.G., Nüesch, R., 2007. Impact of calcite on phosphorus removal and recovery from wastewater using CSH-filled fixed bed filters. J. Residuals Sci. Technol. 4, 73–81.

Blöcher, C., Niewersch, C., Melin, T., 2012. Phosphorus recovery from sewage sludge with a hybrid process of low pressure wet oxidation and nanofiltration. Water Res. 46, 2009–2019. https://doi.org/10.1016/j.watres.2012.01.022

Bontoux, L., 1999. The incineration of waste in Europe: issues and perspectives 47.

Britton, A., Sacluti, F., Oldham, W.K., Mohammed, A., Mavinic, D.S., Koch, F.A., 2007. Value from waste: struvite recovery at the city of Edmontons Gold Bar WWTP. Proc. IWA Spec. Conf. Mov. Forw. - Wastewater biosolids Sustain. 575–581.

Bruschi, M.L. (Ed.), 2015. Mathematical models of drug release, in: Strategies to Modify the Drug Release from Pharmaceutical Systems. Elsevier, pp. 63–86. https://doi.org/10.1016/B978-0-08-100092-2.00005-9

Bunce, J.T., Ndam, E., Ofiteru, I.D., Moore, A., Graham, D.W., 2018. A review of phosphorus removal technologies and their applicability to small-scale domestic wastewater treatment systems. Front. Environ. Sci. 6, 1–15. https://doi.org/10.3389/fenvs.2018.00008

Capdevielle, A., Sýkorová, E., Biscans, B., Béline, F., Daumer, M.L., 2013a. Optimization of struvite precipitation in synthetic biologically treated swine wastewater-Determination of the optimal process parameters. J. Hazard. Mater. 244–245, 357–369. https://doi.org/10.1016/j.jhazmat.2012.11.054

Capdevielle, A., Sýkorová, E., Biscans, B., Béline, F., Daumer, M.L., 2013b. Optimization of struvite precipitation in synthetic biologically treated swine wastewater-Determination of the optimal process parameters. J. Hazard. Mater. 244–245, 357–369. https://doi.org/10.1016/j.jhazmat.2012.11.054

Carlos Escobar Palacio, J., Joaquim Conceição Soares Santos, J., Luiza Grillo Renó, M., Corrêa Furtado Júnior, J., Carvalho, M., Martín Martínez Reyes, A., José Rúa Orozco, D., 2019. Municipal Solid Waste Management and Energy Recovery, in: Energy Conversion - Current Technologies and Future Trends. IntechOpen, p. 13. https://doi.org/10.5772/intechopen.79235

Chimenos, J.M., Fernández, A.I., Villalba, G., Segarra, M., Urruticoechea, A., Artaza, B., Espiell, F., 2003. Removal of ammonium and phosphates from wastewater resulting from the process of cochineal extraction using MgO-containing by-product. Water Res. 37, 1601–1607. https://doi.org/10.1016/S0043-1354(02)00526-2

Choi, H.J., Yu, S.W., Kim, K.H., 2016. Efficient use of Mg-modified zeolite in the treatment of aqueous solution contaminated with heavy metal toxic ions. J. Taiwan Inst. Chem. Eng. 63, 482–489. https://doi.org/10.1016/j.jtice.2016.03.005

Cieślik, B., Konieczka, P., 2017. A review of phosphorus recovery methods at various steps of wastewater treatment and sewage sludge management. The concept of "no solid waste generation" and analytical methods. J. Clean. Prod. 142, 1728–1740. https://doi.org/10.1016/j.jclepro.2016.11.116

Cieślik, B.M., Namieśnik, J., Konieczka, P., 2015. Review of sewage sludge management: Standards, regulations and analytical methods. J. Clean. Prod. 90, 1–15. https://doi.org/10.1016/j.jclepro.2014.11.031

Cordell, D., White, S., 2013. Sustainable phosphorus measures: Strategies and technologies for achieving phosphorus security. Agronomy 3, 86–116. https://doi.org/10.3390/agronomy3010086

Corre, K.S. Le, Hobbs, P., Parsons, S.A., 2009. Technology Phosphorus Recovery from Wastewater by Struvite Crystallization : A Review Phosphorus Recovery from Wastewater by Struvite Crystallization : A Review. https://doi.org/10.1080/10643380701640573

Costa, A.., Ely, C.., Pennington, M.., Rock, S.., Staniec, C., Turgeon, J., 2015. Anaerobic Digestion and its Applications. United States Environ. Prot. Agency 15.

Costamagna, G., Chiabrando, V., Fassone, E., Mania, I., Gorra, R., Ginepro, M., Giacalone, G., 2020. Characterization and use of absorbent materials as slow-release fertilizers for growing strawberry: Preliminary results. Sustain. 12. https://doi.org/10.3390/SU12176854

Cremonez, P.A., Teleken, J.G., Weiser Meier, T.R., Alves, H.J., 2021. Two-Stage anaerobic digestion in agroindustrial waste treatment: A review. J. Environ. Manage. 281. https://doi.org/10.1016/j.jenvman.2020.111854

Czajczyńska, D., Anguilano, L., Ghazal, H., Krzyżyńska, R., Reynolds, A.J., Spencer, N., Jouhara, H., 2017. Potential of pyrolysis processes in the waste management sector. Therm. Sci. Eng. Prog. 3, 171–197. https://doi.org/10.1016/j.tsep.2017.06.003

Dai, L., Tan, F., Wu, B., He, M., Wang, W., Tang, X., Hu, Q., Zhang, M., 2015. Immobilization of phosphorus in cow manure during hydrothermal carbonization. J. Environ. Manage. 157, 49–53. https://doi.org/10.1016/j.jenvman.2015.04.009

Dalahmeh, S.S., Stenström, Y., Jebrane, M., Hylander, L.D., Daniel, G., Heinmaa, I., 2020. Efficiency of Iron- and Calcium-Impregnated Biochar in Adsorbing Phosphate From Wastewater in Onsite Wastewater Treatment Systems. Front. Environ. Sci. 8, 1–14. https://doi.org/10.3389/fenvs.2020.538539

Daneshgar, S., Buttafava, A., Capsoni, D., Callegari, A., Capodaglio, A.G., 2018a. Impact of pH and ionic molar ratios on phosphorous forms precipitation and recovery from different wastewater sludges. Resources 7. https://doi.org/10.3390/resources7040071

Daneshgar, S., Callegari, A., Capodaglio, A.G., Vaccari, D., 2018b. The potential phosphorus crisis: Resource conservation and possible escape technologies: A review. Resources 7.

https://doi.org/10.3390/resources7020037

Demirbas, A., 2004. Effects of temperature and particle size on bio-char yield from pyrolysis of agricultural residues. J. Anal. Appl. Pyrolysis 72, 243–248. https://doi.org/10.1016/j.jaap.2004.07.003

Desmidt, E., Ghyselbrecht, K., Zhang, Y., Pinoy, L., Van Der Bruggen, B., Verstraete, W., Rabaey, K., Meesschaert, B., 2015. Global phosphorus scarcity and full-scale P-recovery techniques: A review. Crit. Rev. Environ. Sci. Technol. 45, 336–384. https://doi.org/10.1080/10643389.2013.866531

Dhal, J.P., Mishra, B.G., Hota, G., 2015. Ferrous oxalate, maghemite and hematite nanorods as efficient adsorbents for decontamination of Congo red dye from aqueous system. Int. J. Environ. Sci. Technol. 12, 1845–1856. https://doi.org/10.1007/s13762-014-0535-x

Doyle, J.D., Parsons, S.A., 2002. Struvite formation , control and recovery 36, 3925–3940.

Drahansky, M., Paridah, M.., Moradbak, A., Mohamed, A.., Owolabi, F. abdulwahab taiwo, Asniza, M., Abdul Khalid, S.H.., 2016. We are IntechOpen , the world ' s leading publisher of Open Access books Built by scientists , for scientists TOP 1 %. Intech i, 13. https://doi.org/http://dx.doi.org/10.5772/57353

Dung, V.B., Van Thien, D., 2014. The equation of backward diffusion and negative diffusivity. J. Phys. Conf. Ser. 537. https://doi.org/10.1088/1742-6596/537/1/012011

EDA, 2020. Annual report 2019/20, European Dairy Association.

Egle, L., Rechberger, H., Krampe, J., Zessner, M., 2016. Phosphorus recovery from municipal wastewater: An integrated comparative technological, environmental and economic assessment of P recovery technologies. Sci. Total Environ. 571, 522–542. https://doi.org/10.1016/j.scitotenv.2016.07.019

Egle, L., Rechberger, H., Zessner, M., 2015. Overview and description of technologies for recovering phosphorus from municipal wastewater. Resour. Conserv. Recycl. 105, 325–346. https://doi.org/10.1016/j.resconrec.2015.09.016

EIP-AGRI, 2017. EIP-AGRI Focus Group. Nutrient Recycling.

Elomaa, H., Seisko, S., Lehtola, J., Lundström, M., 2019. A study on selective leaching of heavy metals vs. iron from fly ash. J. Mater. Cycles Waste Manag. 21, 1004–1013. https://doi.org/10.1007/s10163-019-00858-w

EU, 2019. Regulation (EU) 2019/1009 of the European Parliament and of the Council of 5 June 2019 laying down rules on the making available on the market of EU fertilising products and amending Regulation (EC) No 1069/2009 and (EC) No 1107/2009 and repealing Regulat. Off. J. Eur. Union 2019, 1–114.

EurEau, 2021. Briefing Note Waste water treatment - sludge management.

European commission, 2000. The European parliament directive on the incineration of waste. Off. J. Eur. Communities 52, 1–15.

Fijalkowski, K., Rorat, A., Grobelak, A., Kacprzak, M.J., 2017. The presence of contaminations in sewage sludge – The current situation. J. Environ. Manage. 203, 1126–1136. https://doi.org/10.1016/j.jenvman.2017.05.068

Foletto, E.L., Dos Santos, W.R.B., Mazutti, M.A., Jahn, S.L., Gündel, A., 2013. Production of struvite from beverage waste as Phosphorus source. Mater. Res. 16, 242–245. https://doi.org/10.1590/S1516-14392012005000152

Gelb, R.I., 1971. Conductometric Determination of pKa Values—Oxalic and Squaric Acids. Anal.

Chem. 43, 1110–1113. https://doi.org/10.1021/ac60303a028

Generalic, E., 2019. Solubility product constants."EniG. Periodic Table of the Elements.

Ghanim, B.M., Kwapinski, W., Leahy, J.J., 2018. Speciation of Nutrients in Hydrochar Produced from Hydrothermal Carbonization of Poultry Litter under Different Treatment Conditions. ACS Sustain. Chem. Eng. 6, 11265–11272. https://doi.org/10.1021/acssuschemeng.7b04768

Ghanim, B.M., Kwapinski, W., Leahy, J.J., 2017a. Hydrothermal carbonisation of poultry litter: Effects of initial pH on yields and chemical properties of hydrochars. Bioresour. Technol. 238, 78–85. https://doi.org/10.1016/j.biortech.2017.04.025

Ghanim, B.M., Kwapinski, W., Leahy, J.J., 2017b. Hydrothermal carbonisation of poultry litter: Effects of initial pH on yields and chemical properties of hydrochars. Bioresour. Technol. 238, 78–85. https://doi.org/10.1016/j.biortech.2017.04.025

Gianico, A., Braguglia, C., Gallipoli, A., Montecchio, D., Mininni, G., 2021. Land Application of Biosolids in Europe: Possibilities, Con-Straints and Future Perspectives. Water 13, 103. https://doi.org/10.3390/w13010103

Gorazda, K., Tarko, B., Werle, S., Wzorek, Z., 2018. Sewage sludge as a fuel and raw material for phosphorus recovery: Combined process of gasification and P extraction. Waste Manag. 73, 404–415. https://doi.org/10.1016/j.wasman.2017.10.032

Gotsis skretas, O., Friligos, N., 1990. Contribution to eutrophication and phytoplankton ecology in the Thermaikos Gulf. Thalassografika.

Gutierrez, O., Park, D., Sharma, K.R., Yuan, Z., 2010. Iron salts dosage for sulfide control in sewers induces chemical phosphorus removal during wastewater treatment. Water Res. 44, 3467–3475. https://doi.org/10.1016/j.watres.2010.03.023

Hao, X.D., Wang, C.C., Lan, L., Van Loosdrecht, M.C.M., 2008. Struvite formation, analytical methods and effects of pH and Ca 2+. Water Sci. Technol. 58, 1687–1692. https://doi.org/10.2166/wst.2008.557

Hardman, G., Perkins, S., Brownridge, P.J., Clarke, C.J., Byrne, D.P., Campbell, A.E., Kalyuzhnyy, A., Myall, A., Eyers, P.A., Jones, A.R., Eyers, C.E., 2019. Strong anion exchange-mediated phosphoproteomics reveals extensive human non-canonical phosphorylation. EMBO J. 38, 1–22. https://doi.org/10.15252/embj.2018100847

Heilmann, S.M., Molde, J.S., Timler, J.G., Wood, B.M., Mikula, A.L., Vozhdayev, G. V., Colosky, E.C., Spokas, K.A., Valentas, K.J., 2014. Phosphorus reclamation through hydrothermal carbonization of animal manures. Environ. Sci. Technol. 48, 10323–10329. https://doi.org/10.1021/es501872k

Hermann, L., 2009. Rückgewinnung von Phosphor aus der Abwasserreinigung. Bundesamt für Umwelt Umwelt-Wis, 196.

Holub, M., Balintova, M., Pavlikova, P., Palascakova, L., 2013. Study of sorption properties of zeolite in acidic conditions in dependence on particle size. Chem. Eng. Trans. 32, 559–564. https://doi.org/10.3303/CET1332094

Hövelmann, J., Stawski, T.M., Freeman, H.M., Besselink, R., Mayanna, S., Perez, J.P.H., Hondow, N.S., Benning, L.G., 2019. Struvite crystallisation and the effect of Co2+ ions. Minerals 9, 1–18. https://doi.org/10.3390/min9090503

Huang, H.M., Xiao, X.M., Yang, L.P., Yan, B., 2011. Removal of ammonium from rare-earth wastewater using natural brucite as a magnesium source of struvite precipitation. Water Sci. Technol. 63, 468–474. https://doi.org/10.2166/wst.2011.245

Huchzermeier, M.P., Tao, W., 2012. Overcoming Challenges to Struvite Recovery from Anaerobically

Digested Dairy Manure. Water Environ. Res. 84, 34–41. https://doi.org/10.2175/106143011X13183708018887

Izadi, Parnian, Izadi, Parin, Eldyasti, A., 2020. Design, operation and technology configurations for enhanced biological phosphorus removal (EBPR) process: a review. Rev. Environ. Sci. Bio/Technology 19, 561–593. https://doi.org/10.1007/s11157-020-09538-w

Jarvie, H.P., Withers, J.A., Neal, C., 2002. Review of robust measurement of phosphorus in river water: sampling, storage, fractionation and sensitivity. Hydrol. Earth Syst. Sci. 6, 113–131. https://doi.org/10.5194/hess-6-113-2002

Johansson, S., 2019. Taking Advantage of Autotrophic Nitrogen Removal: Potassium and Phosphorus Recovery From Municipal Wastewater Doctoral Thesis 102.

John, B., 2013. Application of desirability function for optimizing the performance characteristics of carbonitrided bushes. Int. J. Ind. Eng. Comput. 4, 305–314. https://doi.org/10.5267/j.ijiec.2013.04.003

Kabdaşlı, I., Tünay, O., 2018. Nutrient recovery by struvite precipitation , ion exchange and adsorption from source-separated human urine – a review 2515. https://doi.org/10.1080/21622515.2018.1473504

Kahiluoto, H., Kuisma, M., Ketoja, E., Salo, T., Heikkinen, J., 2015. Phosphorus in manure and sewage sludge more recyclable than in soluble inorganic fertilizer. Environ. Sci. Technol. 49, 2115–2122. https://doi.org/10.1021/es503387y

Kapsak, W.R., Rahavi, E.B., Childs, N.M., White, C., 2011. Functional Foods: Consumer Attitudes, Perceptions, and Behaviors in a Growing Market. J. Am. Diet. Assoc. 111, 804–810. https://doi.org/10.1016/j.jada.2011.04.003

Kasina, M., Wendorff-Belon, M., Kowalski, P.R., Michalik, M., 2019. Characterization of incineration residues from wastewater treatment plant in Polish city: a future waste based source of valuable elements? J. Mater. Cycles Waste Manag. 21, 885–896. https://doi.org/10.1007/s10163-019-00845-1

Kataki, S., Hazarika, S., Baruah, D.C., 2017. Investigation on by-products of bioenergy systems (anaerobic digestion and gasification) as potential crop nutrient using FTIR, XRD, SEM analysis and phyto-toxicity test. J. Environ. Manage. 196, 201–216. https://doi.org/10.1016/j.jenvman.2017.02.058

Kataki, S., West, H., Clarke, M., Baruah, D.C., 2016a. Phosphorus recovery as struvite from farm, municipal and industrial waste: Feedstock suitability, methods and pre-treatments. Waste Manag. 49, 437–454. https://doi.org/10.1016/j.wasman.2016.01.003

Kataki, S., West, H., Clarke, M., Baruah, D.C., 2016b. Phosphorus recovery as struvite: Recent concerns for use of seed, alternative Mg source, nitrogen conservation and fertilizer potential. Resour. Conserv. Recycl. 107, 142–156. https://doi.org/10.1016/j.resconrec.2015.12.009

Kazadi Mbamba, C., Tait, S., Flores-Alsina, X., Batstone, D.J., 2015a. A systematic study of multiple minerals precipitation modelling in wastewater treatment. Water Res. 85, 359–370. https://doi.org/10.1016/j.watres.2015.08.041

Kazadi Mbamba, C., Tait, S., Flores-Alsina, X., Batstone, D.J., 2015b. A systematic study of multiple minerals precipitation modelling in wastewater treatment. Water Res. 85, 359–370. https://doi.org/10.1016/j.watres.2015.08.041

Khai, N.M., 2012. Chemical Precipitation of Ammonia and Phosphate from Nam Son Landfill Leachate, Hanoi. Iran. J. Energy Environ. 3, 32–36. https://doi.org/10.5829/idosi.ijee.2012.03.05.06

Khater, E., Ms, S., El, S., Youssif, H., August, J., 2015. Design for Struvite Precipitation from Industrial Wastewater Stream : Res. J. Pharm. , Biol. Chem. Sci. 6, 1586–1599.

Kijo-Kleczkowska, A., Środa, K., Kosowska-Golachowska, M., Musiał, T., Wolski, K., 2015. Mechanisms and kinetics of granulated sewage sludge combustion. Waste Manag. 46, 459–471. https://doi.org/10.1016/j.wasman.2015.08.015

Kim, A.H., Yu, A.C., El Abbadi, S.H., Lu, K., Chan, D., Appel, E.A., Criddle, C.S., 2021. More than a fertilizer: Wastewater-derived struvite as a high value, sustainable fire retardant. Green Chem. 23, 4510–4523. https://doi.org/10.1039/d1gc00826a

Kim, D., Kim, J., Ryu, H.D., Lee, S.I., 2009. Effect of mixing on spontaneous struvite precipitation from semiconductor wastewater. Bioresour. Technol. 100, 74–78. https://doi.org/10.1016/j.biortech.2008.05.024

Kim ten Wolde, 2013. THE ROLE AND OPPORTUNITIES OF FERTILIZER PRODUCTION FOR PHOSPHATE RECYCLING, in: ICL Fertilizers Europe. Symposium Re-Water Braunschweig (6–7. November 2013. Braunschweig. Germany.

Kolev, S., 2017. General Characteristics and Treatment Possibilities of Dairy Wastewater – A Review. Food Technol. Biotechnol. 53, 237–242. https://doi.org/10.17113/ft

Kotoulas, A., Agathou, D., Triantaphyllidou, I., Tatoulis, T., Akratos, C., Tekerlekopoulou, A., Vayenas, D., 2019. Zeolite as a Potential Medium for Ammonium Recovery and Second Cheese Whey Treatment. Water 11, 136. https://doi.org/10.3390/w11010136

Kwapinski, W., Byrne, C.M.P., Kryachko, E., Wolfram, P., Adley, C., Leahy, J.J., Novotny, E.H., Hayes, M.H.B., 2010. Biochar from biomass and waste. Waste and Biomass Valorization 1, 177–189. https://doi.org/10.1007/s12649-010-9024-8

Lavanya, A., Sri Krishnaperumal Thanga, R., 2020. Effective removal of phosphorous from dairy wastewater by struvite precipitation: process optimization using response surface methodology and chemical equilibrium modeling. Sep. Sci. Technol. 00, 1–16. https://doi.org/10.1080/01496395.2019.1709080

Le Corre, K.S., Valsami-Jones, E., Hobbs, P., Parsons, S.A., 2009. Phosphorus recovery from wastewater by struvite crystallization: A review, Critical Reviews in Environmental Science and Technology. https://doi.org/10.1080/10643380701640573

Lei, Y., Zhan, Z., Saakes, M., van der Weijden, R.D., Buisman, C.J.N., 2021. Electrochemical Recovery of Phosphorus from Acidic Cheese Wastewater: Feasibility, Quality of Products, and Comparison with Chemical Precipitation. ACS ES&T Water 1, 1002–1013. https://doi.org/10.1021/acsestwater.0c00263

Lewis, A.E., 2010. Review of metal sulphide precipitation. Hydrometallurgy 104, 222–234. https://doi.org/10.1016/j.hydromet.2010.06.010

Lewis, W.M., Wurtsbaugh, W.A., Paerl, H.W., 2011. Rationale for control of anthropogenic nitrogen and phosphorus to reduce eutrophication of inland waters. Environ. Sci. Technol. 45, 10300–10305. https://doi.org/10.1021/es202401p

Li, C., Ning, Y., Yan, T., Zheng, W., 2019. Studies on nucleation and crystal growth kinetics of ferrous oxalate. Heliyon 5, e02758. https://doi.org/10.1016/j.heliyon.2019.e02758

Li, X., Rubæk, G.H., Müller-Stöver, D.S., Thomsen, T.P., Ahrenfeldt, J., Sørensen, P., 2017. Plant Availability of Phosphorus in Five Gasification Biochars. Front. Sustain. Food Syst. 1, 1–12. https://doi.org/10.3389/fsufs.2017.00002

Liberti, L., Boari, G. and Passino, R., 1984. Method for removing and recovering nutrients from wastewater. U.S. Pat. no. 4,477,355 0–5.

Liberti, L., Petruzzelli, D., De Florio, L., 2001. Rem nut ion exchange plus struvite precipitation process. Environ. Technol. (United Kingdom) 22, 1313–1324. https://doi.org/10.1080/09593330409355443

Libra, J.A., Ro, K.S., Kammann, C., Funke, A., Berge, N.D., Neubauer, Y., Titirici, M.M., Fühner, C., Bens, O., Kern, J., Emmerich, K.H., 2011. Hydrothermal carbonization of biomass residuals: A comparative review of the chemistry, processes and applications of wet and dry pyrolysis. Biofuels 2, 71–106. https://doi.org/10.4155/bfs.10.81

Loewenthal, R. E., U.R.. K. and E.P. van H., 1994. Modellingstruvite_precipitation. Water Sci. Technol. 30, 107–116.

Lv, H., Liu, D., Zhang, Y., Yuan, D., Wang, F., Yang, J., Wu, X., Zhang, W., Dai, X., 2019. Effects of temperature variation on wastewater sludge electro-dewatering. J. Clean. Prod. 214, 873–880. https://doi.org/10.1016/j.jclepro.2019.01.033

Malmberg, C.G., Maryott, A.A., 1956. Dielectric constant of water from 0 to 100 C. J. Res. Natl. Bur. Stand. (1934). 56, 1. https://doi.org/10.6028/jres.056.001

Maneedaeng, A., Flood, A.E., Haller, K.J., Grady, B.P., 2012. Modeling of precipitation phase boundaries in mixed surfactant systems using an improved counterion binding model. J. Surfactants Deterg. 15, 523–531. https://doi.org/10.1007/s11743-012-1353-0

Mansourri, G., Madani, M., 2016. Examination of the Level of Heavy Metals in Wastewater of Bandar Abbas Wastewater Treatment Plant 55–61.

Marinoni, M., Carrayrou, J., Lucas, Y., Ackerer, P., 2017. Thermodynamic equilibrium solutions through a modified Newton Raphson method. AIChE J. 63, 1246–1262. https://doi.org/10.1002/aic.15506

Matynia, A., Wierzbowska, B., Hutnik, N., Mazienczuk, A., Kozik, A., Piotrowski, K., 2013. Separation of Struvite from Mineral Fertilizer Industry Wastewater. Procedia Environ. Sci. 18, 766–775. https://doi.org/10.1016/j.proenv.2013.04.103

Mekmene, O., Quillard, S., Rouillon, T., Bouler, J.M., Piot, M., Gaucheron, F., 2009. Effects of pH and Ca/P molar ratio on the quantity and crystalline structure of calcium phosphates obtained from aqueous solutions. Dairy Sci. Technol. 89, 301–316. https://doi.org/10.1051/dst/2009019

Moerman, W., Carballa, M., Vandekerckhove, A., Derycke, D., Verstraete, W., 2009. Phosphate removal in agro-industry: Pilot- and full-scale operational considerations of struvite crystallization. Water Res. 43, 1887–1892. https://doi.org/10.1016/j.watres.2009.02.007

Moharir, R. V., Gautam, P., Kumar, S., 2019. Waste treatment processes/technologies for energy recovery, Current Developments in Biotechnology and Bioengineering: Waste Treatment Processes for Energy Generation. Elsevier B.V. https://doi.org/10.1016/B978-0-444-64083-3.00004-X

Moletta, R., Verrier, D., Albagnac, G., 1986. Dynamic modelling of anaerobic digestion. Water Res. 20, 427–434. https://doi.org/10.1016/0043-1354(86)90189-2

Möller, K., Müller, T., 2012. Effects of anaerobic digestion on digestate nutrient availability and crop growth: A review. Eng. Life Sci. 12, 242–257. https://doi.org/10.1002/elsc.201100085

Moragaspitiya, C., Rajapakse, J., Millar, G.J., 2019. Effect of Ca:Mg ratio and high ammoniacal nitrogen on characteristics of struvite precipitated from waste activated sludge digester effluent. J. Environ. Sci. (China) 86, 65–77. https://doi.org/10.1016/j.jes.2019.04.023

Morse, G.K., Brett, S.W., Guy, J.A., Lester, J.N., 1998. Review: Phosphorus removal and recovery technologies. Sci. Total Environ. 212, 69–81. https://doi.org/10.1016/S0048-9697(97)00332-X

Müller-Stöver, D.S., Jakobsen, I., Grønlund, M., Rolsted, M.M.M., Magid, J., Hauggaard-Nielsen, H.,

2018. Phosphorus bioavailability in ash from straw and sewage sludge processed by low-temperature biomass gasification. Soil Use Manag. 34, 9–17. https://doi.org/10.1111/sum.12399

Muller, J.A., Gunther, L., Dockhorn, T., Dichtl, N., Phan, L.-C., Urban, I., Weichgrebe, D., Rosenwinkel, K.-H., Bayerle, N., 2007. Nutrient Recycling from Sewage Sludge using the Seaborne Process. Proc. Mov. Forw. Wastewater Biosolids Sustain. Tech. Manag. Public Synerg. 629–633.

Musvoto, E. V., Wentzel, M.C., Loewenthal, R.E., Ekama, G.A., 2000. Integrated chemical-physical processes modelling - I. Development of a kinetic-based model for mixed weak acid/base systems. Water Res. 34, 1857–1867. https://doi.org/10.1016/S0043-1354(99)00334-6

Nadeem, K., Alliet, M., Plana, Q., Bernier, J., Azimi, S., Rocher, V., Albasi, C., 2021. Modeling, simulation and control of biological and chemical P-removal processes for membrane bioreactors (MBRs) from lab to full-scale applications: State of the art. Sci. Total Environ. 151109. https://doi.org/10.1016/j.scitotenv.2021.151109

Nancollas, G.H, Amjad, Z, and Koutsoukos, P., 1979. Calcium Phosphates—Speciation, Solubility, and Kinetic Considerations. Chem. Model. acqeous Syst. 475–497. https://doi.org/10.1021/bk-1979-0093.ch023

Neyens, E., Baeyens, J., 2003. A review of thermal sludge pre-treatment processes to improve dewaterability. J. Hazard. Mater. 98, 51–67. https://doi.org/10.1016/S0304-3894(02)00320-5

Nobel, P.S., Nobel, P.S., 2009. Chapter 6 – Bioenergetics. Physicochem. Environ. Plant Physiol. 276–317. https://doi.org/10.1016/B978-0-12-374143-1.00006-5

Numviyimana, C., Chmiel, T., Kot-Wasik, A., Namieśnik, J., 2019. Study of pH and temperature effect on lipophilicity of catechol-containing antioxidants by reversed phase liquid chromatography. Microchem. J. 145. https://doi.org/10.1016/j.microc.2018.10.048

Numviyimana, C., Warchoł, J., Izydorczyk, G., Baśladyńska, S., Chojnacka, K., 2020. Struvite production from dairy processing wastewater: Optimizing reaction conditions and effects of foreign ions through multi-response experimental models. J. Taiwan Inst. Chem. Eng. 117, 182–189. https://doi.org/10.1016/j.jtice.2020.11.031

Numviyimana, C., Warchoł, J., Khalaf, N., Leahy, J.J., Chojnacka, K., 2022. Phosphorus recovery as struvite from hydrothermal carbonization liquor of chemically produced dairy sludge by extraction and precipitation. J. Environ. Chem. Eng. 10, 106947. https://doi.org/10.1016/j.jece.2021.106947

Numviyimana, C., Warchoł, J., Ligas, B., Chojnacka, K., 2021. Nutrients recovery from dairy wastewater by struvite precipitation combined with ammonium sorption on clinoptilolite. Materials (Basel). 14. https://doi.org/10.3390/ma14195822

Ohtake, H., Tsuneda, S., 2018. Phosphorus Recovery and Recycling. Phosphorus Recover. Recycl. 1–526. https://doi.org/10.1007/978-981-10-8031-9

Ojo, P., Ifelebuegu, A.O., 2019. The effects of aluminium- and ferric-based chemical phosphorus removal on activated sludge digestibility and dewaterability. Processes 7. https://doi.org/10.3390/pr7040228

Oladejo, J., Shi, K., Luo, X., Yang, G., Wu, T., 2019. A review of sludge-to-energy recovery methods. Energies 12, 1–38. https://doi.org/10.3390/en12010060

Olmez-hanci, T., Tunay, O., 2004. Magnesium ammonium phosphate precipitation using seawater.

OSTARA, 2018. Nutrient Recovery Technology Customized To Meet Your Needs Crystal Green Processing – Simple and Fully Automated.

Perera, M.K., Englehardt, J.D., Dvorak, A.C., 2019. Technologies for Recovering Nutrients from Wastewater: A Critical Review. Environ. Eng. Sci. 36, 511–529.

https://doi.org/10.1089/ees.2018.0436

Petzet, S., Peplinski, B., Bodkhe, S.Y., Cornel, P., 2011. Recovery of phosphorus and aluminium from sewage sludge ash by a new wet chemical elution process (SESAL-Phos-recovery process). Water Sci. Technol. 64, 693–699. https://doi.org/10.2166/wst.2011.682

Petzet, S., Peplinski, B., Cornel, P., 2012. On wet chemical phosphorus recovery from sewage sludge ash by acidic or alkaline leaching and an optimized combination of both. Water Res. 46, 3769–3780. https://doi.org/10.1016/j.watres.2012.03.068

Pinatha, Y., Polprasert, C., Englande, A.J., 2017. Adsorption onto ash particles and common ion effect for phosphorus recovery from urinal wastewater. GMSARN Int. J. 11, 33–44.

Polat, S., Sayan, P., 2019. Application of response surface methodology with a Box–Behnken design for struvite precipitation. Adv. Powder Technol. 30, 2396–2407. https://doi.org/10.1016/j.apt.2019.07.022

Popko, M., Michalak, I., Wilk, R., Gramza, M., Chojnacka, K., Górecki, H., 2018. Effect of the new plant growth biostimulants based on amino acids on yield and grain quality of winter wheat. Molecules 23. https://doi.org/10.3390/molecules23020470

Prot, T., Wijdeveld, W., Eshun, L.E., Dugulan, A.I., Goubitz, K., Korving, L., Van Loosdrecht, M.C.M., 2020. Full-scale increased iron dosage to stimulate the formation of vivianite and its recovery from digested sewage sludge. Water Res. 182, 115911. https://doi.org/10.1016/j.watres.2020.115911

Rahman, M.M., Salleh, M.A.M., Rashid, U., Ahsan, A., Hossain, M.M., Ra, C.S., 2014. Production of slow release crystal fertilizer from wastewaters through struvite crystallization - A review. Arab. J. Chem. 7, 139–155. https://doi.org/10.1016/j.arabjc.2013.10.007

Ramprasad, C., Alekhya, D., Bhishmitha, C., Deepika, C.S., 2020. Precipitation of struvite by sustainable waste materials and use as slow release fertilizer-A circular economy approach. IOP Conf. Ser. Mater. Sci. Eng. 955. https://doi.org/10.1088/1757-899X/955/1/012088

Ravindran, R., Hassan, S.S., Williams, G.A., Jaiswal, A.K., 2018. A review on bioconversion of agro-industrial wastes to industrially important enzymes. Bioengineering 5, 1–20. https://doi.org/10.3390/bioengineering5040093

Ravindran, R., Jaiswal, A.K., 2016. Exploitation of Food Industry Waste for High-Value Products. Trends Biotechnol. 34, 58–69. https://doi.org/10.1016/j.tibtech.2015.10.008

Rismiati, 2016. Industrial waste incineration including hazardous waste and sewage sludge.

Robinson, J.S., Baumann, K., Hu, Y., Hagemann, P., Kebelmann, L., Leinweber, P., 2018. Phosphorus transformations in plant-based and bio-waste materials induced by pyrolysis. Ambio 47, 73–82. https://doi.org/10.1007/s13280-017-0990-y

Rodarte, M.P., Dias, D.R., Vilela, D.M., Schwan, R.F., 2011. Atividade proteolítica de bactérias, leveduras e fungos filamentosos presentes em grãos de café (Coffea arabica L.). Acta Sci. - Agron. 33, 457–464. https://doi.org/10.4025/actasciagron.v33i3.6734

Römer, W., Samie, I.F., 2002. Iron-rich sewage sludge is not suitable for phosphorus recycling in agriculture. Wasser und Boden 54, 28–32.

Ronteltap, M., Maurer, M., Gujer, W., 2007. Struvite precipitation thermodynamics in source-separated urine. Water Res. 41, 977–984. https://doi.org/10.1016/j.watres.2006.11.046

Roque-Malherbe, R., 2001. Applications of Natural Zeolites in Pollution Abatement and Industry. Handb. Surfaces Interfaces Mater. 5, 495–522. https://doi.org/10.1016/b978-012513910-6/50069-4

Ruiz, J.L., Del Carmen Salas, M., 2019. Evaluation of organic substrates and microorganisms as bio-fertilisation tool in container crop production. Agronomy 9. https://doi.org/10.3390/agronomy9110705

Samreen, S., Kausar, S., 2019. Phosphorus Fertilizer: The Original and Commercial Sources, in: Phosphorus - Recovery and Recycling. IntechOpen, p. 13. https://doi.org/10.5772/intechopen.82240

Scholz, G., Scholz, F., 2014. First-order differential equations in chemistry. J. Comput. Sci. Technol. 1. https://doi.org/10.1007/s40828-014-0001-x

Schröder, J.J., Cordell, D., Smit, A.L., Rosemarin, A., 2010. Sustainable use of phosphorus Report 357 (European Union tender project ENV.B.1/ETU/2009/0025) 140.

Selby-Pham, S.N.B., Miller, R.B., Howell, K., Dunshea, F., Bennett, L.E., 2017. Physicochemical properties of dietary phytochemicals can predict their passive absorption in the human small intestine. Sci. Rep. 7, 1–15. https://doi.org/10.1038/s41598-017-01888-w

Sena, M., Hicks, A., 2018. Resources , Conservation & Recycling Life cycle assessment review of struvite precipitation in wastewater treatment. Resour. Conserv. Recycl. 139, 194–204. https://doi.org/10.1016/j.resconrec.2018.08.009

Seymour, D., 2009. Can Nutrient Recovery Be a Financially Sustainable Development Objective?

Shaddel, S., Grini, T., Andreassen, J.P., Østerhus, S.W., Ucar, S., 2020a. Crystallization kinetics and growth of struvite crystals by seawater versus magnesium chloride as magnesium source: towards enhancing sustainability and economics of struvite crystallization. Chemosphere 256, 126968. https://doi.org/10.1016/j.chemosphere.2020.126968

Shaddel, S., Grini, T., Ucar, S., Azrague, K., Andreassen, J.P., Østerhus, S.W., 2020b. Struvite crystallization by using raw seawater: Improving economics and environmental footprint while maintaining phosphorus recovery and product quality. Water Res. 173, 115572. https://doi.org/10.1016/j.watres.2020.115572

Shaddel, S., Ucar, S., Andreassen, J.P., Sterhus, S.W., 2019. Engineering of struvite crystals by regulating supersaturation - Correlation with phosphorus recovery, crystal morphology and process efficiency. J. Environ. Chem. Eng. 7, 102918. https://doi.org/10.1016/j.jece.2019.102918

Shaikh, M., 2018. Phosphorus Recovery From Wastewater Treatment & Sewage Sludge: A Review.

Shalaby, M.S., El-Rafie, S., Hamzaoui, A.H., M'nif, A., 2015. Modeling and optimization of phosphate recovery from industrial wastewater and precipitation of solid fertilizer using experimental design methodology. Chem. Biochem. Eng. Q. 29, 35–46. https://doi.org/10.15255/CABEQ.2014.2107

Shi, W., Fenton, O., Ashekuzzaman, S.M., Daly, K., Leahy, J.J., Khalaf, N., Hu, Y., Chojnacka, K., Numviyimana, C., Healy, M.G., 2022. An examination of maximum legal application rates of dairy processing and associated STRUBIAS fertilising products in agriculture. J. Environ. Manage. 301, 113880. https://doi.org/10.1016/j.jenvman.2021.113880

Shi, W., Healy, M.G., Ashekuzzaman, S.M., Daly, K., Leahy, J.J., Fenton, O., 2021. Dairy processing sludge and co-products: A review of present and future re-use pathways in agriculture. J. Clean. Prod. 314, 128035. https://doi.org/10.1016/j.jclepro.2021.128035

Shih, K., Yan, H., 2016. The Crystallization of Struvite and Its Analog (K-Struvite) From Waste Streams for Nutrient Recycling, Environmental Materials and Waste: Resource Recovery and Pollution Prevention. Elsevier Inc. https://doi.org/10.1016/B978-0-12-803837-6.00026-3

Siciliano, A., Limonti, C., Mehariya, S., Molino, A., Calabrò, V., 2018. Biofuel production and phosphorus recovery through an integrated treatment of agro-industrial waste. Sustain. 11, 1–17. https://doi.org/10.3390/su11010052

Sikarwar, V.S., Zhao, M., Clough, P., Yao, J., Zhong, X., Memon, M.Z., Shah, N., Anthony, E.J., Fennell, P.S., 2016. An overview of advances in biomass gasification. Energy Environ. Sci. 9, 2939–2977. https://doi.org/10.1039/c6ee00935b

Silva, R.V.S., Romeiro, G.A., Veloso, M.C.C., Figueiredo, M.K.K., Pinto, P.A., Ferreira, A.F., Gonçalves, M.L.A., Teixeira, A.M., Damasceno, R.N., 2012. Fractions composition study of the pyrolysis oil obtained from sewage sludge treatment plant. Bioresour. Technol. 103, 459–465. https://doi.org/10.1016/j.biortech.2011.10.007

Simoes, F., Vale, P., Stephenson, T., Soares, A., 2018. The role of pH on the biological struvite production in digested sludge dewatering liquors. Sci. Rep. 8, 1–9. https://doi.org/10.1038/s41598-018-25431-7

Smyth, D.P., Fredeen, A.L., Booth, A.L., 2010. Reducing solid waste in higher education: The first step towards "greening" a university campus. Resour. Conserv. Recycl. 54, 1007–1016. https://doi.org/10.1016/j.resconrec.2010.02.008

Solon, K., Flores-Alsina, X., Mbamba, C.K., Volcke, E.I.P., Tait, S., Batstone, D., Gernaey, K. V., Jeppsson, U., 2015. Effects of ionic strength and ion pairing on (plant-wide) modelling of anaerobic digestion. Water Res. 70, 235–245. https://doi.org/10.1016/j.watres.2014.11.035

Stolzenburg, P., Capdevielle, A., Teychené, S., Biscans, B., 2015. Struvite precipitation with MgO as a precursor: Application to wastewater treatment. Chem. Eng. Sci. 133, 9–15. https://doi.org/10.1016/j.ces.2015.03.008

Sugawara, E., Nikaido, H., 2018. COMMISSION IMPLEMENTING DECISION (EU) 2018/1147 of 10 August 2018 establishing best available techniques (BAT) conclusions for waste treatment, under Directive 2010/75/EU of the European Parliament and of the Council, Official Journal of the European Union.

Sun, D., Hale, L., Kar, G., Soolanayakanahally, R., Adl, S., 2018. Phosphorus recovery and reuse by pyrolysis: Applications for agriculture and environment. Chemosphere 194, 682–691. https://doi.org/10.1016/j.chemosphere.2017.12.035

Szymańska, M., Szara, E., Sosulski, T., Wąs, A., Van Pruissen, G.W.P., Cornelissen, R.L., Borowik, M., Konkol, M., 2019. A Bio-Refinery concept for n and p recovery - A chance for biogas plant development. Energies 12, 1–10. https://doi.org/10.3390/en12010155

Takács, I., Murthy, S., Smith, S., McGrath, M., 2006. Chemical phosphorus removal to extremely low levels: Experience of two plants in the Washington, DC area. Water Sci. Technol. 53, 21–28. https://doi.org/10.2166/wst.2006.402

Tamulonis, C., 2002. Environmental Assessment of the Final Effluent Guidelines for Iron and Steel Industry, EPA.

Tang, H., Xu, X., Wang, B., Lv, C., Shi, D., 2020. Removal of ammonium from swine waste water using synthesized zeolite from fly ash. Sustain. 12, 1–15. https://doi.org/10.3390/SU12083423

Tarpani, R.R.Z., Alfonsín, C., Hospido, A., Azapagic, A., 2020. Life cycle environmental impacts of sewage sludge treatment methods for resource recovery considering ecotoxicity of heavy metals and pharmaceutical and personal care products. J. Environ. Manage. 260, 109643. https://doi.org/10.1016/j.jenvman.2019.109643

Taupe, N.C., Lynch, D., Wnetrzak, R., Kwapinska, M., Kwapinski, W., Leahy, J.J., 2016. Updraft gasification of poultry litter at farm-scale - A case study. Waste Manag. 50, 324–333. https://doi.org/10.1016/j.wasman.2016.02.036

Tavazzi, S., Locoro, G., Comero, S., Sobiecka, E., Loos, R., Gans, O., Ghiani, M., Umlauf, G., Suurkuusk, G., Paracchini, B., Cristache, C., Fissiaux, I., Riuz, A.A., Gawlik, B.M., 2012. Occurrence and levels of selected compounds in European sewage sludge samples (FATE SEES).

ec.europa.eu/jrc/sites/default/files. https://doi.org/10.2788/67153

Tian, Y., Cui, L., Lin, Q., Li, G., Zhao, X., 2019. The sewage sludge biochar at low pyrolysis temperature had better improvement in urban soil and turf grass. Agronomy 9. https://doi.org/10.3390/agronomy9030156

Ulex, G.L., 1845. CLXIII. On struvite, a new mineral. Mem. Proc. Chem. Soc. 3, 106–110. https://doi.org/10.1039/MP8450300106

USEPA, 1974. Process design manual for sulfide control in sanitary sewerage systems. Epa Technol.trans. Publ.

Uysal, A., Yilmazel, Y.D., Demirer, G.N., 2010. The determination of fertilizer quality of the formed struvite from effluent of a sewage sludge anaerobic digester. J. Hazard. Mater. 181, 248–254. https://doi.org/10.1016/j.jhazmat.2010.05.004

Van Rensburg, P., Musvoto, E. V., Wentzel, M.C., Ekama, G.A., 2003. Modelling multiple mineral precipitation in anaerobic digester liquor. Water Res. 37, 3087–3097. https://doi.org/10.1016/S0043-1354(03)00173-8

Van Vuuren, D.P., Bouwman, A.F., Beusen, A.H.W., 2010. Phosphorus demand for the 1970–2100 period: A scenario analysis of resource depletion. Glob. Environ. Chang. 20, 428–439. https://doi.org/10.1016/j.gloenvcha.2010.04.004

Varala, S., Dharanija, B., Satyavathi, B., Basava Rao, V. V., Parthasarathy, R., 2016. New biosorbent based on deoiled karanja seed cake in biosorption studies of Zr(IV): Optimization using Box-Behnken method in response surface methodology with desirability approach. Chem. Eng. J. 302, 786–800. https://doi.org/10.1016/j.cej.2016.05.088

Verma, A., Kore, R., Corbin, D.R., Shiflett, M.B., 2019. Metal Recovery Using Oxalate Chemistry: A Technical Review. Ind. Eng. Chem. Res. 58, 15381–15393. https://doi.org/10.1021/acs.iecr.9b02598

Wahono, S.K., Maryana, R., Kismurtono, M., 2009. Biogas purification process to increase gen - Set efficiency. AIP Conf. Proc. 1169, 185–189. https://doi.org/10.1063/1.3243250

Wang, J., Burken, J.G., Zhang, X., Surampalli, R., 2005. Engineered struvite precipitation: Impacts of component-ion molar ratios and pH. J. Environ. Eng. 131, 1433–1440. https://doi.org/10.1061/(ASCE)0733-9372(2005)131:10(1433)

Wang, S., Peng, Y., 2010. Natural zeolites as effective adsorbents in water and wastewater treatment. Chem. Eng. J. 156, 11–24. https://doi.org/10.1016/j.cej.2009.10.029

Warmadewanthi, I.D.A.A., Zulkarnain, M.A., Ikhlas, N., Kurniawan, S.B., Abdullah, S.R.S., 2021. Struvite precipitation as pretreatment method of mature landfill leachate. Bioresour. Technol. Reports 15, 100792. https://doi.org/10.1016/j.biteb.2021.100792

Weigand, H., Bertau, M., Hübner, W., Bohndick, F., Bruckert, A., 2013a. RecoPhos: Full-scale fertilizer production from sewage sludge ash. Waste Manag. 33, 540–544. https://doi.org/10.1016/j.wasman.2012.07.009

Weigand, H., Bertau, M., Hübner, W., Bohndick, F., Bruckert, A., 2013b. RecoPhos: Full-scale fertilizer production from sewage sludge ash. Waste Manag. 33, 540–544. https://doi.org/10.1016/j.wasman.2012.07.009

Wentzel, M.C., Musvoto, E. V., Ekama, G.A., 2001. Application of integrated chemical - physical processes modelling to aeration treatment of anaerobic digester liquors. Environ. Technol. (United Kingdom) 22, 1287–1293. https://doi.org/10.1080/09593332208618189

Werle, S., Sobek, S., 2019. Gasification of sewage sludge within a circular economy perspective: a Polish case study. Environ. Sci. Pollut. Res. 26, 35422–35432. https://doi.org/10.1007/s11356-

019-05897-2

Whitaker, A., Jeffery, J.W., 1970. The crystal structure of struvite, MgNH 4 PO 4 .6H 2 O . Acta Crystallogr. Sect. B Struct. Crystallogr. Cryst. Chem. 26, 1429–1440. https://doi.org/10.1107/s0567740870004284

Wiedner, K., Naisse, C., Rumpel, C., Pozzi, A., Wieczorek, P., Glaser, B., 2013. Chemical modification of biomass residues during hydrothermal carbonization - What makes the difference, temperature or feedstock? Org. Geochem. 54, 91–100. https://doi.org/10.1016/j.orggeochem.2012.10.006

Xu, H., He, P., Gu, W., Wang, G., Shao, L., 2012. Recovery of phosphorus as struvite from sewage sludge ash. J. Environ. Sci. (China) 24, 1533–1538. https://doi.org/10.1016/S1001-0742(11)60969-8

Xue, G., Kwapinska, M., Horvat, A., Li, Z., Dooley, S., Kwapinski, W., Leahy, J.J., 2014. Gasification of miscanthus x giganteus in an air-blown bubbling fluidized bed: A preliminary study of performance and agglomeration. Energy and Fuels 28, 1121–1131. https://doi.org/10.1021/ef4022152

Yadav, H., Fatima, R., Sharma, A., Mathur, S., 2017. Enhancement of applicability of rock phosphate in alkaline soils by organic compost. Appl. Soil Ecol. 113, 80–85. https://doi.org/10.1016/j.apsoil.2017.02.004

Yetilmezsoy, K., Kocak, E., Akbin, H.M., Özçimen, D., 2020. Utilization of struvite recovered from high-strength ammonium-containing simulated wastewater as slow-release fertilizer and fire-retardant barrier. Environ. Technol. (United Kingdom) 41, 153–170. https://doi.org/10.1080/09593330.2018.1491642

Z. X., T., Lal, R., Wiebe, K.D., 2005. Global Soil Nutrient Depletion and Yield Reduction. J. Sustain. Agric. 26, 123–146. https://doi.org/10.1300/J064v26n01_10

Zhang, Tianxi, Bowers, K.E., Harrison, J.H., Chen, S., 2010. Releasing Phosphorus from Calcium for Struvite Fertilizer Production from Anaerobically Digested Dairy Effluent. Water Environ. Res. 82, 34–42. https://doi.org/10.2175/106143009x425924

Zhang, Tao, Ding, L., Ren, H., Guo, Z., Tan, J., 2010. Thermodynamic modeling of ferric phosphate precipitation for phosphorus removal and recovery from wastewater. J. Hazard. Mater. 176, 444–450. https://doi.org/10.1016/j.jhazmat.2009.11.049

Zhang, T., He, X., Deng, Y., Tsang, D.C.W., Jiang, R., Becker, G.C., Kruse, A., 2020. Phosphorus recovered from digestate by hydrothermal processes with struvite crystallization and its potential as a fertilizer. Sci. Total Environ. 698, 134240. https://doi.org/10.1016/j.scitotenv.2019.134240

Zhang, X., Hu, J., Spanjers, H., van Lier, J.B., 2016. Struvite crystallization under a marine/brackish aquaculture condition. Bioresour. Technol. 218, 1151–1156. https://doi.org/10.1016/j.biortech.2016.07.088

Zhao, X., Becker, G.C., Faweya, N., Rodriguez Correa, C., Yang, S., Xie, X., Kruse, A., 2018. Fertilizer and activated carbon production by hydrothermal carbonization of digestate. Biomass Convers. Biorefinery 8, 423–436. https://doi.org/10.1007/s13399-017-0291-5

Zheng, X., Jiang, Z., Ying, Z., Ye, Y., Chen, W., Wang, B., Dou, B., 2020. Migration and Transformation of Phosphorus during Hydrothermal Carbonization of Sewage Sludge: Focusing on the Role of pH and Calcium Additive and the Transformation Mechanism. ACS Sustain. Chem. Eng. 8, 7806–7814. https://doi.org/10.1021/acssuschemeng.0c00031

LIST OF FIGURES

LIST OF TABLES

ABSTRACT

Thermochemical treatment of sludge from dairy industries was applied to obtain products designated as STRUBIAS (struvite, biochar, and ash), which are commercially accepted as fertilizing products. The technologies hereby used include lower temperature incineration to produce a P rich ash and hydrothermal carbonization (HTC) that produces hydrochar, a prototype of biochar, and a nutrient rich process water. The P and N in resulting hydrothermal process water were purified through struvite precipitation. The multiple optimization method was used to find the proper process conditions. These were evaluated on processed cheese wastewater where the desirability function enabled the minimizing effect of foreign ions while enhancing struvite precipitation from calcium rich whey. The approach was improved by addition of clinoptilolite natural zeolitic materials for struvite precipitation combined with ammonium sorption. This enhanced the ammonium removal, process thermodynamic and obtaining a fertilizer formulation encapsulating more nitrogen in the sorbent active sites, thus a managed nutrient release.

The particular attention was given to chemically produced dairy sludge with iron salts as coagulants. Such a sludge is characterized with very low P availability to plant, while high level of iron becomes threatening for some plants. On one side of the study, the incineration ashes were leached with phosphoric acid supplemented with hydrochloric acid followed by struvite precipitation after ammonium and magnesium dosage. For better cost effectiveness, the study with ash has combined the magnesite and dairy sludge ash co-leached together in acidic solution followed by struvite precipitation. The combination of dairy sludge ash and magnesite were as effective in struvite crystallization as the magnesium chloride use.

The HTC process leaves a bigger volume of nutrient-rich liquor. The recovery of phosphorus (P) by direct precipitation was criticized for product quality. The product iron content was 17.96%, a value higher than accepted limits for purity of phosphate fertilizers. Thus, the HTC liquor P extraction followed by struvite precipitation was studied. The use of oxalic acid extracted 86.7% of P from HTC liquor, while 86.6% of iron was removed. The process conditions of pH 9, and salt dosage of 1.73:1.14:1 for $Mg:NH_4^+:P$ mole ratio for struvite precipitation were obtained with a P recovery of 99.96%, and the effluent P concentration below 2 $mg \cdot L^{-1}$.

The quality of products as fertilizers was tested by both in-vitro and in-vivo assays. High iron content in the product demonstrated a negative effect on plant germination, whilst the precipitation product from P extract demonstrated an advantage of P purification into struvite

for plant macro and micronutrient availability. The used method of P extraction followed by struvite precipitation is useful for both P and iron recovery into two separate products with agricultural and chemical applications, respectively.

Finally, a business model of sludge valorization into biochar and struvite was illustrated. The struvite precipitation cost effectiveness was evaluated on the hydrothermal carbonization liquor at full scale by adopting the use of fluidized bed reactors. The product cost was nearly 1.11 USD/Kg struvite. Along with that, the recovered iron oxalate byproducts can be commercialized as Fe and Ca sources for further chemical applications.

ABSTRAKT

Zastosowano termochemiczną obróbkę osadów z przemysłu mleczarskiego w celu uzyskania produktów oznaczonych jako STRUBIAS (struwit, biowęgiel i popiół), które są komercyjnie uznawane jako produkty nawozowe. Zastosowane technologie obejmują spalanie w niższej temperaturze w celu wytworzenia popiołu bogatego w fosfor i hydrotermalną karbonizację (HTC), która wytwarza hydrochar, prototyp biowęgla oraz wodę bogatą w składniki odżywcze. Fosfor i azot w otrzymanej w tym procesie hydrotermalnej wodzie oczyszczono poprzez wytrącanie struwitu. W celu znalezienia odpowiednich warunków procesu zastosowano metodę wielokrotnej optymalizacji. Zostały one określone, badając serwatkę, dzięki funkcji spełnienia wymagań (desirability function) określono efekt minimalizujący wpływ obcych jonów, jednocześnie zwiększając wytrącanie struwitu z bogatej w wapń serwatki. Podejście to zostało ulepszone przez dodanie naturalnego zeolitu – klinoptylolitu, aby wytrącić struwit w połączeniu z sorpcją amonu. To usprawniło usuwanie amonu, termodynamikę procesu i uzyskanie składu nawozu, który w miejscach aktywnych sorbentu zawiera więcej azotu, a tym samym zachodzi kontrolowane uwalnianie składników odżywczych.

Szczególną uwagę zwrócono na chemicznie wytworzone osady mleczne z solami żelaza jako koagulantami. Taki osad charakteryzuje się bardzo niską dostępnością P dla roślin, podczas gdy wysoki poziom żelaza staje się dla niektórych roślin zagrożeniem. Z jednej strony badania popioły pozostałe po spaleniu były ługowane kwasem fosforowym z dodatkiem kwasu solnego, następnie po dodaniu amonu i magnezu następowało wytrącenie struwitu. W celu uzyskania lepszej opłacalności procesu, połączono magnezyt i popiół z osadów mlecznych, które były ługowane w roztworze kwaśnym, a następnie wytrącono struwit. Połączenie popiołu

z osadów mlecznych i magnezytu było tak samo skuteczne w krystalizacji struwitu, jak użycie chlorku magnezu.

Proces HTC pozostawia większą ilość bogatego w składniki odżywcze roztworu. Odzyskiwanie fosforu (P) przez bezpośrednie strącanie zostało zbadane w celu polepszenia jakości produktu. Zawartość żelaza w produkcie wynosiła 17,96% i była wartością wyższą od dopuszczalnej wartości czystości nawozów fosforowych. Dlatego wykonano ekstrakcję roztworu P w HTC, a następnie wytrącono struwit. Zastosowanie kwasu szczawiowego wyekstrahowało 86,7% P z ługu HTC, podczas gdy usunięto 86,6% żelaza. Dla warunków procesu pH 9 i dodatku soli w stosunku molowym ($Mg:NH_4^+:P$) 1,73:1,14:1 do wytrącenia struwitu odzyskano 99,96% P i stężeniu P w odcieku poniżej 2 $mg \cdot L^{-1}$.

Jakość produktów jako nawozów została przetestowana zarówno w testach in-vitro, jak i in-vivo. Wysoka zawartość żelaza w produkcie wykazywała negatywny wpływ na kiełkowanie roślin, podczas gdy produkt strącania z ekstraktu P wykazał przewagę oczyszczania P do struwitu dla dostępności makro i mikroelementów dla roślin. Zastosowana metoda ekstrakcji P, po której następuje strącanie struwitu, jest przydatna zarówno do odzyskiwania P, jak i żelaza, oddzielnych produktów do zastosowań odpowiednio rolniczych i chemicznych.

Na koniec zilustrowano model biznesowy waloryzacji osadów do biowęgla i struwitu. Opłacalność wytrącania struwitu została oceniona na roztworze po hydrotermalnej karbonizacji w pełnej skali przy zastosowaniu reaktorów ze złożem fluidalnym. Koszt produktu wyniósł około 1,11 USD/kg struwitu. Wraz z tym odzyskane produkty uboczne szczawianu żelaza mogą być skomercjalizowane jako źródła Fe i Ca do dalszych zastosowań chemicznych.

.

SCIENTIFIC ACHIEVEMENTS

Published work under PhD study:

1. **C. Numviyimana**, J. Warchoł, N. Khalaf, J.J. Leahy, K. Chojnacka. Phosphorus recovery as struvite from hydrothermal carbonization liquor of chemically accumulated dairy sludge through extraction and precipitation. Journal of Environmental Chemical Engineering, Vol 10, Issue 1, 2022, **IF=5.9**
2. **C. Numviyimana**, J. Warchoł, B. Ligas, K. Chojnacka. Nutrients Recovery from Dairy Wastewater by Struvite Precipitation Combined with Ammonium Sorption on Clinoptilolite. Materials, Vol 14, Issue 19, 2021, **IF=3.6**
3. W. Shi, O. Fenton, S.M. Ashekuzzaman, K. Daly, J.J. Leahy, N. Khalaf, Y. Hu, K. Chojnacka, **C. Numviyimana**, M.G. Healy. An examination of maximum legal application rates of dairy processing and associated STRUBIAS fertilizing products in agriculture. Journal of Environmental management, Vol 301, 2022, **IF=6.78**
4. **C. Numviyimana**, J. Warchoł, G. Izydorczyk, S. Baśladyńska, K. Chojnacka. Struvite production from dairy processing wastewater: Optimizing reaction conditions and effects of foreign ions through multi-response experimental models. Journal of the Taiwan Institute of Chemical Engineers, Vol 117B, 2020, **IF=5.8**

Other published work:

5. **C. Numviyimana**, T. Chmiel, A. Kot-Wasik, J. Namieśnik. Study of pH and temperature effect on lipophilicity of catechol-containing antioxidants by reversed phase liquid chromatography. Microchemical Journal, Vol 145, Page 380-387, 2019, **IF=4.8**

Participation in scientific conferences:

1. Desirability function for optimization of metal interferences and process conditions for struvite precipitation from processed cheese wastewater. Poster, International conference of biotechnology and fungi, BioTop, March 12th , 2022 Wroclaw.
2. Hydrothermal carbonization process coupled to struvite precipitation for valorization of dairy sludge to commercial phosphorus fertilizing products. Oral presentation in X Congress of Chemical Technology, 12th May 2022, Wroclaw Poland.

AWARDS

2019-2022 EU-H2020, ITN-Maria Skłodowska-Curie scholarship award, REFLOW project, grant no:814258. Wroclaw University of Science and Technology (**Poland**).

2016-2018 EU-Joint Master Program-Erasmus mundus master's scholarship award, EMQAL 9th edition, University of Algarve (**Portugal**) – Gdańsk University of Technology (**Poland**).

2015 ARES-CCD scholarship award (A Belgian cooperation award), for postgraduate training, University of Liege (**Belgium**).

SUPPLEMENTARY MATERIALS

S. 1. Additional dosage in experimental struvite precipitation: Calculation formula of molar ratios, excess and limiting reagents.

-Calculate the molar ratio Ca/P, Mg/P and NH4+/P in the sample using results of elemental concentration C_x from sample analysis.

Molar ratio (R) of element (x): $R_x = \frac{n_x}{n_p} = \frac{C_x\left(\frac{mg}{kg}\right) \Big/ Mm_x\left(\frac{g}{mol}\right) * 1000\left(\frac{mg}{g}\right)}{C_P\left(\frac{mg}{kg}\right) \Big/ Mm_P\left(\frac{g}{mol}\right) * 1000\left(\frac{mg}{g}\right)}$

-On 250 mL of wastewater volume (Vs) measured using graduated cylinder, add recalculated amount of reagents as follow.

1. When Calcium is needed in excess, adjust its molar ratio to design of experiment matrix (R_{DOE})

$$n_{Ca_{add\ to\ 1L}} = R_{Ca/P} * n_P - n_{Ca}$$

$$V_{CaCl_2 1Molal\ added\ (mL)} = (n_{Ca\_added\ (mol)/1kg} * V_{s(kg)} * 1000(\frac{mL}{1L})) \,/\, (M_{\left(\frac{mol}{kg}\right)} * Density)$$

2.When P is needed in excess i.e $R_{\frac{Ca}{P}} \leq 1$,

$$n_{P_{add\ to\ 1L}} = \frac{\left(n_{Ca} - n_{\frac{Ca}{P}\_DOE} * n_P\right)}{n_{\frac{Ca}{P}\_DOE}}$$

$$V_{K_2HPO_4\ 1Molal\ added\ (mL)} = (n_{P\_added\ (mol)/1kg} * V_{s(kg)} * 1000(\frac{mL}{1L})) \,/\, (M_{\left(\frac{mol}{kg}\right)} * Density)$$

3. Magnesium is then calculated by molar ratio to actual P concentration in design of experiment (DOE).

$$n_{Mg\ needed} = R_{Mg/P} * n_{P\_DOE}$$

$$n_{Mg\ added\ to\ 1L} = n_{Mg\ added\ to\ 1L} - n_{Mg_{in\ 1L\ sample}}$$

$$V_{MgSO_4\ 2Molal\ added\ (mL)} = (n_{Mg\_added\ (mol)/1kg} * V_{s(kg)} * 1000(\frac{mL}{1L})) \,/\, (M_{\left(\frac{mol}{kg}\right)} * Density)$$

4. Ammonium is calculated as excess on Mg/P ratio. Thus $R_{NH_4^+/P} = R_{NH_4^+\ DOE} * R_{Mg/P}$

$$n_{NH_4^+\ needed} = R_{NH_4^+/P} * n_{P\_DOE}$$

$$n_{NH_4^+\ added\ to\ 1L} = n_{NH_4^+\ added\ to\ 1L} - n_{NH_4^+\ in\ 1L\ sample}$$

$$V_{NH_4Cl\ 4Molal\ added\ (mL)} = (n_{NH_4^+\_added\ (mol)/1kg} * V_{s(kg)} * 1000(\frac{mL}{1L})) \,/\, (M_{(\frac{mol}{kg})} * Density\ )$$

S. 2. ***Matrices of experimental data: Actual factors and responses***

Box–Behnken design for pH, Mg:P, Ca:P, and NH_4^+ excess. The number of experiments for struvite precipitation from processed cheese wastewater is 27 experiments. The table of experimental results of phosphorus recovery are given in table below:

Run	Factor 1 A:pH	Factor 2 B:Mg/P	Factor 3 C:Ca/P	Factor 4 D:NH_4^+	P_i	P_{out}	Response 1 X-recP %	Response 2 X-NH_4^+ %
1	8	1.5	0.625	2	1015	237.1	76.643	4.50
2	9.5	1.5	0.625	1	1015	55.9	94.499	4.13
3	11	1	0.625	3	990	93.5	90.551	2.05
4	9.5	1.5	1	2	634	37.8	94.039	3.13
5	9.5	0.5	0.625	1	1015	255.3	74.857	1.30
6	9.5	1	0.625	2	1015	62.6	93.829	4.13
7	11	0.5	0.625	2	1015	239.6	76.398	0.56
8	9.5	0.5	0.25	2	2528	699.9	72.424	4.29
9	8	1	0.625	3	1015	219.2	78.414	4.10
10	8	1	0.625	1	1015	280.0	72.420	2.91
11	8	1	1	2	635	195.1	69.253	2.44
12	11	1	0.625	1	1003	57.9	94.225	0.44
13	9.5	1	0.625	2	1015	40.8	95.982	3.24
14	11	1.5	0.625	2	1015	44.2	95.646	1.15
15	9.5	1	0.625	2	993	34.8	96.495	2.93
16	9.5	1.5	0.25	2	2518	36.1	98.566	5.92
17	11	1	0.25	2	2443	64.6	97.356	1.32
18	9.5	1	0.25	3	2377	57.6	97.578	5.60
19	9.5	1	0.25	1	2538	57.5	97.736	4.38
20	9.5	1	1	3	595	41.6	93.003	2.20
21	9.5	1.5	0.625	3	1005	35.6	96.459	4.88
22	8	1	0.25	2	2444	244.4	89.998	6.37
23	8	0.5	0.625	2	1015	406.9	59.926	1.95
24	11	1	1	2	626	57.5	90.806	0.27
25	9.5	0.5	0.625	3	1006	222.5	77.883	1.88
26	9.5	1	1	1	631	49.6	92.135	0.96
27	9.5	0.5	1	2	627	136.9	78.159	0.46

S. 3. ANOVA for Quadratic models for minimizing effect of foreign ions

Source	df	P rec				X-NH4+				Significance
		Sum of Squares	Mean Square	F-value	p-value	Sum of Squares	Mean Square	F-value	p-value	
Model	14	3070.97	219.35	20.03	< 0.0001	79.49	5.68	17.53	< 0.0001	significant
A-pH	1	809.48	809.48	73.91	< 0.0001	22.66	22.66	69.98	< 0.0001	
B-Mg/P	1	1136.82	1136.82	103.8	< 0.0001	14.69	14.69	45.35	< 0.0001	
C-Ca/P	1	110.42	110.42	10.08	0.0080	28.31	28.31	87.41	< 0.0001	
D-NH4+	1	5.40	5.40	0.493	0.4961	3.61	3.61	11.16	0.0059	
AB	1	1.43	1.43	0.131	0.7239	0.9577	0.9577	2.96	0.1111	
AC	1	50.76	50.76	4.63	0.0524	2,07	2.07	6.38	0.0266	
AD	1	23.55	23.55	2.15	0.1683	0.0444	0.0444	0.1370	0.7178	
BC	1	26.53	26.53	2.42	0.1456	0.2690	0.2690	0.8307	0.3800	
BD	1	0.2857	0.2857	0.026	0.8744	0.0072	0.0072	0.0221	0.8843	
CD	1	0.2650	0.2650	0.024	0.8790	0.0000	0.0000	0.0001	0.9941	
A^2	1	489.28	489.28	44.67	< 0.0001	5.42	5.42	16.75	0.0015	
B^2	1	441.01	441.01	40.26	< 0.0001	0.3275	0.3275	1.01	0.3344	
C^2	1	0.7251	0.7251	0.066	0.8013	0.1224	0.1224	0.3780	0.5502	
D^2	1	5.86	5.86	0.535	0.4784	0.1427	0.1427	0.4407	0.5193	
Residual	12	131.43	10.95			3.89	0.3238			
Lack of Fit	12	127.40	12.74	6.32	0.1442	3.11	0.3114	0.8069	0.6695	not significant
Pure Error		4.03	2.02			0.7719	0.3860			
Cor Total		3202.40				83.38				

S. 4. Multi-response optimization for effect of foreign ions

In this case both responsees are maximized, errors minimized and othors factors in the range. The overall desirability is deduced as geometric mean of both responses using desirability function, and inputs data. The lamp graph as follow:

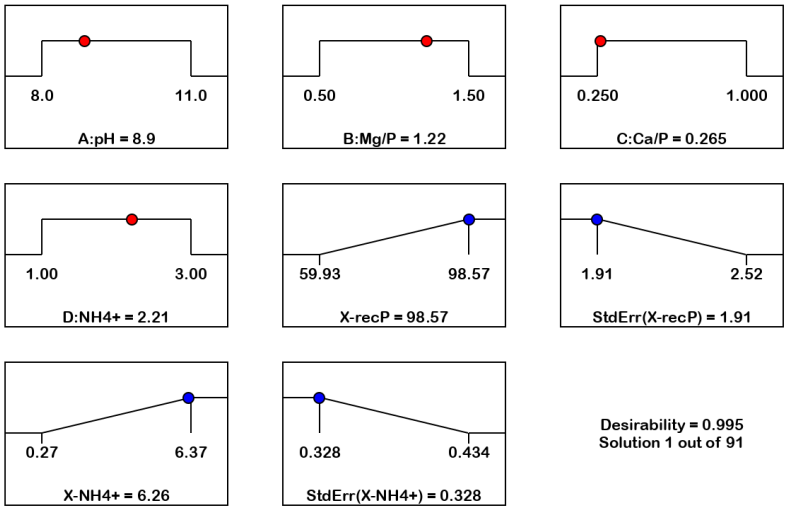

S. 5 Elemental composition of dairy wastes samples (S1 and S2)

	Concentrations ($mg \cdot kg^{-1}$)						
Analyte	**S1**	**S2**	**S3**	**S4**	**S5**	**S6**	**S7**
pH	4.35	4.34			6.96	-	-
C [%]	1.81	3.33	48.7	12.94	3.72	-	16.1*
Al	0.68	0.94	6116	3242.87	421	0.22*	-
B	1.14	10.83	1.65.00	55.45	2.52		-
Ba	0.30	0.11	16	15.39	0.55	45	-
Ca	1310	404	49205	37783.2	5538	15*	0.54*
Cr	0.12	0.39	2.12	6.04		-	-
Fe	88.2	3.44	128741	53212.1	9033	25*	106.6
K	1640	1635	15256	5558.03	2382	2.4*	147.7
Mg	108	82.33	2874.7	1843.6	278.6	0.83*	31.04*
Mn	1.53	0.06	181.69	131.4	19.21	390	-
N [%]	0.1	0.14	5.15	2.69	1.05	-	-
Na	490	488.39	3039.2	1834.99	557.7	0.57*	279.9
Ni	-	0.74	6.96	2.9	< LOD	-	
P	698	412	57177	52402.1	4517	16*	**154**
Pb	0.70	4.96	4.26	29.96	0.07	12	**<LOD**
S	88.2	126.43	4321.4	-	1302	152	-
Sb	-	5.78	9.96	15.66	1.35	4.26	-
Si	7.50	136.88	62.3	84.64	53.4	-	-
Ti	0.13	3.34	580.2	414.47	1.64	-	-
V	-	0.34	5.53	-	0.38	-	
Zn	2.83	2.54	125.8	103.7	15.2	280	-
NH_4^+	600	364	-	-	5850	-	-
Density	1.02	1.0	-	-	1.0	-	-

*:Values in % as unit. S1: cheese wastewater from District Dairy Cooperative in Krzepice, and S2, at the Sery Lutomierskie, Poland; S3: Dairy Sludge, S4: Hydrochar, S5: HTC liquor, S6: sludge ash, S7: Magnesite.

S. 6. Ash mineral extraction efficiencies

	(Ca+P):P	0M_HCl	±	2M_HCl	±	4M_HCl	±
Mg (%)	0.15	1.27	0.11	35.19	0.00	64.51	1.17
	0.25	4.03	0.37	32.25	0.00	80.14	13.68
	0.50	15.64	0.98	24.63	0.00	60.21	5.47
	0.75	16.49	1.83	23.75	0.88	73.89	7.04
	1.00	9.82	7.77	10.03	1.11	28.15	4.69
Ca (%)	0.15	19.89	0.33	78.67	9.33	78.22	0.00
	0.25	23.00	1.44	74.67	0.00	90.67	12.44
	0.50	21.44	0.78	62.67	6.67	80.00	5.33
	0.75	28.89	2.22	64.00	16.00	80.00	5.33
	1.00	13.33	8.44	54.67	6.67	69.33	8.89
Fe (%)	0.15	0.94	0.12	34.72	5.60	14.34	3.58
	0.25	0.68	0.29	21.50	0.90	52.27	4.48
	0.50	0.41	0.21	15.90	1.79	61.23	4.48
	0.75	1.95	0.66	17.14	3.92	56.75	5.97
	1.00	5.36	3.98	12.66	1.23	50.77	5.97

S. 7 Ash dissolution real-time measurement data

Time (min)	P	Ca	Fe	Mg	K
	mg.kg-1				
0	4.29	7.03	0.63	1.89	0
4	477.95	816.58	227.85	2138.69	85.66
10	1325.49	2080.32	602.16	7201.17	226.35
15	1974.29	3092.48	916.86	10763.90	322.14
20	2557.05	3876.43	1225.18	11223.60	461.56
27	2850.74	4062.40	1431.95	12856.30	546.08
35	2888.00	4090.02	1682.96	17091.30	672.4
50	2918.49	4270.93	1842.72	21190.70	827.94
75	3037.41	4465.78	1826.27	24852.80	865.68
110	3489.27	4622.28	2045.16	26332.70	835.02
150	3485.04	4896.96	2114.31	26065.00	739.4
210	3377.43	5035.22	2066.02	28056.40	735.65

Time (min)	Mg(mg.kg^{-1}) With MgCl2	With magnesite	P (mg.kg^{-1}) With MgCl2	With magnesite
0	10349.85	11359.33	5587.00	4917.00
1.5	7060.85	8457.91	1940.10	1372.14
4	4917.96	6969.73	16.84	15.00
6	4751.79	6738.29	8.12	9.62
8	4735.56	6764.32	5.42	6.12
10	4766.24	6387.72	4.92	4.97
13.5	4942.12	6993.98	4.78	4.25
17	4775.04	6805.59	3.90	4.11
22	4819.55	6920.12	3.38	3.51
27	5006.44	6900.10	3.20	3.21
35	4789.51	6861.32	2.89	3.15
45	4660.47	7050.18	1.73	3.02
60	4907.45	6943.86	2.46	3.33

S. 8. Mass balance estimates for cost effectiveness

$$V_{R2} = V_{R1} * \Delta V$$

$$V_{H3PO4} = \frac{1}{purity} * \left(\frac{C_{NH4+} * \Delta C_{NH4+}}{R_{\frac{N}{P}} * M_{m_{NH4+}}} - \frac{C_P * \Delta C_P}{Mm_P} * Mm_{H3PO4} * V_{R1} * \Delta V \right)$$

$$V_{R2} = V_{extract} + V_{MgCl2} + V_{H3PO4} + V_{NaOH}$$

$$m_{MgCl2}(kg) = \frac{P_{in}(kg) * V_{R1} * \Delta V * R_{Mg/P}}{Mm_P(\frac{kg}{mol})}$$

$$m_{NaOH\ 6M} = \frac{39.47 * V_{R1} * \Delta V}{0.24}$$

Estimated mass of cake:

$$m_{cake} = \frac{Fe_{cake}(kg)}{\%Fe_{cake} * 10^{-2}}$$

$$Fe_{cake}(kg) = (C_{Fe}\left(\frac{mg}{kg}\right) * V_{R1}(m^3) * 1000\frac{kg}{m^3} * \frac{10^{-6}kg}{mg} * \%RE_{Fe} * 10^{-2}$$

$$C_P\ upgrade\ (C_{P_{in}})\ for\ N{:}P\ 1.14\ = \frac{C_{NH4+} * \Delta C_{NH4+} * Mm_P}{100 * R_{\frac{N}{P}} * Mm_{NH4+}}$$

$$\Delta C_{NH4+}(\%) = 100 - \frac{\%NH4_{cake} * m_{cake}}{V_{R1} * 10^3 * C_{NH4+} * 10^{-6}}$$

$$P_{waste\ fraction}(P_R) = C_P * \frac{\Delta C_P}{C_{P_{in}}}$$

$$V_{extract} = \frac{L_c * P_R * 10^{-3}}{C_P * \Delta P * 10^{-2} * 10^{-6}}$$

$$V_{R1} = \frac{V_{extract}}{\Delta V * 10^{-2}}$$

$$m_{H2C2O4} = (V_{R1} * 0.375 * 10^3 * Mm_{H2C2O4} * 10^{-3})$$

$$P_{cake}(kg) = C_p * V_{R1} * 10^3 * 10^{-6} * RE_P * 10^{-2}$$

$$P_{rec}(kg) = P_{in}(kg) * \frac{RecP(\%)}{100}$$

$$Struvite\ product\ mass\ estimate = \frac{P_{rec}(kg)}{\%P2O5 * \frac{62}{142} * 10^{-2}}$$

S. 9. Quantitative estimation results for proposed industrial production model (energy, maintenance, operation, chemicals, installation and production costs)

	Reactor type	Pearl 500	Pearl 2K	Pearl 10K
	Load capacity (kg PO4_P/day) (Lc)	65.00	250.00	1250.00
Sample property	[P] liquor (mg/kg) (C_P)	4517.00	4517.00	4517.00
	C_{Fe}	9033.00	9033.00	9033.00
	C_{Ca}	5538.00	5538.00	5538.00
	[NH4] liquor 9 (mg/kg), C_{NH4+}	5850.00	5850.00	5850.00
Reactor 1 & mass balance	NH_4^+ (%) in cake, $\%NH4_{Cake}$	1.72	1.72	1.72
	dNH4 for second reactor (%), ΔCNH4+	79.16	79.16	79.16
	P upgrade for N:P to be 1.14 (CP_{in})	6995.94	6995.94	6995.94
	dP for second reactor influent, ΔCP	86.70	86.70	86.70
	P liquor fraction, P_R	0.56	0.56	0.56
	V liquor licheate (m3), $V_{extract}$	9.29	35.74	178.68
	dV for second reactor influent, ΔV	82.40	82.40	82.40
	Feed liquor volume, V_{R1}	11.28	43.37	216.84
	Mass (kg) of Oxalic acid added (up to 0.375M), m_{H2C2O4}	380.55	1463.66	7318.31
	Fe accumulated (%), $\%Fe_{cake}$	86.60	86.60	86.60
	Ca Accumulated (%),	93.13	93.13	93.13
	P accumulated (%)	13.40	13.40	13.40
	P in cake (%P2O5)	0.34	0.34	0.34
	Fe in cake ($\%Fe_{cake}$)	11.04	11.04	11.04
	Ca in cake ($\%Ca_{cake}$)	7.30	7.30	7.30
	P in cake for used substrate mass (kg), P_{cake} (kg)	6.82	26.25	131.25
	Fe in cake for used substrate mass (kg), Fe_{cake} (kg)	88.20	339.25	1696.24
	Ca in cake for used substrate mass (kg), Ca_{cake} (kg)	58.15	223.67	1118.35
	Estimated mass (kg) of cake (CaC2O4 and FeC2O4), m_{cake} (kg)	798.95	3072.89	15364.47
Reactor2	V H3PO4 85% added for N:P 1.14 adjust, V_{H3PO4} (kg)	106.42	409.31	2046.53
	$MgCl_2$ (kg) added for Mg:P 1.73 adjust, m_{MgCl2}(kg)	344.60	1325.40	6627.02
	VNaOH 6M added for pH ~8.5-9 adjust, $m_{NaOH\ 6M}$ (kg)	1528.00	5876.92	29384.61
	Influent Liquor leachate total Volume, V_{R2}	11.27	43.35	216.73
	RecP (%)	99.96	99.96	99.96
	P_in (Kg)	65.00	250.00	1250.00
	P_Rec (Kg)	64.97	249.90	1249.50
	P_2O_5 in product (%)	28.18	28.18	28.18
	Struvite product mass (kg)	528.07	2031.06	10155.28
Cost	Reactor (USD) (20 years)	1800000.00	1800000.00	1800000.00
	Lifetime of the reactor (years)	20.00	20.00	20.00
	Labor Usd/h	0.35	0.35	0.35
	Electricity (KWh)	320.00	320.00	320.00
	Electricity cost (USD)/KWh	0.15	0.15	0.15
	P recovery cost USD 2.4-3.7/Kg P for 15 years since 2009	3.70	3.70	3.70
	Maintainace cost /1 reactor (15000-27000 USD/year	27000.00	27000.00	27000.00
	Building space (SF) with 160-200USD/SF	2400.00	2400.00	2400.00
Chemicals	Magnesium Chloride (USD/tonne) as per Ostara	250.00	250.00	250.00
	NaOH cost (USD/tone)	340.00	340.00	340.00
	Oxalic Acid Cost (USD/tone)	640.00	640.00	640.00
	H_3PO_4 (USD/tonne)	800.00	800.00	800.00
TAC /day	Infrastructure cost	885.40	885.40	885.40
	Chemicals cost	539.52	2075.10	10375.48
	TAC	1424.93	2960.50	11260.88
	PE_k	64.97	249.90	1249.50
	CE	21.93	11.85	9.01
	PC/kg struvite (USD)	2.70	1.46	1.11